Functional importance of metabolic pathways in the tumour microenvironment to tumour development and progression

AMIRAH ALBAQAMI

UNIVERSITY OF LIVERPOOL
OCT-2018 / DEC-2022

Acknowledgment

First of all, I would like to express my huge gratitude to my supervisors Daimark and Vijay for their constant support, and for always encouraging me to push myself to achieve and to obtain the best results. I thank them for sharing their knowledge with me and for giving me excellent advice when I needed it. Without their guidance, I can honestly say that I would not have written or accomplished this excellent work. Thank you for cooperating with me and thank you to all my lovely colleagues in the lab as well as the cell imaging center team.

I also have such huge thanks to express to my son, Hussein, who has been my constant companion throughout this PhD journey. You were the best companion, and I hope that you will read this work of mine later and excuse me for my shortcomings with you. I love you very much.

To my friend Reem, her husband, and their children, thank you from the bottom of my heart for standing by my side during the COVID-19 period. You gave me and my son such great support at difficult times, and I will always be very grateful to you.

Munira, my sister and friend, I dedicate this achievement to you because you trusted me and supported me, and you always believed that I was capable of successfully completing this academic degree, and because of that, I believed it myself.

I cannot forget the love and support shown to me by my sisters Moudi, Malak, Arwa and Rawabi and my brother Nawaf. It meant a lot to me to know that you were by my side the whole way through this project, even when we could not be physically together. I hope that obtaining this degree will be a strong motivation for you and all of your children to continue seeking knowledge, just as our honourable mother, Nadha, prepared us to do.

Mother, I know that my success is your success, but I know that I could not have achieved this without your ground preparation. You were my first teacher and my ideal role model, always and forever. I also dedicate this work to my beloved father, who has supported me unreservedly throughout my journey. The love of my family was a constant motivator for me to continue and strive for success. I hope that I have made you proud.

Abstract

Altered energy metabolism is one of the hallmarks of cancer and is receiving much attention as a therapeutic target. The changes affect a wide range of metabolic pathways. In this study, we focussed our attention on fatty acid and amino acid metabolism, as two less well studied pathways with clear translational potential. We used the *Drosophila* eye epithelium as a cancer model. Knockdown of the metabolism genes found to be essential to eye development showed that the metabolic regulator Carnitine palmitoyltransferase 2 (*CPT-2*) in either immune cells or Ras^{V12}*/S100A4*-induced tumours was the most effective suppressor of tumour growth and invasion. We therefore focussed on *CPT-2* in our translational studies. Remarkably a role for *CPT-2* in the TME is consistent with clinical data that has been mined in collaboration with Dr Vijay Sharma, showing that *CPT-2* expression in tumour or immune cells is associated with poor prognosis, especially when there is low mutation burden. In a separate collection of breast cancer patient samples, the association between *CPT-2* expression and patient outcome was significant. High expression of *CPT-2* prevented recurrence of DCIS. The findings show that *CPT-2* has a protective effect at the *in-situ* stage in preventing recurrence of *in-situ* disease. These are surprising findings as *CPT-2* has been a hitherto neglected component of the fatty acid oxidation pathway in cancer studies. It may have a role both as a biomarker of progression and as a therapeutic target, although its effects are complex, switching from a protective effect at the *in-situ* stage to a broadly negative effect at the invasive stage. The latter effect is in keeping with our experimental observations.

In the second study, we probed the amino acid metabolism pathways using a dietary manipulation approach. Using an experimental model of tumourigenesis in *Drosophila*, we removed non-essential amino acids (NEAAs) from the food and we found that, of all the amino acids we tested,

glycine deprivation suppressed the tumour growth the most. Knockdown of the glycine transporter in neural cells had the same effect. We hypothesise that these effects may be mediated by circuitry in the brain controlling circadian clock because it has previously been shown that circadian neurobiology is a key target of glycinergic signalling. Interestingly, our preliminary mass spectrometry findings confirmed that Ecdysone is upregulated in animals with neuronal glycine transporter (*GlyT*) knockdown. This raises the possibility that nutritional inputs mediate changes in the neuronal circadian clock, ultimately impacting on tumour growth and progression, via steroid hormone production. Overall, glycine represents a metabolic vulnerability in rapidly proliferating cancer cells that could in principle be translated into human studies and be targeted for therapeutic benefit.

In summary, we have, through these studies, identified and characterised two therapeutic targets, *CPT-2* and glycine metabolism, which showed the strongest effects in our experimental models, and can now be further investigated in translational studies.

Table of Contents

List of Figures and tables :

List of abbreviations :

Ala - alanine
Asp - aspartate
Asn - sparagine
ATP- adenosine 5'-triphosphate
AttP - phage attachment
AttB -bacterial attachment
ACLY - ATP citrate lyase
ASNS - asparagine synthase enzyme
Br - Broad
BL - Bloomington fly stock center
CTPsyn - CPT synthase
CS- carnitine system
CDF - chemically defined food
CyO - curly wings
Chinmo - chronologically inappropriate morphogenesis
CLL - lymphocytic leukaemia
CPT-1 - Carnitine palmitoyltransferase I
CPT-2- Carnitine palmitoyltransferase II
CAC - citric acid cycle
CS- Carnitine system
Crb - Crumbs
CycE - Cyclin E
CLL - lymphocytic leukaemia
Cys- cysteine
Dac- Dachshund
DCIS- Ductal carcinoma in situ
Dlg- discs-large
Ey- eyeless
Eya- eyes absent
eyFLP - eyeless flipase
EGFP - encoding enhanced GFP
EcR - ecdysone receptor subunit
EcRE - ecdysone response element
Elav - Embryonic lethal abnormal vision
eya - Eyes absent
Eno- Enolase
ETC- electron transport chain
ER - estrogen receptor
FRT- flippase recognition target
FLP- Flpase
FAO- fatty acid oxidation
FAT - fatty acid translocase
FASN - Fatty-acid synthase
Gal4 - galactose-induced genes.
GDP- guanosine diphosphate

GlyT - glycine transporter
GLUT1- glucose transporter
GLS - glutamine synthesis
GFP- Green fluorescent protein
G6PDH- Glucose-6-phosphate dehydrogenase
Gs1- Gs1- Glutamine synthetase 1
Glt- Glutamate
Gln -glutamine
GTP - guanosine triphosphate
Hpo - Hippo
He - head involution defective
HCC - hepatocellular carcinoma
HER2- human epidermal growth factor receptor 2
JNK- c-Jun N-terminal Kinase
ILPs- insulin-like protiens
IL- interleukin
IR- inverted repeats
LACS - Long-chain acyl-CoA synthetase
LD- lipid droplets
Lo- LexAoperator
Let-7- lethal-7
L3- mid larvae stage 3
Mpc1- Mitochondrial pyruvate carrier
MMP1- Matrix Metallopeptidase 1
MAGK - membrane-associated guanylate kinase
ND-49- NADH dehydrogenase (ubiquinone) 49 kDa subunit
NAFLD- non-alcoholic fatty liver disease
NF -normal food
NEAAs- Non-essential amino acids
Puc- Puckered
PBS – Phosphate buffer saline
PBTB- (1X PBS, 0.2% Tween 20, 5% fetal bovine serum)
PBST - (1X PBS, 0.2% Tween 20)
PDAC - pancreatic ductal adenocarcinoma
PFK- Phosphofructokinase
PHGDH - phosphoglycerate dehydrogenase
PTTH - prothoracicotropic hormone
PR - progesterone receptors
PIG-H - Phosphatidylinositol glycan anchor biosynthesis class H
PI3K - phosphophatidylinositol-3 kinase
Pals1- protein associated with caenorhabditis elegans Lin-7 protein (Pals1) and
Patj - Pals1-associated TJ protein
Par - partitioning defective
Pro-Proline
ROS - reactive oxygen species
RNAi - RNA interference
RFP- Red fluorescent protein
Scrib - scribbled
Ser- serine
SREBPs - sterol regulatory element binding proteins
Sav - Salvador
So- sine oculis
SLC - solute carrier
SAM -S- adenosylmethionine
Toy- twin of eyeless
TME- Tumour microenvironment
TCA- tricarboxylic acid
TNF- Tumor Necrosis Factor

TRiP - transgenic RNAi Project

USP- ultraspiracle

UAS - upstream activating sequence

UP-TORR - Updated Targets of RNAi Reagents

VDRC - Vienna Drosophila RNAi Center

Wats - Warts

Yki - Yorkie

ZBTB - complex/Tramtrack/Bric-à-brac Zinc-finger

20E - 20-hydroxyecdysone

αKG - α-ketoglutarate

+/- presence or absence

Chapter 1: Introduction

1.1. Introduction

Cancer is a disease that is characterised by the accumulation of genetic changes that allow cells to acquire distinctive biological properties, or hallmarks. These hallmarks include sustained cell signalling proliferation, induction of angiogenesis, resistance to apoptosis, the capability of invasion and evasion of growth suppressors (Hanahan and Weinberg, 2011). Another two hallmarks have emerged in the last decade, including evading destruction by the immune system and remodelling energy metabolism (Pavlova and Thompson, 2016, Hanahan and Weinberg, 2011). Furthermore, tumours exhibit another level of complexity by creating the tumour microenvironment (TME), in which stromal cells are recruited to contribute to the acquisition of hallmark capabilities that enable tumourigenesis and malignancy. Consequently, tumour biology cannot be simply understood by studying the intrinsic features of tumour cells - the TME contribution to tumourigenesis must also be taken into account (Hanahan and Weinberg, 2011). The TME consists of immune cells, vasculature, fibroblasts and extracellular matrix proteins (Maan et al., 2018). During tumour cell proliferation, the tumour microenvironment can be acidic, nutrient-deprived, and hypoxic. In response to these conditions, the tumour cells and the surrounding stromal cells remodel their metabolism in a way that allows tumour proliferation and invasion (Maan et al., 2018). One type of metabolic reprogramming that has received great attention in the last few years, is that of alterations to glucose metabolism (Gaglio et al., 2011, Gatenby and Gillies, 2004). However, other nutrients including amino acid and fatty acid metabolism are also altered in cancer, and there are also a growing number of studies on lipid metabolism

alteration (Maan et al., 2018). A few studies in a limited number of cancer types, have demonstrated the association of metabolic changes with different subtypes and outcome by using genomic data and/or metabolite analysis of fresh samples from human tumour tissue (Chang et al., 2015, Tang et al., 2014). However, neither the association between cancer subtypes and metabolic changes and genetic events nor the interaction between TME and tumour cells has been systematically addressed. Understanding the intricacies of these factors will ultimately expand our understanding of cancer progression and metastases and provide possible therapeutic strategies targeting this interaction.

1.2. Cancer metabolism overview

1.2.1 Glucose metabolism

Energy metabolism in normal cells, under aerobic conditions, converts glucose to pyruvate in the cytosol. Then only few amounts of this pyruvate are converted to lactate and the rest to carbon dioxide in the mitochondria, via the tricarboxylic acid (TCA) cycle, known also as citric acid cycle (CAC) or Krebs cycle, to produce the energy-storing molecule adenosine 5'-triphosphate (ATP)**.** Meanwhile, under anaerobic conditions, oxidative metabolism stops, and glycolysis becomes the sole source of energy, leading to the conversion of pyruvate into lactate in the cytosol **(Figure 1.1)** (Matthew et al., 2009, Kim and Dang, 2006). In this condition, glycolysis becomes the sole source of energy generated from glucose, and because the pyruvate generated by glycolysis has nowhere to go it is then converted to lactate. Under aerobic conditions, energy from glucose is derived from both glycolysis and oxidative metabolism in the mitochondria, but because oxidative metabolism produces much more ATP, the proportion of energy generated by glycolysis is smaller.

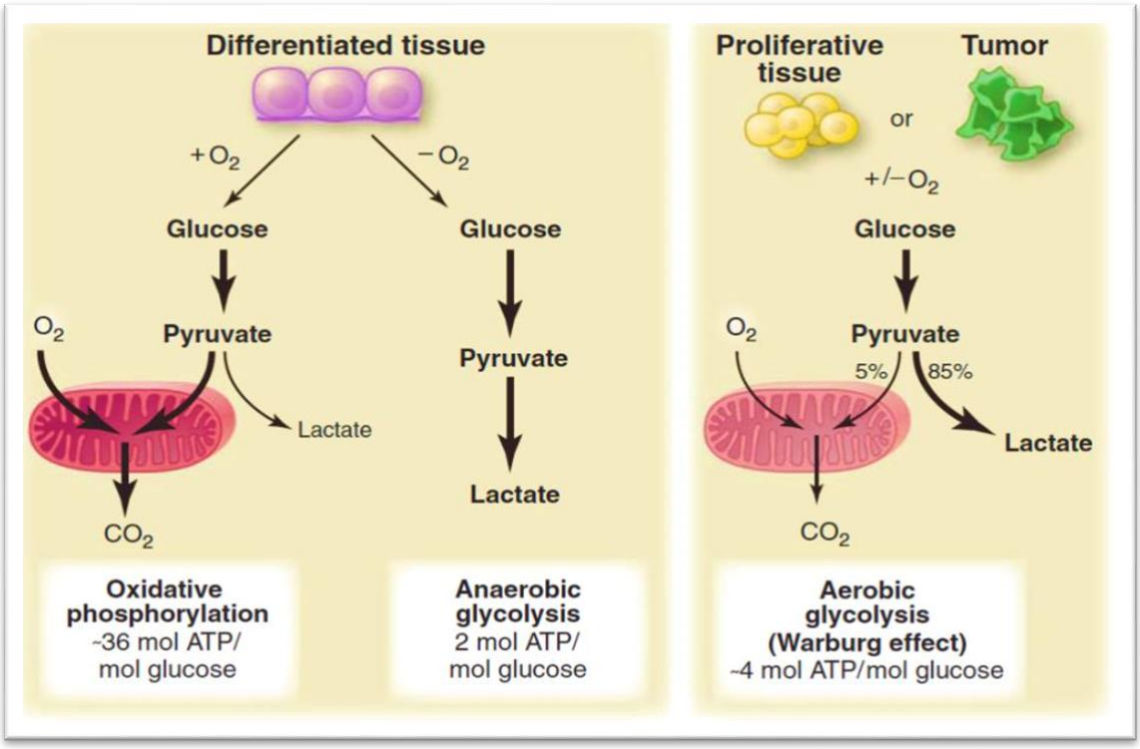

Figure 1.1 Glucose metabolism pathway.

Differentiated tissues (normal cells) rely on oxidative phosphorylation which generates 36 ATP in the presence of oxygen, while in anaerobic conditions they switch to glycolysis which generates 2 ATP. In proliferative tissue and cancer cells, regardless to the level of oxygen, most of the pyruvate is converted to lactate via glycolysis and only (5%) is used for ATP production. Figure reproduced from (Fung, 2018).

Malignant cancer cells can be hypoxic in some regions due to an increased distance between blood vessels and tumour cells (Muz et al., 2015). Warburg suggested that cancer cells rely on aerobic glycolysis (the Warburg effect), for energy production (Otto, 1956). In fact, cancer cells use Warburg metabolism, aerobic glycolysis, to adapt to the hypoxic environment and also to generate the substrate needed for progression and not just for energy production (Petan et al., 2018). Cell division requires many cellular components, building blocks such as Acetyl-Co-A, ribose sugar for nucleotide synthesis, amino acids for protein synthesis and lipids for bio-membrane synthesis. Thus, cancer cells degrade glucose and use some for energy and the rest for biomass to support biosynthesis and expansion (Fadaka et al., 2017). Moreover, the aerobic glycolysis pathway

reduces the consumption of oxygen, which ensures cell survival by protecting cells from being anoxic (Denko, 2008).

The glycolysis pathway is inefficient for energy production as only 4 ATP molecules are produced for each molecule of glucose. To overcome this inefficiency, there is an increased uptake of glucose via the *glucose transporter (GLUT1)* in cancer cells and thus more glycolysis events occurs (Fadaka et al., 2017). Increased glycolysis rates also underline TME acidosis (Maan et al., 2018). Moreover, in cases of glucose-derived energy production deficiency, cancer cells rely on lipid metabolism to ensure their survival, explained in more details in **Section 1.2.2.**

1.2.2. Lipid metabolism

Lipids, including sterols, phospholipids and di-/tri-acylglycerols are integrated in cell membranes and are used for energy production, storage, and cellular signalling. Lipid synthesis is regulated by the sterol regulatory element binding proteins (SREBPs), which are membrane-bound transcription factors that control the expression of enzymes involved in the synthesis and uptake of FA and cholesterol. SREBPs respond to upstream signalling networks, for example, phosphophatidylinositol-3 kinase (PI3K)/AKT and mammalian target of rapamycin (mTOR), pathways and to the nutrition status such as lipid depletion (Peck and Schulze, 2019).

Lipids are stored in lipid droplets (LDs) and degraded by lipolysis and autophagy when needed (Farese Jr and Walther, 2009). Fatty acids consist of phospholipids, hydrophobic tails and glycolipids (Birsoy et al., 2015). FAs are stored as triglycerides (TGs) in the adipose tissue (Maan et al., 2018). In the case of energy depletion, TGs are degraded to release FAs and then they undergo oxidation to release energy. In the cytoplasm, FAs are activated to form acyl CoA, which will

then be transported to the mitochondria with the help of *carnitine palmitoyltransferase 1 (CPT1)* (Carracedo et al., 2013). *CPT1* is the rate- limiting enzyme for fatty acid oxidation (FAO). In mitochondria, fatty acids obtained by lipolysis undergo a cyclic series of reactions for oxidation of the ß-carbon of the fatty acid and they generate acetyl Co-enzyme A (acetyl CoA), NADH and FADH2 (**Figure 2.1.2**). Acetyl-CoA enters the Krebs cycle, and NADH and FADH2 then enter the electron transport chain (ETC) to produce ATP (Camarda et al., 2016, Carracedo et al., 2013).

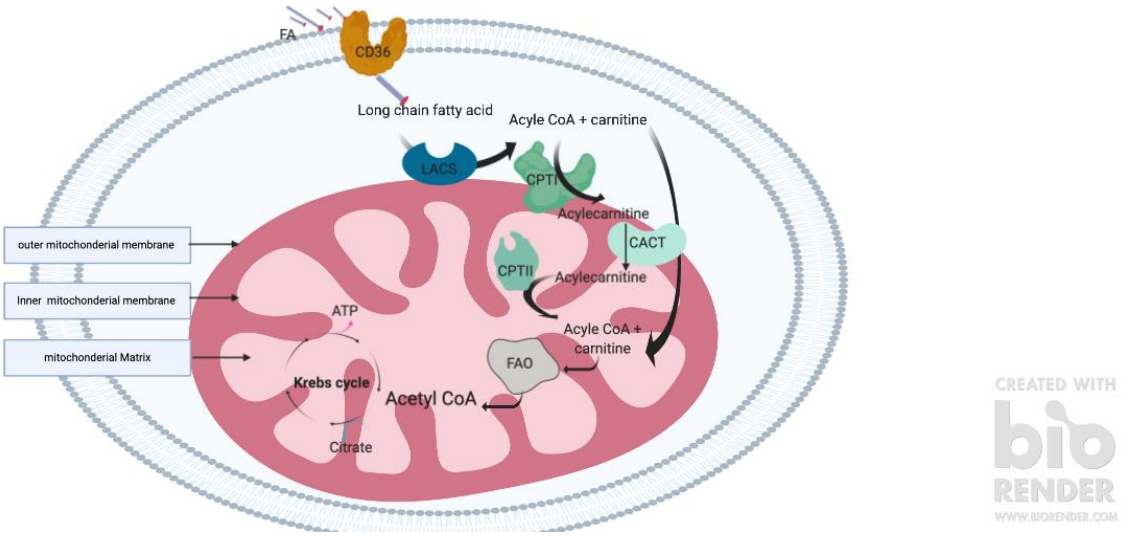

Figure 2.1.2: FAO regulation on the mitochondrial membrane.

FA is taken via CD36, a transmembrane channel protein, and fatty acid translocase (FAT). Long-chain acyl-CoA synthetase (*LACS*) is catalysed and then long-chain fatty acid is transformed into acyl-CoA. This acyl-CoA is transported to the mitochondrial matrix by *CPT1*: acyl-CoA is converted into acylcarnitine by *CPT1*. Acylcarnitine carnitine Translocase (CACT) exchanges carnitine and acylcarnitine between the outer and inner mitochondrial membranes. *CPTII* converts acylcarnitine into acyl-CoAs for oxidation. Figure and information were reproduced with slight changes from (Maan et al., 2018) .

In cancer cells, FA synthesis and FAO are often increased, leading to increased accumulation of LDs (Beloribi-Djefaflia et al., 2016). Lipid metabolic changes in

cancer cells involve FAO, *de novo* lipogenesis and lipid storage as LDs (**Figure 3.1.3**).

Moreover, FAO plays an important role in the condition of acidosis where there is a reduction of glucose-derived acetyl CoA; this helps ensures cancer cell survival (Kalyanaraman, 2017). Targeting these starving cancer cells of their insatiable metabolic requirements by using drugs (that are non-toxic to the normal cells) can inhibit cancer cell proliferation (Bristow, 2000).

Fatty-acid synthase (FASN) catalyzes *de novo* biosynthesis of saturated fatty acids (SFA) (Carracedo et al., 2013). Over-expression of FASN is reported in several cancers including ovarian, breast, colorectal and prostate (Menendez and Lupu, 2007, Milgraum et al., 1997, Chavarro et al., 2013). Conversely, inhibition of FASN has been shown to reduce tumour progression and invasion in hepatocellular carcinoma cells (Hao et al., 2014).

ATP citrate lyase (*ACLY*) overexpression has been reported in gastric adenocarcinoma (Qian et al., 2015), whereas RNAi knockdown of *ACLY* leads to a reduction in cell proliferation and invasion in lung, prostate, osteosarcoma and cervical cancer cells (Xin et al., 2016).

Acetyl CoA carboxylase (Jaccard et al.) is the rate limiting step of FAS pathway. There are two isoforms of *ACC, ACC1* (cytosolic isoform) is present in lipogenic tissues and involved in lipid synthesis (Wang et al., 2016). *ACC2* (mitochondrial outer membrane) is present in lipid oxidizing tissues and it is involved in inhibition of lipid degradation (Camarda et al., 2016). *ACC1* is frequently upregulated and *ACC2* is inhibited in different cancers, supporting increased FAS and FAO in cancer cells (Carracedo et al., 2013).

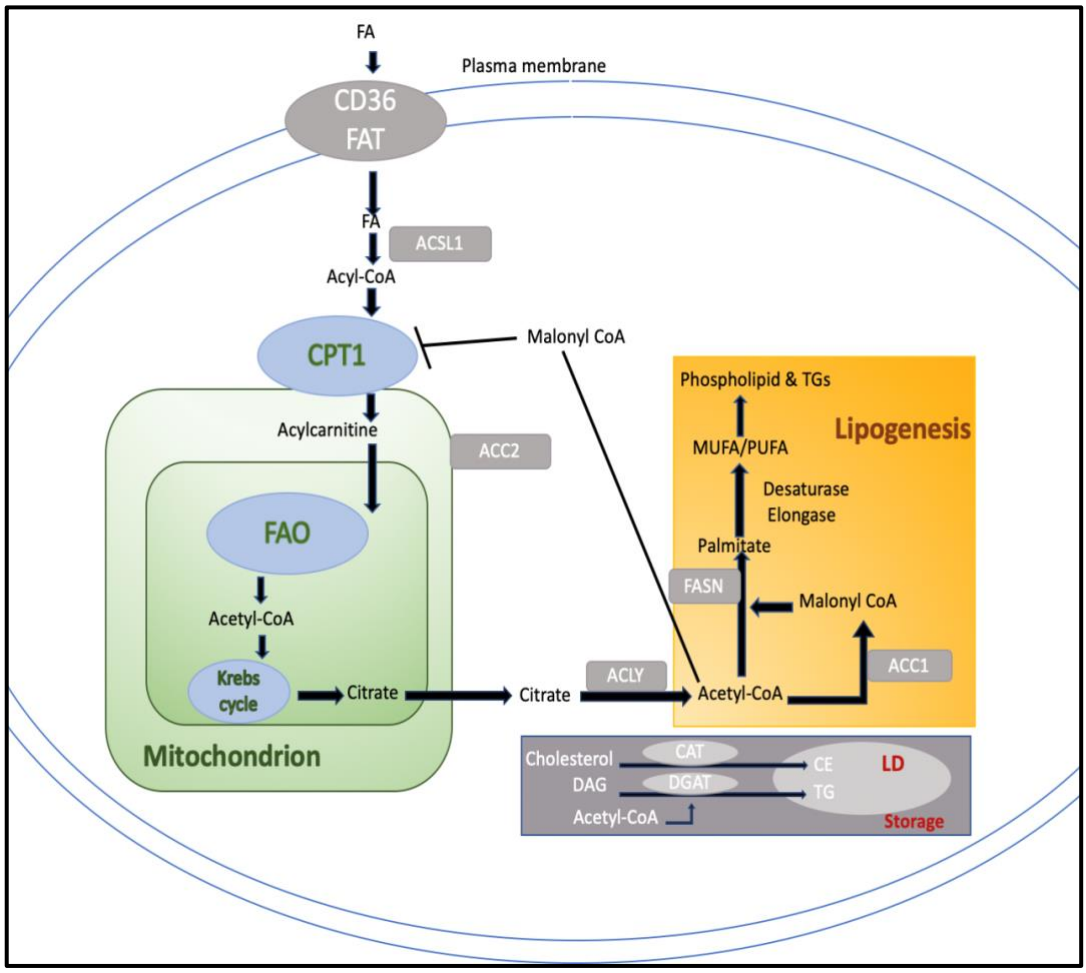

Figure 3.1.3: Schematic representation of lipid metabolism in cancer cells.

FA uptake increased via CD36 and FAT. Then, FA undergoes ß-oxidation in the mitochondria, more details are in figure 5. The end product of FAO, Acetyl CoA, can either enter Krebs cycle, or is transported in the form of citrate to the cytosol for fatty acid synthesis. Cytosol citrate is converted to Acetyl CoA again by *ACLY*. Then, *ACC1* catalyzes the carboxylation of Acetyl CoA to malonyl CoA. *FASN* forms palmitic acid by using acetyl-CoA molecule and malonyl-CoA molecules. The final product palmitate is then elongated by *ELOVL6* (elongation of very long chain fatty acids protein 6) or desaturated by SCDs. In lipid droplets, formation of triacylglycerol and cholesterol ester (CE) is made by esterification of excess acyl CoA with cholesterol or diacylglycerol (DAG) (Maan et al., 2018).

Carriers in the carnitine system (CS), which transport Acyl-CoA from cytosol to mitochondria and vice versa, play a crucial role in switching between fatty acid and glucose metabolism (Melone et al., 2018). Therefore, in recent studies, regulation of CS at both epigenetic and enzymatic levels is suggested to be a way to trigger the metabolic pathway of cancer cells (Melone et al., 2018).

Drosophila melanogaster is a powerful model to investigate the lipid metabolic regulators that support tumour growth and development. Often, disruption of individual regulatory enzymes leads to specific phenotypes, thus revealing their involvement in cell proliferation, growth and differentiation. For example, mutation of two enzymes involved in citric acid cycle (TCA cycle) led to preventing the larval salivary glands from dying at the onset of metamorphosis (Wang et al., 2010, Dianne et al., 2017). This result suggests that cell death activation in the salivary glands is dependent on the TCA cycle and reveal an unexpected relationship between central carbon metabolism and metamorphosis (Pletcher et al., 2019). Such phenotype-driven studies are essential for investigating how metabolism and cancer development are coordinated. Furthermore, cancer metabolism is shaped by interaction with TME including stromal and endothelial cells, fibroblasts as well as nutrient and oxygen availability (Anastasiou, 2017).

In this regard, we are particularly interested in the requirement of metabolic reprogramming of tumours and the TME for neoplastic growth and invasion. This necessitates the use of tractable model systems in which the TME can be readily manipulated. Studies of how tumours use evolutionary conserved pathways in model systems to promote metastatic dissemination will guide studies in human cancer patients; by measuring the expression levels of factors in human cancer samples, we will be able to determine whether they have prognostic significance. Critically, a comprehensive understanding of the genes needed for successful invasion to occur may offer new therapeutic strategies.

1.3. *Drosophila* as a cancer model

Drosophila models have many features that lend themselves to use as a subject for experimentation, including a short life cycle and the fact that it is possible to examine large numbers of flies in well-targeted genetic screens (Héctor and Stephen, 2017). Consequently, *Drosophila* is useful for exploring the machinery of complex developmental biology and behaviour as well as contributing to our knowledge regarding different aspects of tumours in humans (Héctor and Stephen, 2017). There has been a significant increase in the use of D*rosophila* as a cancer model in the last 20 years, suggesting its relevance to cancer research (**Figure 4.1.4**)(warr, 2019).

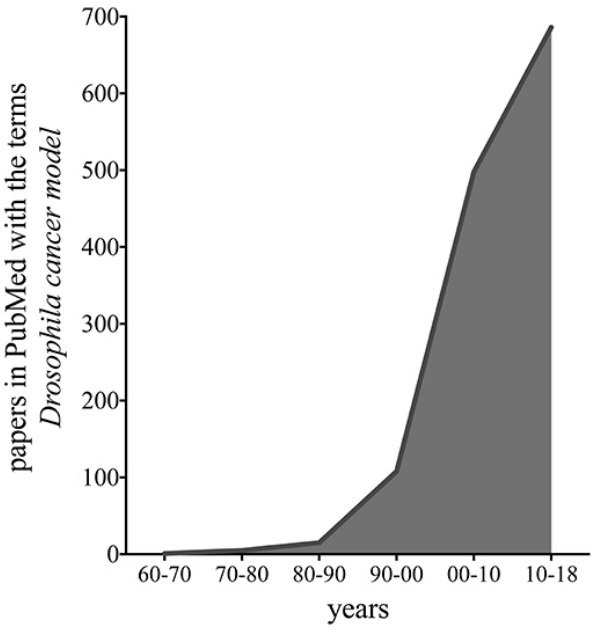

Figure 4.1.4: Number of publications.

Number of publications in PubMed used the term (*Drosophila* cancer model) in the last 48 years. Figure reproduced from (Zhasmine et al., 2019).

The fact that *Drosophila melanogaster* has substantial genetic, metabolic, and functional similarities with humans and ~75% of human disease-causing genes are conserved has made it a valuable model for neurological disorders, cancer and other diseases (Hales et al., 2015). Many cellular regulators were first identified in *Drosophila* and involved in cancer development in humans, including *Hedgehog, Notch, Salvador (Sav), Hippo (Hpo)* and *Warts (Wats)* (Gonzalez et al., 2013). Thus, these genes can be studied and manipulated in *Drosophila*, where the *in vivo* setting also enables assessing the microenvironment role in tumour progression (Gonzalez et al., 2013). Furthermore, studies on *Drosophila* have given insights into epithelial cancer development, including apoptosis-induced compensatory proliferation, cell competition and oncogenic co-operation (Vidal and Cagan, 2006).

In our experiments, we are using the *Drosophila* eye epithelium as a cancer model. There is an anatomical difference between human eyes and flies eyes. However, number of genes involved in orchestrating the proper temporal and spatial organization of the eye components such as *atonal (ato)* or in eye specification such as *eyeless (ey), twin of eyeless (toy), eyes absent (eya), dachshund (dac) and sine oculis (so)* are highly conserved, and mutations result in retinal defects in both systems alike. *Drosophila* imaginal discs (including eye/antennal disc) offer the opportunity to model epithelial tumours *in vivo* – and is therefore broadly relevant to many tumour types (Hodgson et al., 2021). It is therefore a valuable genetic model in which to test interactions between cancer-related genes found to drive the development or progression of tumours in humans (Kumar, 2001).

1.3.1. *Drosophila* genetic tools

1.3.2. Chromosomal balancer

Drosophila models benefit from over a hundred years of accumulated knowledge, tools, and resources. Collections of *Drosophila* mutations are available for functional genomic studies and have been generated by exposure to X-ray and other chemical mutagenetic approaches, such as alkylating agent ethyl methane sulphonate (EMS) (Muller, 1927). These mutations can occur anywhere in the genome and with the development of balancer chromosomes mutations can be mapped to a defined region of the genome and stably maintained over many generations. The **chromosomal balancer** is a multiple inverted segment used to suppress recombination and it has a dominant phenotypic marker such as curly wings (*CyO*) to enable tracking of chromosomes across generation (Hentges and Justice, 2004). They are recessive lethal so the balancer chromosome cannot exist in the homozygous state and the chromosomal of interest will be stable in a heterozygous state (Hentges and Justice, 2004). Many phenotypically- marked chromosomes with recessive mutations are available at the Bloomington *Drosophila* Stock Center.

1.3.3. P transposable elements

Balancer mutagenesis screens can provide a systematic functional analysis of the genes and help facilitate a functional annotation of the fly genome sequence. This is particularly possible after having *Drosophila* genome sequenced successfully in March 2000. Information from such studies is curated in the online database (Flybase).

Gene function can be studied by using *plasmid (P)* transposon element mediated transgenesis. *P* transposon element is a mobile genetic element (transposon) encoding the transposase enzyme, which together with the inverted repeats found on the terminus of the DNA element allow movement within the genome (Gerald and Allan, 1982). A modified version of the *P* element lacking the transposase, which is typically provided on a separate plasmid, and carrying selectable markers can be injected into G0 *Drosophila* embryos for stable transformation of transgenic constructs (Venken and Bellen, 2005). Typically, the *white* (w^+) eye color marker gene is used to identify transformants. Another use of *P* elements is in a technique called GENE-TRAP where transposable *P* elements contain sequences encoding enhanced GFP (EGFP) or a temperature-sensitive splicing protein introns (or INTEINS). These introns are spliced out and result in a functional protein at the permissive temperature. However, at the restrictive temperature (29°C), the splicing does not occur and the protein will be inactive (Venken and Bellen, 2005).This approach is particularly important for experiments using recessive lethal gene mutations, as it induces expression of mutant transgenes after lethal stage. Using the (GFP-TRAP) carried by a transposable P-element allow rapid access to the distribution and localization of the endogenous protein of the tarped genes (Morin et al., 2001).

However, generating transgenics with large (>40kb) DNA fragments using *P*-elements is challenging, not least because such DNA is often not stable in high copy number plasmids for amplification in bacteria (Venken and Bellen, 2005). Consequently, sufficient DNA cannot be generated for microinjection. Furthermore, insertion into the genome occurs randomly and to identify the desired site specific transgenic insertion it will require genetic screening (Venken and Bellen, 2005). To overcome these limitation, an efficient site-specific recombination method was developed using bacteriophage phi C31(φC31) integrase (Groth et al., 2004). Transgenes are integrated into the genome using

φC31integrase, which catalyses recombination between its recognition sites in *Drosophila*, the phage attachment (*attP*) and bacterial attachment (*attB*) (Venken and Bellen, 2005). The *attP* site integrated in drosophila genome with a *P* element. The φC31 integrase is then injected into *Drosophila* embryos to promote integration of an *attB*-containing plasmid into the *attP* site, resulting in adults producing transgenic offspring (Groth et al., 2004).

1.3.4. *GAL4/UAS* and *LexA/Lexop* based gene expression

GAL4 is a yeast transcription factor which binds to the upstream *activating sequence* (*UAS*), an enhancer that is specific to *GAL4. LexA* is a transcription factor which binds to Lexop, *LexA* operator sequences to activate transcription (Hales et al., 2015), (**Figure 5.1.5**.). *GAL4* drives the expression in specific tissue when binds to *UAS*, which could be expressing gene mutagenesis or RNAi construct. These bipartite expression systems place the gene of interest indirectly under control of the promoter/enhancer that is driving expression of *GAL4*. The key advantage is that it allows a lot of flexibility, such that a single transgenic construct (for example, *UAS-gene*) can be induced in different ways by interbreeding. The *LexA*/ *Lexop* system works using a similar principle.

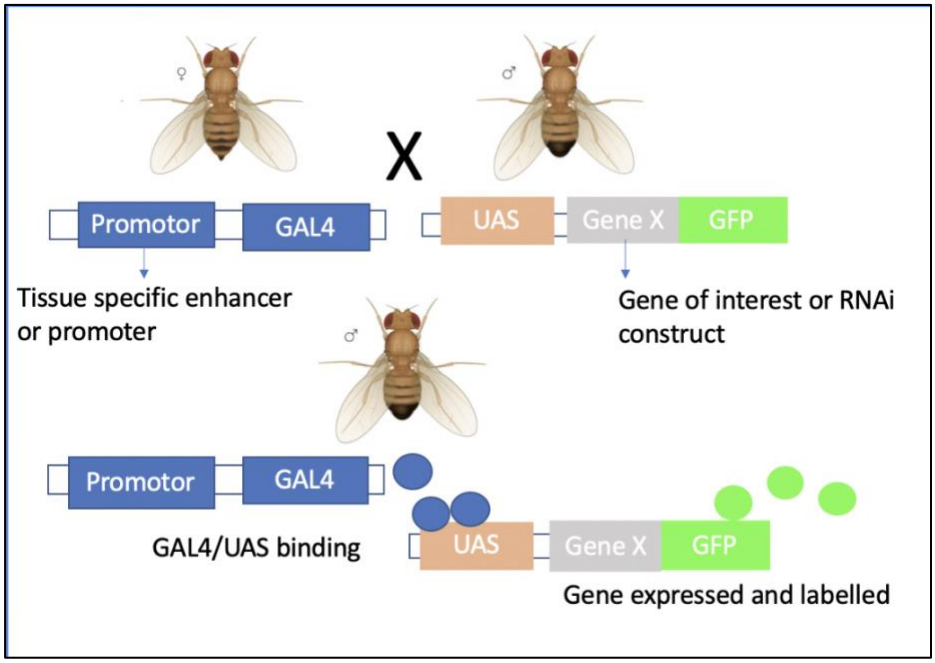

Figure 5.1.5.: GAL4/UAS binary expression system.

A *P*-element carrying a *UAS* with gene of interest is in one fly and the *GAL4* with the tissue specific promoter is in another fly and when crossed to each other , GAL4 protein will bind to the *UAS* and trigger the expression of the gene at the tissue that the promoter is specific for (Hales et al., 2015).

Expression of GAL4 can be controlled using the GAL80 repressor, which binds to the carboxy terminal of GAL4 and prevents transcription activation. GAL80 can be used to temporally control GAL4 expression with the temperature sensitive variant ($GAL80^{ts}$). $GAL80^{ts}$ represses GAL4-meditated expression of UAS when raised at 25°C, but at 37°C repression is relieved and expression of UAS by GAL4 is activated (McGuire et al., 2003).

A large number of *GAL4* drivers are available to express genes in various tissue including imaginal discs, brain testis and ovaries. *GAL4* can be combined with RNA interference (RNAi) to knockdown gene of interest at specific tissue and at any developmental stage (Dietzl et al., 2007). DNA fragments of the gene of interest are cloned as inverted repeats (IR), which, when expressed, form double stranded RNA (dsRNA) that is processed by the endogenous RNAi machinery to

target the endogenous target (complementary) mRNA for degradation. Inverted repeat constructs typically consist of either short hairpin, 21bp, or long repeats, 300-500bp. Transgenic flies carrying short hairpins, generated by the transgenic RNAi Project (TRiP) at Harvard Medical School, and φC31meditated integration is used for these lines (Perrimon et al., 2010, Dietzl et al., 2007). RNAi lines are available from Bloomington fly stock center and Vienna *Drosophila* RNAi Center (VDRC). It is important to know that these RNAi lines can cause non-specific defects or might not result in the complete knock-down of the protein-encoding mRNA. Off-target effects of certain RNAi lines could be predicted by using the computation tools (UP-TORR).

1.3.5. Flippase (Flp) and flippase recognition target (FRT) system:

FLP/FRT system is used to generate mosaic tissues (**Figure 6.1.6).**

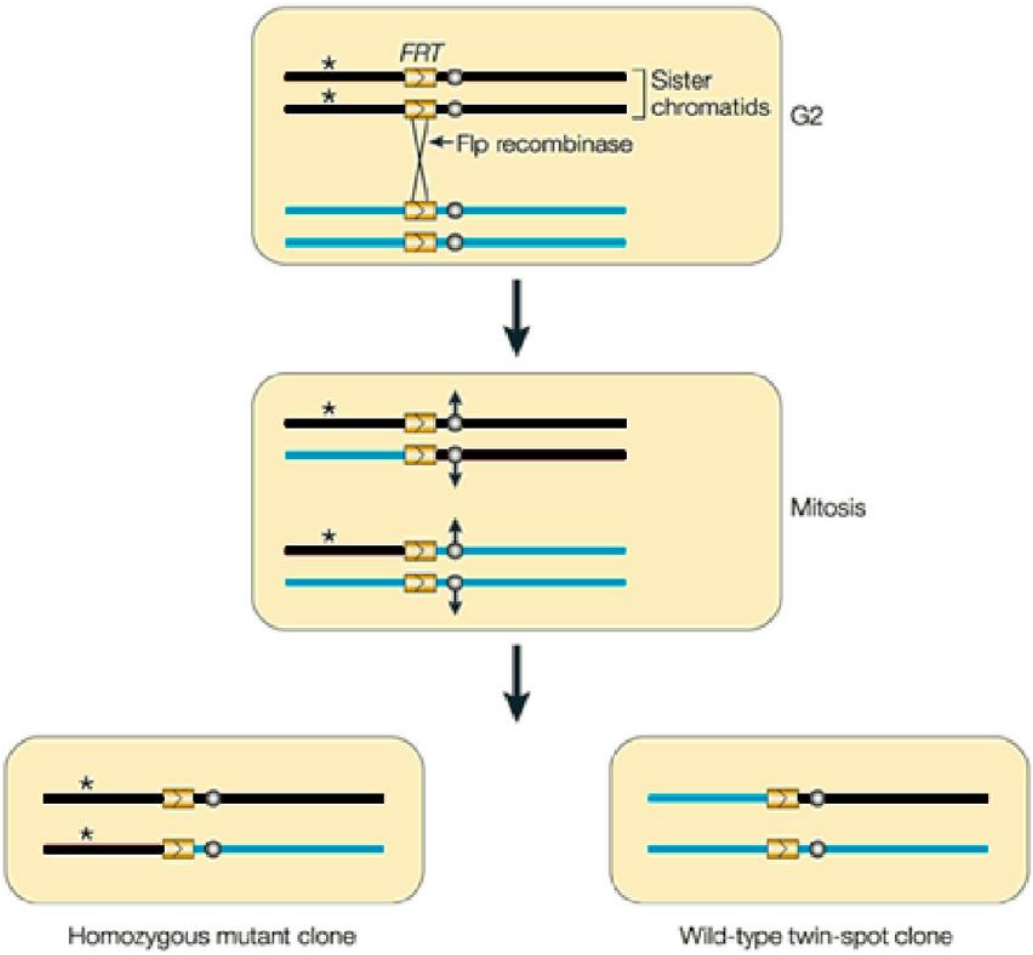

Figure 6. 1.6. FLP/FRT system in *Drosophila*.

The FLP/ FRT system is designed to allow mosaic analysis of a particular mutation (represented diagrammatically in the figure above by the star symbol). The upper panel represents pair of homologous chromosomes, with sister chromatids present for both, in a single cell in phase G2 of the cell cycle. The cell is heterozygous for the mutation and therefore phenotypically normal. FRT sequences are present on both chromatids of both chromosomes at identical positions. Recombination event between FRT sequences of the homologous pair is induced by the enzyme Flp recombinase, expressed from another chromosome in the cell. This causes the two chromatids containing the mutation to be attached to different centromeres (middle panel), and during segregation of each chromosome pair to the daughter cells, one cell receives two sister chromatids bearing the mutation, while the other receives two copies of the wild type of sister chromatids (lower panel). At completion of mitosis, a mosaic pattern has been generated, with one cell homozygous for the mutation and the other wild type. Reproduced from (Beckingham et al., 2005).

1.4. Using *Drosophila* to study tumours and the TME

Thanks to *Drosophila*'s genetic tractability, genetically-defined tumours can be induced in specific epithelial tissues in developing *Drosophila,* such as the eye-antennal imaginal discs of larvae (Singh et al., 2012). Fluorescently labelled tumour cells can then be monitored over time to determine effects on cancer hallmarks such as uncontrolled growth and dissemination. We are using two models, both of which utilise oncogenic Ras (Ras^{Val12}) to drive benign tumour formation.

Ras belongs to a superfamily of small intracellular GTPase enzymes, which convert guanosine triphosphate (GTP) hydrolysis to guanosine diphosphate (GDP) and are involved in transducing external signals to the interior of cells. There are multiple *Ras* isoforms in humans including *H-Ras, K-Ras and N-Ras*. They are implicated in oncogenic transformation when constitutively activated by mutation (reviewed by Prior et al., 2012). Within this family, the R-Ras subfamily proteins, which could also promote oncogenic transformation (Trabalzini and Retta, 2014). For example, point mutation in *RAS* proteins includes substitute single amino acid at codon 12, 13 or 61 of Ras p21 protein and it results in aberrant *RAS* proteins that disrupt GTPase activity and lead to tumour formation (Lowy and Willumsen, 1993). Codon 12 mutation, identified to be the most predominant mutation and it substitutes 12 Glycine residue by Valin residue. *Drosophila's Ras* has a conserved function as human and interestingly it has conserved glycine at position 12 as well which when substituted by Valine cause benign tumour formation (Shira Neuman-Silberberg et al., 1984).

By combining *Ras^{Val12}* with other genetic changes it is possible to drive tumour invasion and spreading to more distant sites (Singh et al., 2012). One such model utilises overexpression of the human metastasis-inducing protein *S100A4*, a member of the S100-calcium-binding protein family (Du et al., 2018). *S100A4* overexpression enables invasion, cell migration and extracellular matrix remodelling in flies and humans alike (Ismail et al., 2017). The advantage of this *Ras^{Val12}/S100A4* model is that *S100A4* overexpression has been reported to be clinically related to different types of metastatic malignancies in humans including, breast pancreas, oral mucosa, prostate, bladder, colorectum, oesophagus, stomach, thyroid glands and lung carcinomas (Fei et al., 2017). Therefore, mechanisms of tumour development uncovered through studies of *Ras^{Val12}/S100A4* tumours in the fly may have direct translational relevance in humans.

Other, extensively studied *Drosophila* cancer models utilise *Ras^{Va12}* combined with disruption of a cell polarity gene such as *scribbled* (*scrib*), *discs-large* (*dlg*) or *lethal (Pharma) giant larvae* (*lgl*) (Singh et al., 2012). *Scrib* encodes a leucine-rich-repeat protein with four PDZ domains (Bilder and Perrimon, 2003); *Dlg* is a membrane-associated guanylate kinase (MAGK) that contains three PDZ domains (Brumby and Richardson, 2003b). The PDZ has major role in *scrib* and *dlg* localization and their functions is highly dependent on their localization to septate (basolateral) junctions of the epithelial cell membrane, which is analogous to the tight junction of vertebrate cells (**Figure 7.1.7.**) (Brumby and Richardson, 2003b).

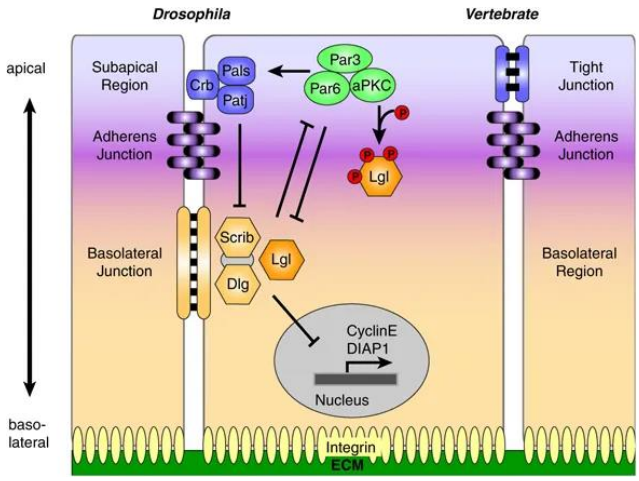

Figure 7.1.7. *Drosophila* cell polarity components.

The apicobasal polarity of epithelial cells in *Drosophila* is maintained by three polarity modules including the Crumbs complex, composed of (Crumbs (Crb), protein associated with caenorhabditis elegans Lin-7 protein (Pals1) and Pals1-associated TJ protein (Patj)), the partitioning defective (Par) complex, composed of (*Par3, Par6* and kinase-dead *Drosophila* atypical (*aPKC)*) and the Scribble polarity module, composed of (*Dlg, Scrib* and *Lgl*). Crumbs and Par complexes are localized to the subapical region and the Scribble polarity complex is localized to the basolateral region. The Scribble polarity module regulates cell proliferation by inhibiting the expression of Cyclin E (*cycE*), a key cell cycle regulator. It also promotes apoptosis by blocking the expression of *DIAP1* the apoptosis inhibitor. Figure and information are reproduced from (Humbert et al., 2008).

Scrib, *dlg* and *lgl* are dominant suppressors of *cycE* and mutation in these suppressors leads to elevation in *CycE* level and thereby increased the number of S-phase cells, providing a more direct link between these tumour suppressors and the cell cycle machinery (Brumby and Richardson, 2003a, Brumby et al., 2004). Indeed *Scrib, Dlg*, and *Lgl* play a rate-limiting role in regulating cell cycle progression, as well as in apicobasal cell polarity.

Furthermore, when mutated, these tumour suppressor genes lead to c-Jun N-terminal Kinase (JNK, encoded by *Basket* in *Drosophila*) activation and cell death (La Marca and Richardson, 2020). However, in the context of the strong survival signals provided by Ras^{Val12}, activated JNK promotes invasiveness of the cancer cells by upregulating the expression of Matrix Metallopeptidase 1

(MMP1), a basement membrane protein (**Figure 8.1.8.**) (Tapon, 2003, Wu et al., 2017)

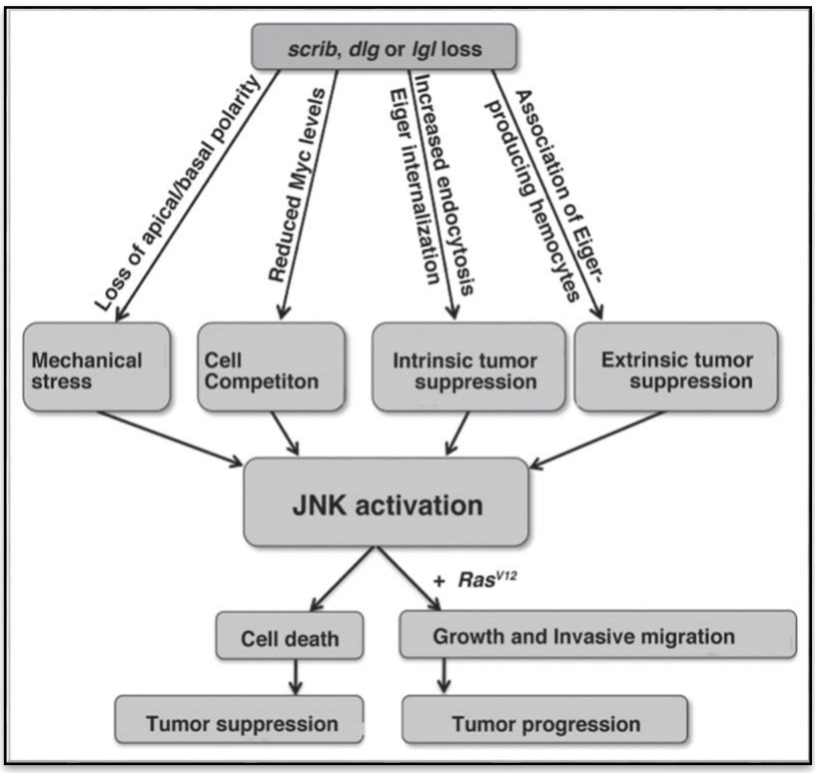

Figure 8.1.8.: Pathways upstream and downstream of *JNK* activation when cell polarity genes are mutated.

Mutant cells for *scrib, dlg or lgl* become resistant to JNK-meditated death upon *Ras*^{Val12} expression. Figure reproduced from (Vidal, 2010).

1.4.1. *Drosophila* JNK and Hippo pathways

JNK signaling, in *Drosophila,* has conserved dual functions, including anti- and pro-tumor activities in imaginal epithelia **(Figure 9.1.9.)**, indicating the advantage of using the *Drosophila* imaginal disc model to understand the basic principle of tumour signaling pathways (Enomoto and Igaki, 2011, Enomoto et al., 2015). The *Hippo (Hpo*) pathway components include *Yorkie (Yki*), a transcriptional coactivator which promotes tissue growth, and two kinases: *Hpo*

and *Warts (Wts*). Loss of function of these kinases results in *Yki* activation and overgrowth of imaginal discs (Halder and Johnson, 2011).

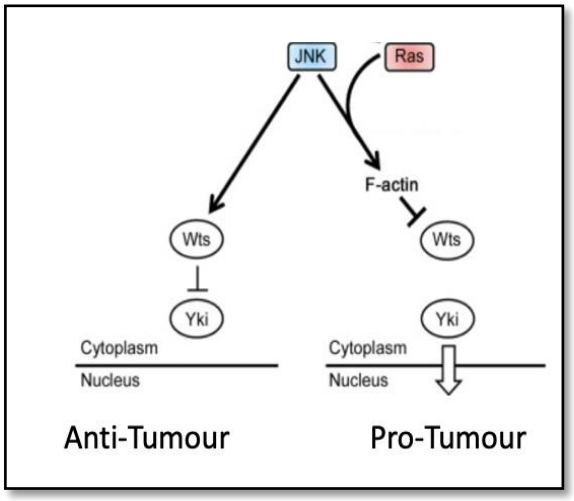

Figure 9.1.9.: JNK dual activities.

JNK signaling suppresses growth of tissue by inhibition the activity of (*Yki*) through Wts elevated activity. However, in the presence of hyperactive *Ras*, *JNK* signaling promotes tissue growth by activating *Yki* through F-actin accumulation which then inactivate the Hippo pathway in cells. Figure reproduced from (Enomoto et al., 2015).

Drosophila has a developmental checkpoint to delay the onset of metamorphosis in cases of tissue damage. This is to ensure that cells have time for any wound healing. Flies respond similarly when harbouring cancer cells and mount an innate immune response via the recruitment of macrophage-like haemocyte cells in an attempt to combat tissue overgrowth. Haemocyte-derived *Eiger* (*Drosophila* orthologue of mammalian Tumor Necrosis Factor, TNF) signaling serves to eliminate *scrib* or *dlg* deficient cells from epithelia (La Marca and Richardson, 2020). However, this host response is diverted to enhance tumour progression in the presence of Ras^{Val12}oncogene (Vidal, 2010), illustrating the importance of the TME in tumour dissemination.

The overgrowth and invasion in the *Ras/Dlg* cancer model is accelerated by an inflammation response. The inflammation response includes the recruitment of haemocytes, which secrete *Eiger* (TNF), thereby activating *JNK* signaling. In the case of loss of *scrib* or *dlg* cells, activated *JNK* functions to remove the aberrant

cells. However, in the presence of (RAS^{Val12}), *JNK* function is diverted into pro-oncogenic function to promote tumor overgrowth and invasion by triggering the expression of multiple signalling pathways (Doggett et al., 2015).

1.4.2. *Differences between Drosophila* and human metabolism

Organs involved in coordinating metabolism in *Drosophila* perform similar physiological and cellular functions as in humans **Figure10.1.10.** (Warr et al., 2018).

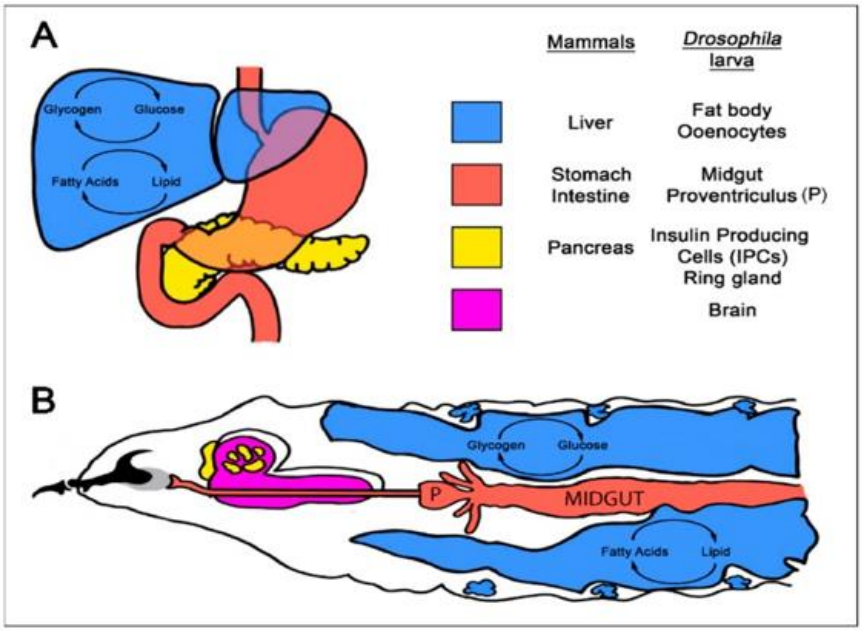

Figure 10.1.10.: Schematic representation of conserved metabolic organs in human and *Drosophila*.

A) Human metabolic organs: liver, gut, and pancreas. (B) *Drosophila* larval tissues performing conserved metabolic functions. In *Drosophila*, fat body and coenocyte cells (in blue) perform similar functions to the human liver and adipose tissue, storing and releasing energy. Glucagon and insulin secreted by pancreas in human while in *Drosophila*, the ring gland and insulin producing cells located anterior to the larvae brain (labelled yellow) secrete glucagon, insulin and insulin-like protiens (ILPs) to maintain glucose levels. Figure and information were reproduced from (Warr et al., 2018).

In flies, metabolic homeostasis is regulated by *adipokinetic hormone (AKH)* and the *ILPs*. A glucagon-like molecule and sugar intake trigger *Ilps* productions in the brain to convert glycogen to glucose. *AKH* is released in response to low levels of circulating sugar (Warr et al., 2018).

1.4.3. Macrophage metabolism in *Drosophila*

Drosophila immune response relies only on innate immunity to fight against tumours and pathogens. There are three types of hemocytes to initiate an innate immune response through cytokine release and phagocytosis: Plasmatocytes have a phagocytic function and are equivalent to mammalian macrophages; crystal cells which involved in melanin deposition in wounds and around foreign objects; and, lamellocytes, appears when parasitoid wasps infest the larvae (Carl-Johan et al., 2004). Hemocytes originate from the lymph glands and the embryonic hemocytesn (King and Akai, 1982). Haemocytes role in *Drosophila* tumours include blood and lymphatic vessel formation, invasion, as well as immune suppression (Carl-Johan et al., 2004).

Similar to human cancer cell metabolism described above, oxygen availability and cytokines have an impact on macrophage metabolism. Activated macrophages (pro-inflammatory M1 macrophages) change their metabolism to elevate anaerobic glycolysis, protein and fatty acid synthesis and pentose phosphate pathway activation. Whereas macrophages activated by M2-inducing stimuli such as *interleukin (IL) - 4 (IL-4)*, *IL-10*, and *IL-13* rely on enhanced oxidative phosphorylation, with no changes in glycolysis (reviwed by Ciana and Eva, 2018).

Interestingly, the metabolic characteristics of macrophages in the context of cancer have not been heavily investigated, so it remains unknown if a change in TME metabolism could influence their phenotype and thus affect cancer growth and metastasis.

In experiments described in this thesis Haemocytes were labelled with GFP. We used *Hemese-GAL4* (he-GAL4) driver which is expressed in all classes of circulating larval hemocytes and in the hematopoietic organs (Carl-Johan et al., 2004). However, it is important to note that *he-GAL4*, unlike the endogenous *Hemese* gene, it is expressed in only ~80% of the circulating hemocytes and it shows little expression in the lymph glands, affecting at most a few scattered cells (Carl-Johan et al., 2004).

1.5. Goals of this thesis

We plan to study tumour development in the context of its host microenvironment in a small, harmless fruit fly, *Drosophila* melanogaster, which has been intensively studied for almost a century because of its many attractive features for genetic research.

We plan to capitalise on these genetic features and publicly available genome-wide resources, such as transgenic RNAi libraries (Dietzl et al., 2007, Zirin et al., 2020). Aside from being more selective (not-withstanding potential off-target effects), dsRNAs for genes of interest can be targeted to specific cell types within the tumour microenvironment, enabling us to elucidate the potential interplay between metabolic changes within the tumour and surrounding host cells.

Our hope is that by obtaining a comprehensive list of the candidates that normally limit the spread of cancer cells in an intact animal, we can help develop ways to boost resistance of healthy tissues, preventing them from being overrun by cancer

cells whilst other treatments acting on the cancer have time to have their effect, leading to better overall patient survival.

1.6. Aims

1. Develop genetic tools to facilitate interrogation of the tumour microenvironment in two genetically defined *Drosophila* cancer models.
2. Interrogate the requirement for metabolic regulators in the TME for tumour growth and dissemination in these models.
3. Correlate our findings from metabolic regulators in flies with findings from cancer patient samples.
4. Interrogate the role of non-essential amino acids (NEAAs) in tumour growth and invasion.
5. Interrogate the mechanism by which glycine depletion reduces tumour progression in the Ras/Dlg cancer model.

Chapter 2: Methods

In this chapter the Methods used to generate *Drosophila* cancer models and the related fly-work including immunohistostaining and imaging are presented. This is followed by a description of methodologies used for immunostaining and analysing human tissue samples.

2.1. *Manipulating the TME in genetically-defined tumour models*

To make the necessary strains for to study tumour and tumour microenvironment we used the scheme below, **Figure 11.2.1**.

Capitalising on *Gal4/UAS* system and LexA/ *Lexop*, dual expression systems (Hales et al.), we have been able to generate spatially-restricted, genetically-defined tumours, whilst simultaneously, but independently, manipulating the surrounding healthy tissue **(Figure 11.2.1).** This allows us to interrogate the involvement of haemocytes and other components of the TME in tumour development and progression.

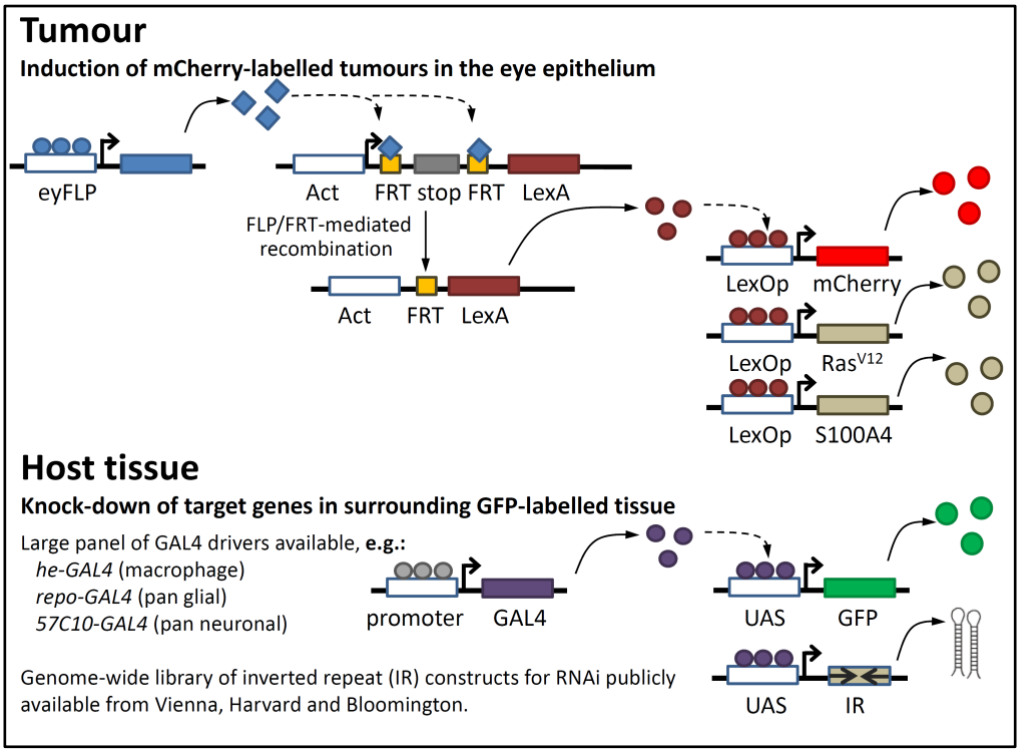

Figure 11.2.1: Overview of approach used for induction of tumours alongside independent manipulation of the host tissue.

For carrying out site-specific recombination, we use a yeast site-specific recombinase (eyFLP), an eye specific *eyeless* promoter that drive transcription of (LexA). The *eyFLP* recombinase recognize FRT sites on tow arm of homologous chromosome and catalyse "flip-out" a linker sequence, resulting in inducement of mitotic recombination between the two arms and removal of the GAL80 repressor. *eyFLP* here repositions the *LexA* gene under the constitutive actin promoter and with the removal of *Gal80*, expression of *LexAop- RasV12*, human *S100A4* and mCherry is activated, resulting in *mCherry*-labelled tumours in the eye disc epithelium. By contrast, cells with *Gal80* repressor, inhibits the upregulation of LexAop- Ras^{V12}, human *S100A4* and *mCherry*. Thus, clones of cells will be homozygous mutant for genes such as (*S100A4* with gain of function mutation, *scrib* and *dlg* with loss of function mutation), which with the activated oncogene *Ras* results in invasive and metastatic behaviour. *GAL4-UAS* system is used for manipulating healthy tissue, in which the tissue-specific expression of the *GAL4* transcription factor triggers expression of UAS element. The expression of UAS-GFP, with or without inverted repeat transgenes for RNAi knockdown (*UAS-IR*), is activated by the same way as *Lexop* and result in GFP-labelled host tissue including haemocytes, glial, neural, fat body and *UAS-IR* expression in specific tissues. reviewed by (Hales et al., 2015, Venken and Bellen, 2005, Matthews et al., 2005, Raymond and Tian, 2003). Figure contributed by Daimark Bennett.

*LexAop was referred to as Lo in the following genetic schemes.

2.2. Generating genetic strains:

Our ultimate goal is to induce tumours whilst simultaneously manipulating host tissue with the RNAi lines of gene of interest. Broadly speaking, three sets of genetic schemes A, B and C, as presented in the figures below, were used to create the necessary tools to achieve this goal. **Table 2.1** summarises the components that were needed to be brought together in a single strain, illustrating the complexity of the task.

Table 1.1. Elements required for both cancer models with their respective purpose

Cancer models	Genetic manipulation of host tissue	Tumour formation in the eye
Ras^{Va12}/Dlg	*promoter-GAL4*, tissue-specific driver UAS-GFP, labelling of host tissue conditional on GAL4 *UAS-RNAi*, knockdown of host tissue	*ey (3.5) FLP*, site specific recombination in the eye *Act>LexA*, overexpression of LexA conditional on flippase activity *dlg^{GFP}*, Lo-*mCherry-GFPi*, knockdown of *dlg* and labelling with RFP *Lo-Ras^{Val12}*, overexpression of oncogenic Ras
Ras^{Val12}/S100A4	*promoter-GAL4*, tissue-specific driver UAS-GFP, labelling of host tissue conditional on GAL4 *UAS-RNAi*, knockdown of host tissue	*ey (3.5) FLP*, site specific recombination in the eye *Lo-Ras^{V12}-S100A4-mCherry*, overexpression of human S100A4, and labelling with RFP (S100A4-mCh fusion protein); weak expression of oncogenic Ras *Lo-Ras^{Val12}*, overexpression of oncogenic Ras

A)- Generating RNAi "tester" strains for use in fly cancer models:

Transgenic UAS RNAi lines (inserted on the 2nd or 3rd chromosome) for metabolic regulatory genes (Table 1.2) were combined with *ey (3.5)FLP, dlg^{GFP}, UAS-td-GFP* (on the X) for use with the *Ras^{Val12}/Dlg* model (**Figure 12.2.2.).** Similar crosses were performed with *ey(3.5)FLP, UAS-td-GFP* for use with the *Ras^{Val12}/S100A4* model. In the case of the *Ras^{Val12}/Dlg* model, the *ey(3.5)FLP, dlg^{GFP}, UAS-td-GFP* strain contains a GFP-trap insertion in the *dlg* locus which

is expressed as a *dlg-GFP* fusion gene. This weak *dlg* allele is then targeted by RNAi using dsRNAs against the GFP coding sequence present in the expressed mRNA. Direct targeting of *dlg* with *LexA*-driven RNAi is not effective. In the *S100A4* model, the *dlg* allele is not required.

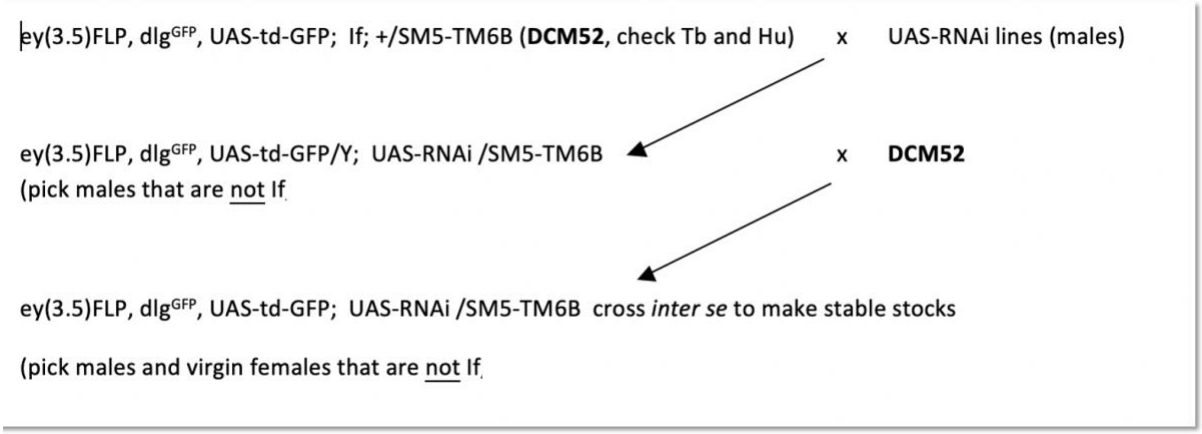

Figure 12.2.2. Combining RNAi lines with *Drosophila* cancer model *Dlg^{GFPi}*

ey(3.5)FLP constructs of both cancer models carries balancers or/and markers that can be traced thanks to their visible phenotypes. For example, *If* results in rough eyes, so after crossing that construct with UAS-RNAi lines we can determine which flies in the progeny have both UAS-RNAi lines and *ey (3.5)FLP, dlg^{GFP}, UAS-td-GFP* by excluding flies that have rough eyes and pick only male flies. We crossed them back to *ey(3.5)FLP* constructs then we made a stable stock for both cancer models. Similar genetic schemes were performed on the other cancer model ***Ras^{Val12}/S100A4.***

B)- Recombining drivers to label host tissues with GFP

To utilise the tester strains above, they need to be crossed to strains carrying the other elements required for the dual expression system to work: *Lexop Ras^{V12}*, *Lexop-GFP^{IR}-mCherry (or Lexop-S100A4-mCherry)*, *Act>y>LexA* (which responds to FLP-mediated recombination) and the desired GAL4 line for tissue-specific expression of the RNAi. To help generate stable strains in which all these elements have been introduced it was necessary to first make a set of recombinant chromosomes in which the GAL4 lines were introduced onto the same chromosome as the *Act>y>LexA* transgene (**Figure 13.2.3.).**

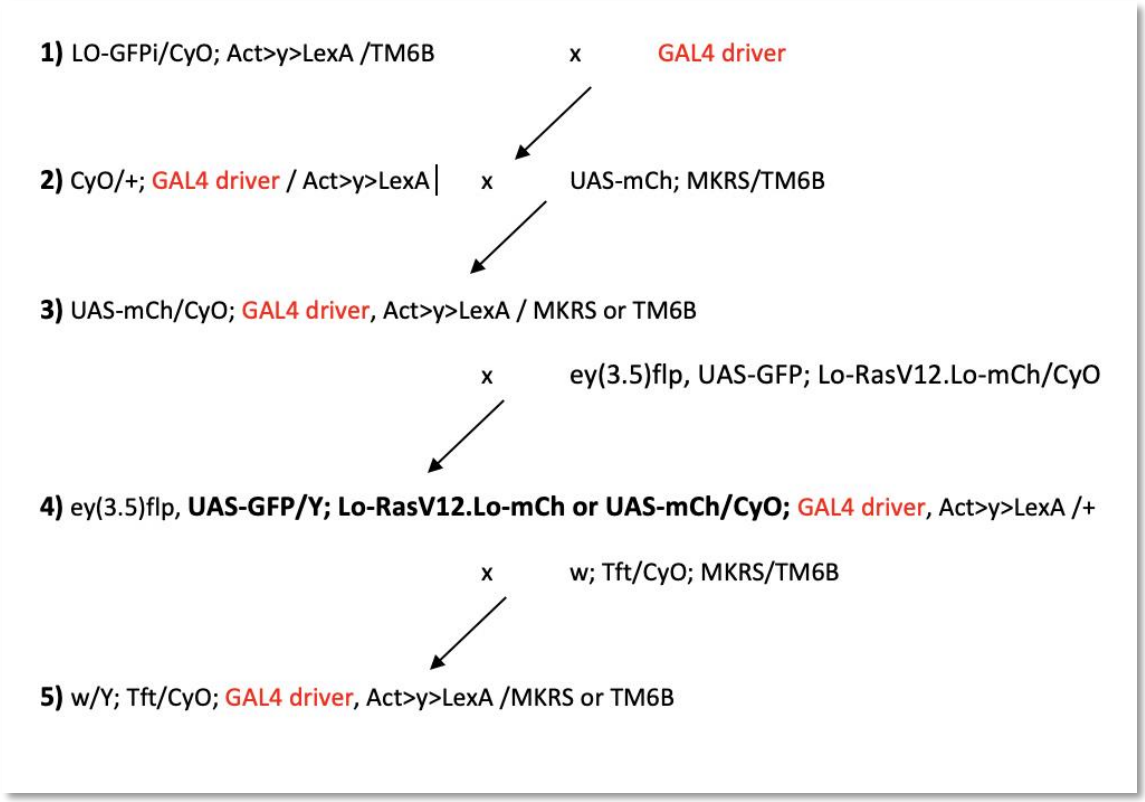

Figure 13. 2.3. Genetic scheme to recombine CAL4 drivers with Act-LexA.

1)To carry out Act-LexA recombinants we combined GAL4 drivers *(he-Gal4, lpp-Gal4, nSyb-Gal4, repo-Gal4)* with a fly possessing *Act>y>LexA (Lo-GFPi/CyO; Act>y>LexA /TM6B).* **2)** we combined that new strain *(CyO/+; GAL4 driver/ Act>y>LexA*) with a construct that has *UAS-mCherry (UAS-mCh; MKRS/TM6B). **3)** GAL4* drivers construct now have both elements *Act-LexA* and *UAS-mCherry*, however, to allow the expression of GAL4 driver and label host tissue with GFP, and express *UAS-Cherry* we crossed the strain to another one that has eyFLP and *LexAop-mCherry (ey(3.5)flp, UAS-GFP; Lo-RasV12.Lo-mCh/CyO)* and then we picked flies that have recombinant GAL4 driver and Act>y>LexA on the same chromosome on the basis of RFP in the eye and host tissue and GFP fluorescence in the host tissue *(ey(3.5)flp, UAS-GFP/Y; Lo-RasV12.Lo-mCh or UAS-mCh/CyO; GAL4 driver , Act>y>LexA /+*). **4 and 5)** Since only needed the recombinant elements on that construct, we rebalanced the strain using *w; Tft/CyO; MKRS/TM6B, picking UAS-mCh/CyO; A>GAL4, A>lexA/+* flies and crossing them back again to the same strain w*; Tft/CyO; MKRS/TM6B* then picking flies of the following genotype to cross *inter se: Tft/CyO; A>GAL4, Act>y>Lex/MKRS.*

C)- Combining GAL4 drivers with cancer models

Having generated recombinant GAL4 strains, the recombinant chromosomes were then combined with *lex-operator* insertions (**Figure 14. 2.4.).**

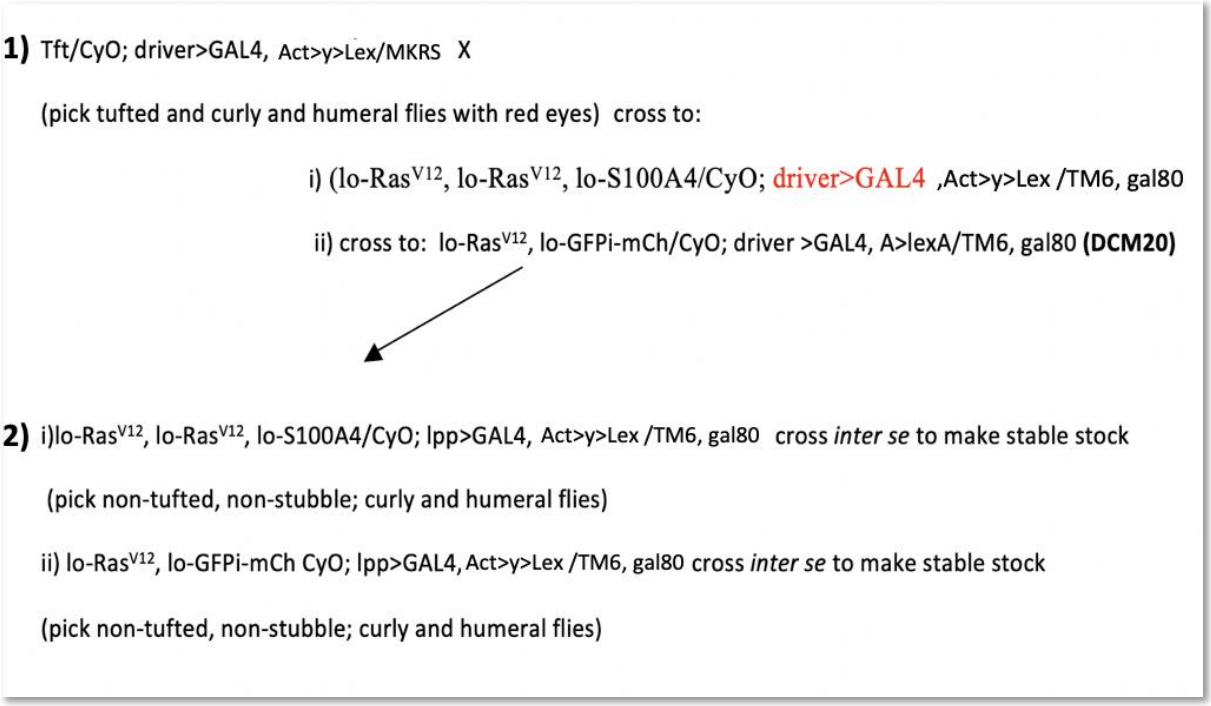

Figure 14.2.4. Combining GAL4 drivers with cancer model.

1) From the previous step in **(B)** theGAL4 drivers labelled with GFP in this strain (*Tft/CyO; GAL4 driver, Act>y>Lex /MKRS*) were combined with our cancer models *Ras^{Val12}/Dlg* and *Ras^{Val12}/S100A4* by crossing to i) and ii), respectively. **2)** From theses crosses we picked flies of this genotype *lo-Ras^{V12}, lo-GFPi-mCh CyO; driver>GAL4, Act>y>Lex/ TM6, gal80 and lo-Ras^{V12}, lo-Ras^{V12}, lo-S100A4/CyO; driver>GAL4, Act>y>Lex/ TM6, gal80* and we made a stable stock for these crosses by crossing males and females carrying the same genotype.

From these crosses we have generated flies that have *GAL4* drivers and *lo-Ras^{V12}, lo-GFPi-mCh or lo-Ras^{V12}, lo-Ras^{V12}, lo-S100A4-mCh*, balanced in the presence of *tub-GAL80 (GAL80* driven constitutively with the tubulin promoter) which blocks *GAL4 and LexA*-mediated expression. Using the approach described above (B and C), we have strains that should make it possible to label and genetically manipulate other cells in TME including haemocytes (*Drosophila* macrophages) with *hemese-GAL4*, glial cells with *repo-GAL4*, fat body (adipocytes) with *Lpp-GAL4* (Musselman and Kuehnlein, 2018), neural cells with *nSyb-GAL4* and the tumour itself with *Act>CD2>GAL4* (**Table 3.)**. Images of

the resulted tumours flies and the only those used for this thesis are shown below, **Figure 15.2.5 and Figure 16. 2.6.**

Table 2. Genotypes of different cell types in TME.

Cell Types	***Ras^{Val12}/S100A4* cancer model Genotype**	***Ras^{Val12}/Dlg* cancer model Genotype**
Glia cell: transgenic transposon is (Repo-Gal4)	*Lo-S100A4,Lo-Ras$^{X2;}$* ***repo-GAL4,*** */SM6-TM6B, tub-GAL80*	*lo-Ras^{V12}, lo-GFPi-mCh CyO;* ***Repo>GAL4****, Act>y>Lex / SM6-TM6B, tub-GAL80*
Neural cells: transgenic transposon is (nSyb-Gal4)	*Lo-S100A4,Lo-Ras$^{X2;}$* ***nSyb-GAL4,*** */SM6-TM6B, tub-GAL80*	*lo-Ras^{V12}, lo-GFPi-mCh CyO;* ***nSyb****>GAL4, Act>y>Lex / TM6,gal80*
Fat body: transgenic transposon is (Lpp-Gal4)	*Lo-S100A4,Lo-Ras$^{X2;}$* ***lpp-GAL4,*** */SM6-TM6B, tub-GAL80*	*lo-Ras^{V12}, lo-GFPi-mCh CyO;* ***lpp>GAL4****, Act>y>Lex / TM6,gal80*
Haemocytes also known as macrophage like-haemocytes: transgenic transposon is (he-Gal4)	*(hs-hid) Y/; Lo-S100A4,Lo-Ras$^{X2;}$* ***he-GAL4****,A>lexA/SM6-TM6B, tub-GAL80*	*Lo-Ras^{v12},Lo-mCh-GFPi;****he-G4****, Act>y>Lex / SM6-TM6B, tub-GAL80*
Act>CD2>GAL4: **ubiquitous driver, but only expressed after Flip-out of a FRT-flanked linker (>CD2>). Together with ey(3.5)FLP, will drive expression in the eye imaginal disc.**	*(hs-hid) Y/; Lo-S100A4,Lo-Ras$^{X2;}$* ***Act>CD2>GAL4****, A>lexA/SM6-TM6B, tub-GAL80*	*Lo-Ras^{v12},Lo-mCh-GFPi;* ***Act>CD2>GAL4****, Act>y>Lex/SM6-TM6B, tub-GAL80*

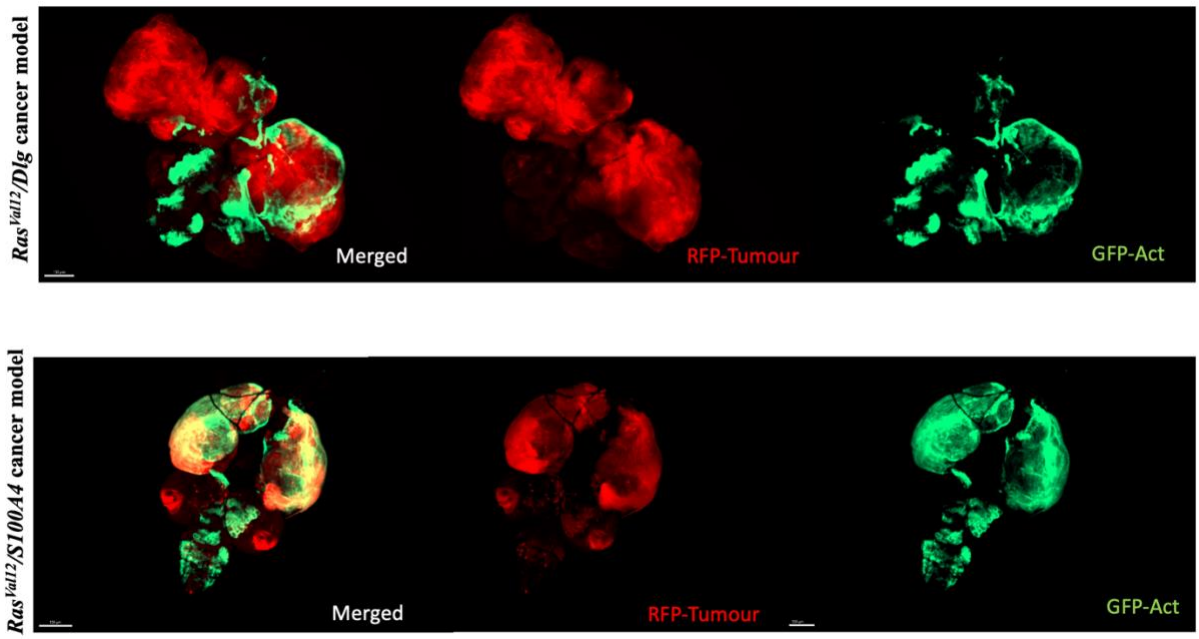

Figure 15.2.5. *Ras^{Va12}/Dlg* and *Ras^{Va12}/S100A4* cancer models with Act-Gal4 driving GFP expression in tumours cells.

***Ras^{va12}/Dlg* cancer model genotype** : *eyFLP, UAS-GfP;lo-Ras^{V12}, lo-GFPi-mCh CyO; Act-GAL4,A>lexA /SM6-TM6B, tub-GAL80.* ***Ras^{va12}/S00A4* cancer model genotype**: *eyFLP, UAS-GfP; Lo-S100A4,Lo-Ras^{X2} ; Act-GAL4,A>lexA /SM6-TM6B, tub-GAL80. In Ras^{Va12}/S100A4* cancer model, *Act-Gal4* is expressed in the same place as tumour cells (RFP-labelled). However, in *Ras^{Va12}/Dlg* animals the GFP expression in eye discs is suppressed. This is to be expected because knockdown of the *dlg* in the *ey(3.5)FLP, dlg^{GFP}, UAS-td-GFP* strain makes use of GFP-RNAi to knockdown expression of the *dlg-GFP* fusion gene. Targeting of the weak *dlg* allele, which expresses mRNA containing the GFP coding sequence, therefore also functions to knockdown the GFP marker expressed in the same cells. 100µm scale is shown.

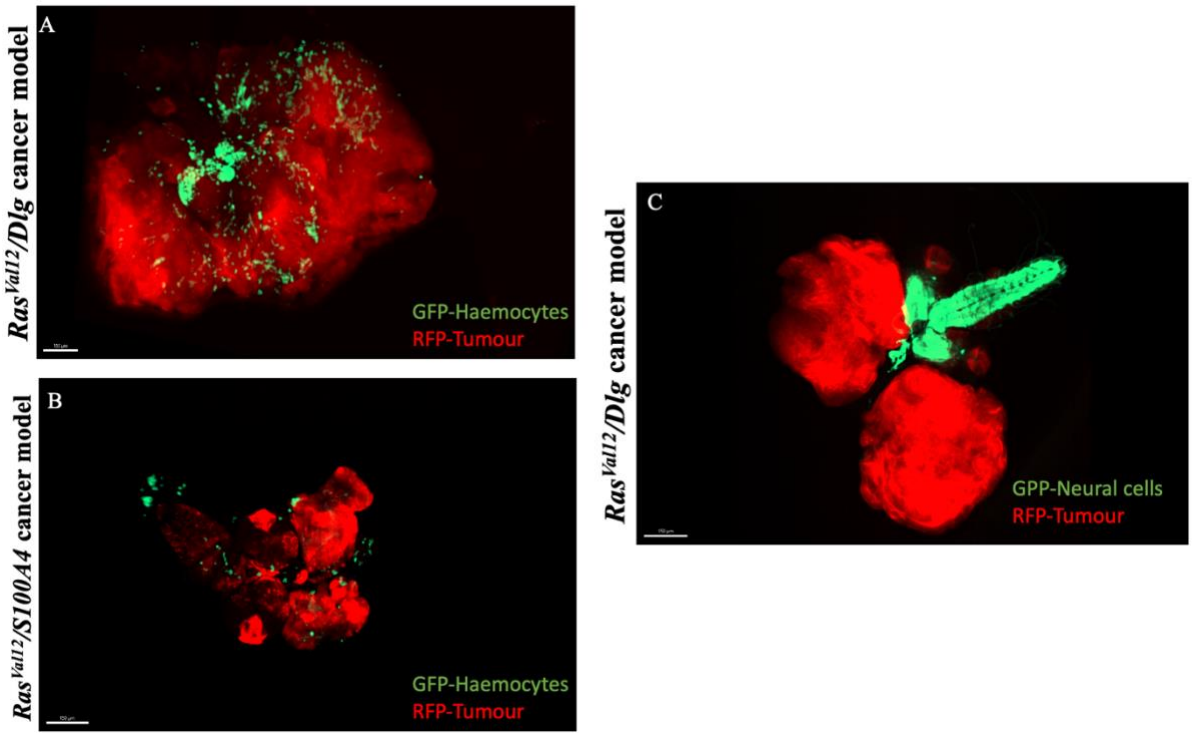

Figure 16.2.6.Representive images of *Ras^{Va12}/Dlg* and *Ras^{Va12}/S100A4* cancer models .

Ras^{Va12}/Dlg and *Ras^{Val2}/S100A4* cancer models with he-Gal4 driving GFP expression (green) in haemocytes and nSyb-Gal4 driving expression in neural cells of *Ras^{Val2}/Dlg* cancer models. Tumour cells are labelled with mCherry (red). Scale bar, 100µm. **A) Genotype :** *eyFLP, UAS-GfP;lo-Ras^{V12}, lo-GFPi-mCh CyO; he-GAL4,A>lexA /SM6-TM6B, tub-GAL80.* B) **Genotypes:** *eyFLP, UAS-GfP; Lo-S100A4,Lo-Ras^{X2} ; he-GAL4,A>lexA/ SM6-TM6B, tub-GAL80.* ***C*) Genotype**: *eyFLP, UAS-GfP; Lo-S100A4,Lo-Ras^{X2} ; nSyb>GAL4,A>lexA /SM6-TM6B, tub-GAL80.*

2.3. Further improvements to GAL4-containing strains:

Preliminary experiments using the above strains by knocking down metabolic regulators in haemocytes with *he-GAL4* in our *Ras^{Va12}/S100A4* cancer model indicated that it might be difficult to obtain sufficient animals for analysis. To resolve this issue, we replaced separate 2nd and 3rd chromosome balancers (CyO and TM6) with a co-joined balancer containing *tub-GAL80* (to block *GAL4/LexA*-mediated expression): this reduces the number of possible genotypes in the offspring, increasing the frequency of the desired type. The new strains also have a “virginiser” to help facilitate collection of virgin females for test crosses. This

is comprised of a transgenic insertion of the proapoptotic gene *head involution defective* (Yao et al.), under the control of the heat shock promoter on the Y chromosome (*Y*, [*hs-hid*]), which when exposed to heat, kills males (Ung et al., 2019).

Previous strain: *Lo-Ras^{X2}, lo-S100A4/CyO; he-GAL4, Act>y>Lex / TM6, gal80*

New strain: *Y, [hs-hid]/; Lo-Ras^{X2}, Lo-S100A4 ; he-GAL4, Act>y>lexA/SM6-TM6B, tub-GAL80.*

2.4. Studying JNK activity in *Drosophila*

The *JNK* reporter *puc-lacZ* was used to visualise *JNK* activity; expression of puc-lacZ is induced after *JNK* activation. Puckered (*puc*) gene, regulates signaling through the *JNK* pathway by encoding *JNK* phosphatase (Martin-Blanco et al., 1998). The puc gene was identified through a *P(lacZ)* insertional mutation that highlights the most dorsal epidermal cells as they finish proliferation and causes defects during dorsal closure (Ring and Martinez-Arias 1993).

To make strains that combine *JNK* reporter *puc-lacZ* into our model by the method described in **Figure 17.2.7.**

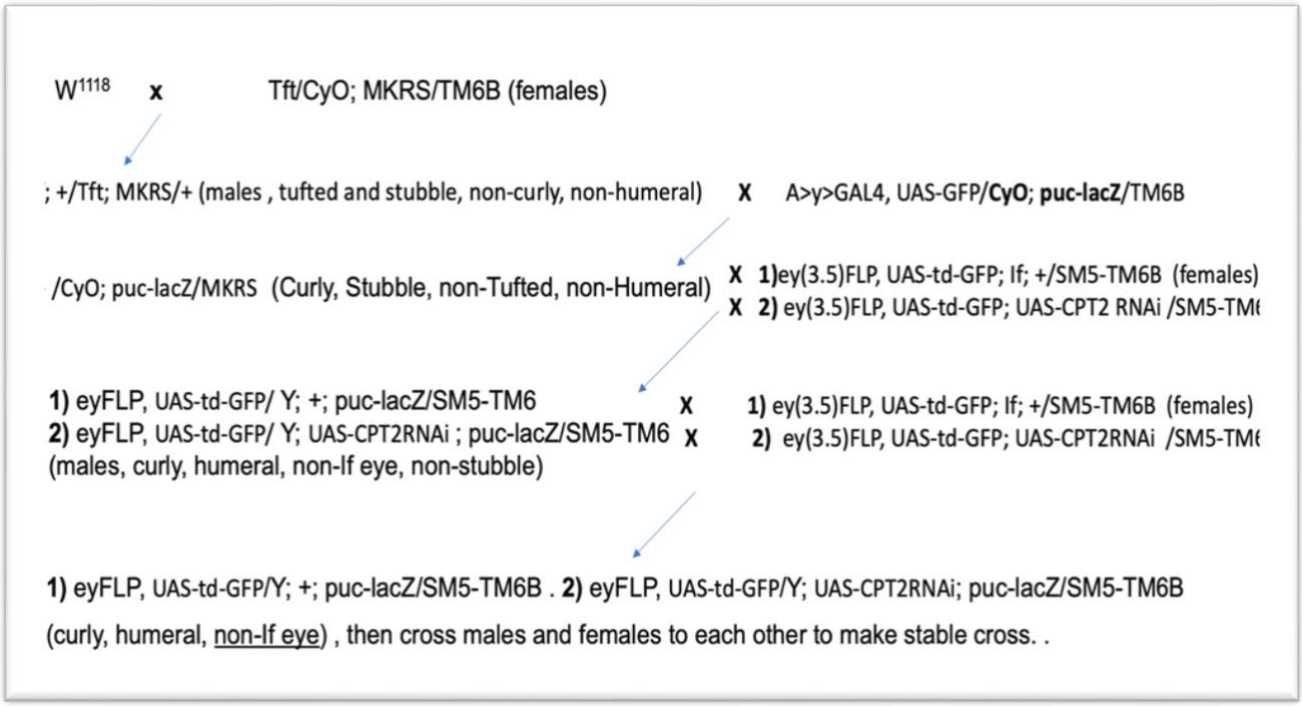

Figure 17.2.7. Making puc-lacZ strains.

The phenotype and genotype of each of the strains are described in the figure for our control model. **1)** represents steps of combining our tumour control with *puc-lacZ and* **2)** for combining CPT2 RNAi line (62455) with *puc-lacZ.*

Males of these strains **(**Figure 17.2.7. Making puc-lacZ strains.**)** were then crossed to females from our cancer model which described previously (haemocytes model) and (cancer model) Error! Reference source not found.

Table 3. Genotypes of flies expressing Puc-lacZ.

Model	**Genotype**
A).Haemocyte control	*eyFLP, UAS-GfP; Lo-S100A4,Lo-Ras^{X2} ; he-GAL4,A>lexA: puc-lacZ*
B). Haemocytes , CPT2 RNAi line	*eyFLP, UAS-GfP; Lo-S100A4,Lo-Ras^{X2} ; he-GAL4,A>lexA / UAS-CPT2 RNAi; puc-lacZ*
C). Cancer model control	*eyFLP, UAS-GfP; Lo-S100A4,Lo-Ras^{X2} ; Act>CD2>GAL4, A>lexA: puc-lacZ*
D). Cancer model and CPT2 RNAi line	*eyFLP, UAS-GfP; Lo-S100A4,Lo-Ras^{X2} ; Act>CD2>GAL4, A>lexA/ UAS-CPT2 RNAi; puc-lacZ*

The progeny are females dissected at 7 days old and they are expressing *β-galactosidase (β-gal)* which could be visualised by staining with *β-ga*l antibody.

2.5. Fly maintenance and immunofluorescent staining method

Flies were raised and crossed at 25°C according to standard procedures. Brain and eyes disc of third instar larvae were dissected, where the eye tissues we are driving our tumours are expressed and the brain where the tumour disseminated. Age of dissected Larvae were staged for each experiment (7 days for *S100A4/Ras^{va12}* cancer model, 10 days for *Dlg/Ras^{va12v}* and 11 days for *Scrib/Ras^{va12}* cancer models) . The age controlled by allowing flies to mate for 24hrs and moving them to another vail. Brains and eyes were dissected in 1x PBS (Phosphate buffer saline) and fixed with 3.7% paraformaldehyde in PBS. Then washed with PBST (1X PBS, 0.2% Tween 20) 3 times for 15 minutes. Brains and eye imaginal discs were then blocked with PBTB (1X PBS, 0.2% Tween 20, 5% fetal bovine serum) for 1 hour at room temperature. Then were stained with primary antibodies in PBTB at 4°C overnight. The following primary antibodies were used for immunostaining (**Table 5).**

Table 4. List of primary antibodies used in our studies and their concentrations.

Antibody	**Concentration**
MMP1 mix of 3A6B4, 3B6D12 and 5H7B11 mix (1:1:1), Thermo Fisher.	1:10
β-**gal (**A-11132), Thermo Fisher.	1:500
Caspase 3 (9H19L2), Thermo Fisher.	1:100
CPT2 (SN06-70), Thermo Fisher.	1:50
HCS LipidTOX™ (H34477), Thermo Fisher.	1:500

The primary antibodies were washed with PBST 4 times for 15 mins and then brains and eyes were incubated with Alexafluor-conjugated secondary antibodies (1:500, Life technologies) in PBTB (in dark place) at room temperature. Then washed 3 times with PBST for 15 minutes then 1x PBS for 15 minutes. Samples were mounted with Hardset ™ Antifaded Mounting Medium (VECTASHIELD) and prepared for imaging.

2.6. Confocal Fluorescence Microscopy

Samples were imaged using the high-speed confocal platform Dragonfly (Andor an Oxford instrument company). Images were acquired with a 10x/25x objectives using the Fusion acquisition software. Samples were excited with three laser lines including 488 nm, 561 nm and 633 nm wavelengths. Images were processed and analysed by using the Imaris software version 5 and 3. We created a surface to calculate the tumour volume and spots for the calculation of the number of haemocytes or any stained cells. The data were analysed without pre-processing. The same creation parameters were consistently used.

Different spots sizes were used depending on (objective and cancer model used). Then, from that surface and spots statistical information (volume, spots number and intensity) were extracted and plotted using Prism 8 (GraphPad) application. Some Figures were made using FigureApp in OMERO (Burel et al., 2015) and final assembly in Adobe Photoshop. Some figures were too large to be uploaded/ opened in OMERO, therefore PowerPoint was used to make these figures.

2.7. Human related work Method

2.7.1. Ethical approvement:

Ethical approval was obtained from Northwest - Greater Manchester South Research Ethics Committee, REC reference number: 21/NW/0076.
Date of favourable ethical opinion: 30th March 2021
Sponsor: Liverpool University Hospitals NHS Foundation Trust.
Note: Work done on CPT2 marker was funded by Amirah's sponsor, Saudi Arabia cultural burau .

2.7.2. Immunohistochemistry:

Immunohistochemistry staining was performed by using formalin fixed paraffin embedded tissue was cut into 10-micron thick sections. We stained breast tissue sections for each patient with (1:50, CPT2 (SN06-70) antibody, Thermo Fisher) via using bond machine. Then scanned the slides with the digital scanner. Qu path then was used to identify Ductal carcinoma *in situ* (DCIS) and measure CPT2 intensity in these DCIS. The statistical data then were used to measure the survival ratio for each group.

2.7.3. Sample type:

Cohort 1 are patients from both Merseyside and the surrounding regions who presented in the era before breast screening when the diagnosis of DCIS was rare. The value of this cohort is that pharmacological treatments that patients tend to get these days were not available, so this is an opportunity to study the pure biology.

Cohort2 is a screening population where everybody screened and we are picking who have DCIS detected but there is also many receiving treatment. Unfortunately, this cohort was not ready to be done during my PhD, therefore the data presented are only from cohort 1, which was for 32 patients.

2.7.4. Statistical analysis:

Data were split based on quartiles, DCIS degree and median to know what level define the threshold to allow us to see an effect. Kaplan-Meier survival analysis was then performed using StatsDirect software.

We also performed ANOVA to find the differences in *CPT-2* expression between the pure DCIS, recurrence, and progression groups.

2.7.5. Kaplan-Meier survival analysis

The **Kaplan–Meier survival analysis** (Rich et al., 2010) was used to measure the length of time for patients with DCIS to have DCIS recurrence or to have DCIS progression into invasion depending on *CPT2* level.

Each patient was characterized by three variables:

1) The time to the outcome (recurrence or progression)

2) Their status at the end of their serial time (DCIS recurrence, DCIS progression into invasion, no recurrence or progression); this information was available because the cohort was retrospective and clinical follow up data was available.

3) The *CPT2* expression level.

To determine the best cut-off by which to define high and low *CPT-2* expression, *CPT-2* levels were quantified using Qu Path, and the analysis was performed using cut offs at the first, second and third quartiles to divide the groups into low and high *CPT-2* expressors (Rich et al., 2010). The best cut off was found to be the first quartile. Values represent the Hazard Ratio and p-value.

2.8. Bioinformatics: Online Method

Assessment of the predictive and prognostic effect of *CPT2* expression on breast cancer at mRNA level was assessed using the KM plotter tool (www.kmplotter.com).

The prognostic effect at protein level was assessed for different cancer types using the Human Protein Atlas (www.proteinatlas.org). Mutations in *CPT2* were assessed using the cBioPortal tool, and the prognostic effect of *CPT2* mutation assessed using G2O tools (www.g-2-o.com). The effect of *CPT2* on treatment response was assessed using the ROC Plotter tool (www.rocplotter.com). Network association analysis was performed using the Oncomine platform (www.oncomine.org). Summary of immune interaction with CPT2 depending on cancer stages and mutation burden was performed using KM plotter. The immune interaction of *CPT-2* with immune cell infiltration, immunomodulator genes and chemokines was assessed using the TISIDB platform (cis.hku.hk/TISIDB/). The gene concepts for the cancer hallmarks, including immune regulation, were based on the NanoString concept (Eastel et al., 2019).

The gene concepts for the epigenetic pathways were obtained from the EpiFactor website (https://epifactors.autosome.ru) (Medvedeva et al., 2015).

2.9. Chemically-defined media method:

Chemically-defined media lacking individual non-essential amino acids were made according to Piper *et al.* (2014), **(Table 6)**. Each treatment was referred to according to amino-acid that was missing: glutamate, glutamine (Gln), glycine (Gly), serine (Ser), alanine (Ala), aspartate (Asp), asparagine (Asn), proline (Pro), tyrosine (Tyr), cysteine (Cys), food lack of all NEAAs (NEAAs). We used for our control a chemically-defined media that has all NEAAs and EAAs (All).
We also used the regular yeast-based fly food (AGS media) to compare it with chemically-defined media. AGS media will be referred to hereafter as normal food (NF) and is composed of (10g agar, 85g sugar, 60g Maize meal, 20g yeast, 1L water, 25ml Nipagin and 3ml Propionic acid).

Table 5. Composition of chemically-defined food

Name of stock (concentration)	Components	For stock per Liter	For 200 ml food
Added Before Autoclaving			
Gelling agent	Agar powder		4 g
Low-solubility amino acids	isoleucine		0.36g
	leucine		0.24g
	tyrosine		0.85g
Sugar	sucrose		3.42g
Cholesterol stock (66.67x)	cholesterol	20g	3ml
Acetate Buffer (10X)	Glacial Acetic Acid	30 ml	20 ml
	KH2PO4	30 g	
	NaHCO3	10 g	
Metal Ions (1000X)	CaCl2.6H2O	250 g	0.20 ml
	MgSO4	250 g	0.20 ml
	CuSo4.5H2O	2.5 g	0.20 ml
	FeSO4.7H2O	25 g	0.20 ml
	MnCl2.4H2O	1 g	0.20 ml
	ZnSO4.7H2O	25 g	0.20 ml
Added After Autoclaving			
Nucleic acids and lipid 125X)	Choline Chloride	6.25 g	1.6 ml
	Myo-Inositol	0.63 g	
	Inosine	8.31 g	
	Uridine	7.50 g	
Essential Amino Acids (16.53X)		**For stock per 200 ml**	
	F (L-phenylalanine)	3.03	12.10ml
	H (L-histidine)	2.24	
	K (L-lysine)	5.74	
	M (L-methionine)	1.12	
	R (L-arginine)	4.7	
	T (L-threonine)	4.28	
	V (L-valine)	4.42	
	W (L-tryptophan)	1.45	
No-Essential Amino Acids (16.53X)	A (L-alanine)	5.25	12.10 ml
	D (L-aspartate)	2.78	
	G (glycine)	3.58	

	N (L-asparagine)	2.78	
	P (L-proline)	1.86	
	Q (L-glutamine)	6.02	
	S (L-serine)	2.51	
Sodium Glutamate Stock 66.09 X	Sodium Glutamate	100 g	3.64 ml
Vitamin Solution 47.6X	thiamine	0.067 g	4.20 ml
	riboflavin	0.033 g	
	Nicotinic acid	0.399 g	
	Ca pantothenate	0.516 g	
	pyridoxine	0.083 g	
	biotine	0.007 g	
Folic Acid 1000X	Folic Acid	0.5 g	0.20 ml
Preservatives	Proionic Acid		1.20 ml
	Nipagine		3 ml
Cysteine stock	Cysteine	50 g	1.05 ml

Male flies of genotype *eyFLP; A>y>GAL4, UAS-GFP; FRT82B tubGAL80* were crossed with virgin flies of the genotype *w; UAS-RasV12; FRT82B scrib-/TM6B* and were reared at 25 °C on the chemical defined food. From the progeny of that cross, only female larvae will carry GFP-labelled tumours, with the genotype *eyFLP/+; UAS- RasV12/A>y>GAL4, UAS-GFP; FRT82B tubGAL80/scrib-* mutant.

Brain and eyes disc of GFP-labelled female larvae, aged 12 days, were dissected in 1x PBS and fixed with 3.7% paraformaldehyde in PBS. Samples were stained with primary mouse anti-Mmp1 (1:1:1 mix of 3A6B4, 3B6D12 and 5H7B11 with final dilution 1:10) and secondary anti-mouse AlexaFluor555 antibody (1:500). Then, they were mounted with Hardset Vectasheild mounting medium (Vectorlabs) and prepared for imaging.

2.10. Mass Spectrometry experiment

This instructional video (https://www.youtube.com/watch?v=im78OIBKlPA) demonstrates how to collect hemolymph from third-instar larvae or adult fruit flies. Note : 3-5 third instars was needed to isolate one microliter hemolymph.

2.10.1. Sample Extraction:

A methanol extraction protocol was used to extract samples. 20 µL of liquid from a pooled sample was added to a 2 mL Eppendorf tube. Either 380 µL of -48 °C MeOH or 320 µL of MeOH and 40 µL of standard spike was added to the tube and vortexed for 15 seconds. The tube was centrifuged at 13,300 G for 20 minutes at 4 °C. 200 µL of the supernatant was then transferred to a fresh 2 mL Eppendorf tube and dried in a Savant vacuum centrifuge. The dried samples were stored at -80 °C.

2.10.2. Sample Reconstitution:

To reconstitute the dried samples, 100 µL of cold (4 °C) water was added to a 2 mL tube containing the dried sample. The tube was vortexed for 15 seconds and centrifuged at 13,300 G for 10 minutes at 4 °C. The dissolved sample was then sub-aliquoted to 2 mL amber glass sample vials fitted with fused 300 µL glass inserts.

2.10.3. Sample Analysis:

The samples were analyzed using a LCMS system consisting of a Themo Scientific Vanquish LC and a Thermo Scientific gTSQ Fortis triple quad MS.

The LC method used a Water + 0.1% Formic Acid (A) / Methanol + 0.1% Formic Acid (B) gradient for 15 minutes at a flow rate of 0.4 mL/min. The column used was a Thermo Scientific Hypersil Gold aQ C18 100x2.1 mm 19 µm column at a temperature of 50 °C.

The MS method monitored precursor m/z 481.316 and product ions m/z 371.208, 445.292, and 463.208 corresponding to 20-Hydroxyecdysone. Collision energies were optimized for fragmentation paths and m/z 371 and 445 transitions were used for quantitation and confirmation.

Quantitation was based on an external peak area calibration curve and limited standard addition approaches. Normally, standard addition would be used to determine the amount of the test analyte present in the non-spiked sample, but the sample numbers were too few for this approach. Instead, the data from the external calibration was used, but sample numbers were still too few for statistical significance. The data from the external calibration broadly supported that from the standard addition.

Note: This methodology was contributed by Nigel Gott.

2.11. 20E Feeding experiments:

20-hydroxyecdysone (20E) (Steroids Inc), was dissolved in 100% Ethanol to make 20 E stock with concentration (20mg/ml = 20ug/ul). Then 10ul of 20 E stock were added to every 1ml of molten food and 10ul of just ethanol were added to the food for the control (Di Cara and King-Jones, 2016).

Chapter 3: Metabolic regulatory enzymes studies

3.1. Metabolic regulators interruption in macrophages and in cancer cells:

It is known that TME shapes immune cells metabolism, in particular macrophages, and their functionality is altered accordingly (Geerarts et al., 2017). These changes occur to fulfill cellular needs, such as growth and survival or to carry out specific effector functions, such as production of cytokine and phagocytosis (O'Neill et al., 2016, Erika et al., 2013). This metabolic reprogramming of immune cells is required for both inflammatory and anti-inflammatory responses.

In tumours, immune cells metabolism is known to be regulated by different signals including cytokines, oxygen levels, growth factors and nutriention availability (O'Neill et al., 2016, Erika et al., 2013). Aside from these signals, there are critical pathways in cancer metabolism and targeting these pathways may provide an insight into haemocyte-like macrophage metabolism. We therefore selected genes representative of and critical for many of the key metabolic pathways (**Table 7**). These were selected from a list of metabolic genes that had previously been studies in a screen for genes involved in normal eye development in *Drosophila* (Pletcher et al., 2019).

We utilised the RNAi strains we made, described in Table 9, for a thorough analysis of their effects on tumour development or progression. To reduce the possibility of off-target effects, RNAi lines were selected based on published studies validating their effect or using UP-TORR analysis.

Table 6. Metabolic regulators and metabolic pathways they are involved in.

The additional information was compiled from Flybase (https://flybase.org/).

Gene names and UAS-RNAi	**Pathway**
Carnitine palmitoyltransferase II (CPT-2), UAS-CPT2	Oxidative Phosphorylation
(NADH dehydrogenase (ubiquinone) 49 kDa subunit (ND-49), UAS ND-49	Oxidative Phosphorylation
Carnitine palmitoyltransferase I (CPT-1), (known as withered in Drosophila), UAS-CPT1	Oxidative Phosphorylation
Enolase (Eno), UAS-Eno	Glycolysis and the TCA cycle
CPT synthase (CTPsyn), UAS-CTPsyn	Glutamine metabolism
Mitochondrial pyruvate carrier (Mpc1), UAS-Mpc1	Glycolysis and the TCA cycle
Glutamine synthetase 1 (Gs1), UAS-Gs1	Glutamine metabolism
Glucose-6-phosphate dehydrogenase (G6PDH); known as Zwischenferment (ZW)	Pentose Phosphate Pathway
Phosphatidylinositol glycan anchor biosynthesis class H (PIG-H)	Glycosylphosphatidylinositol (GPI)-Anchor Synthesis
Phosphofructokinase (Pfk)	Glycolysis and the TCA cycle

Transgenic RNAi lines for each of these genes were selected with reference to the literature and following off-target searches using UP-TORR (Updated Targets of RNAi Reagents; www.flyrnai.org/up-torr), an online database of *in vivo* RNAi reagents from all the major public collections (Hu et al., 2013). These were then combined with our *Ras*^{Val12}*/S100A4* cancer model by fly breeding to generate a panel of "tester" strains **(**see Methods, Figure 12.2.2. Combining RNAi lines with *Drosophila* cancer model *Dlg*). This resulted in the genotypes described in Table 9.We also looked at the eye phenotype associated with these RNAi lines according to (Pletcher et al., 2019), which reports the phenotypic effect of expressing RNAi lines using the *eyes absent composite enhancer-GAL4* (*eya composite*-GAL4) driver during development of the eye imaginal disc (**Table 8.)**

Table 7. Transgenic RNAi lines and their off-target effect.

	UAS-RNAi, transgenic ID	**Eyes phenotype according to (Pletcher et al., 2019).**
1	*CPT2*, 62455	Rough
2	*ND-49*, 28573	Glossy, rough
3	*CPT1*, 33635	Wild type (WT)
4	*Eno*,64496	Eyes absent
5	*CPT1*, 34066	WT
6	*CTPsyn*, 31924	WT
7	*Mpc1*, 67817	Eyes absent
8	*Gs1*, 40836	Eyes absent
9	*G6PDH*, 50667	Rough
10	*PIG-H*, 67330	WT
11	*Pfk*, 34336	WT
12	*CTPsyn*, 12759	Not tested
13	*CPT1*, 105400	Not tested
14	*CPT1*,4046	Not tested
15	*CPT2*,51900	WT

Transgenic flies carrying short hairpins, generated by the transgenic RNAi Project (TRiP) at Harvard Medical School (Perrimon et al., 2010) , were obtained from the Bloomington fly stock center. While flies carrying long double strand dsRNA hairpins (308, 385, 292 bp, lines 12-14 respectively), were from the Vienna *Drosophila* RNAi Center (VDRC).

Below are the genotypes of flies we generated from combining *UAS-RNAi* lines with our cancer models **(Table 9.).**

Table 8.Metabolic RNAi lines genotypes *Ras^{Val12}/S100A4* cancer models

Ras^{Val12}/S100A4 **cancer model Genotype**
ey(3.5)FLP, UAS-td-GFP; UAS-CPT2^{IR} /SM5-TM6B
ey(3.5)FLP, UAS-td-GFP; UAS-ND-49^{IR} /SM5-TM6B
ey(3.5)FLP, UAS-td-GFP; UAS-CPT1^{IR} /SM5-TM6B
ey(3.5)FLP, UAS-td-GFP; UAS-Eno^{IR}/SM5-TM6B
ey(3.5)FLP, UAS-td-GFP; UAS-CPT1^{IR} /SM5-TM6B
ey(3.5)FLP, UAS-td-GFP; UAS-CTPsyn^{IR} /SM5-TM6B
ey(3.5)FLP, UAS-td-GFP; UAS-MPC1^{IR} /SM5-TM6B
ey(3.5)FLP, UAS-td-GFP; UAS-Gs1^{IR} /SM5-TM6B
ey(3.5)FLP, UAS-td-GFP; UAS-G6PDH /SM5-TM6B
ey(3.5)FLP, UAS-td-GFP; UAS-PIG-H^{IR}/SM5-TM6B
ey(3.5)FLP, UAS-td-GFP; UAS-PfK^{IR} /SM5-TM6B
ey(3.5)FLP, UAS-td-GFP; UAS-CTPsyn^{IR} /SM5-TM6B
ey(3.5)FLP, UAS-td-GFP; UAS-CPT1^{IR} /SM5-TM6B
ey(3.5)FLP, UAS-td-GFP; UAS-CPT1^{IR}/SM5-TM6B

3.2. Determining the effect of metabolic regulators on *Ras^{Va12}/S100A4* tumour growth and progression

We used the strains from the list in (Table 9) to drive the expression of the metabolic regulator's knockdown in haemocytes-like macrophages and in tumour cells. By crossing flies with genotypes in Table 9 with flies with *He-Gal4 (Y/; Lo-S100A4,Lo-Ras$^{X2;}$* ***he-GAL4****,A>lexA/SM6-TM6B, tub-GAL80)* and *Act-Gal4 (Y/; Lo-S100A4,Lo-Ras$^{X2;}$* ***Act>CD2>GAL4****, A>lexA/SM6-TM6B, tub-GAL80).* Resulting in tumorous females' larvae with genotypes *eyFLP, UAS-GfP; Lo-*

S100A4,Lo-Ras^{X2} ; he-GAL4,A>lexA / UAS- RNAi and eyFLP, UAS-GfP; Lo-S100A4,Lo-Ras^{X2} ; Act>CD2>GAL4, A>lexA/ UAS- RNAi. Larvae were then dissected and imaged as prescribed in sections 2.5. Fly maintenance and immunofluorescent staining method 2.6. Confocal Fluorescence Microscopy

3.3. Results

3.3.1. Effect of perturbing metabolic regulators in haemocytes on growth of *Ras^{V12}/S100A4* tumours

Tumorous female larvae with genotypes (*eyFLP, UAS-GfP; Lo-S100A4,Lo-Ras^{X2} ; he-GAL4,A>lexA / UAS- RNAi and eyFLP, UAS-GfP; Lo-S100A4,Lo-Ras^{X2} ; Act>CD2>GAL4, A>lexA/ UAS- RNAi*) were dissected and imaged according to the methods described in sections 2.5 and 2.6. Results are shown below **(Figure 18. 3.1) and (Figure 19. 3.2).**

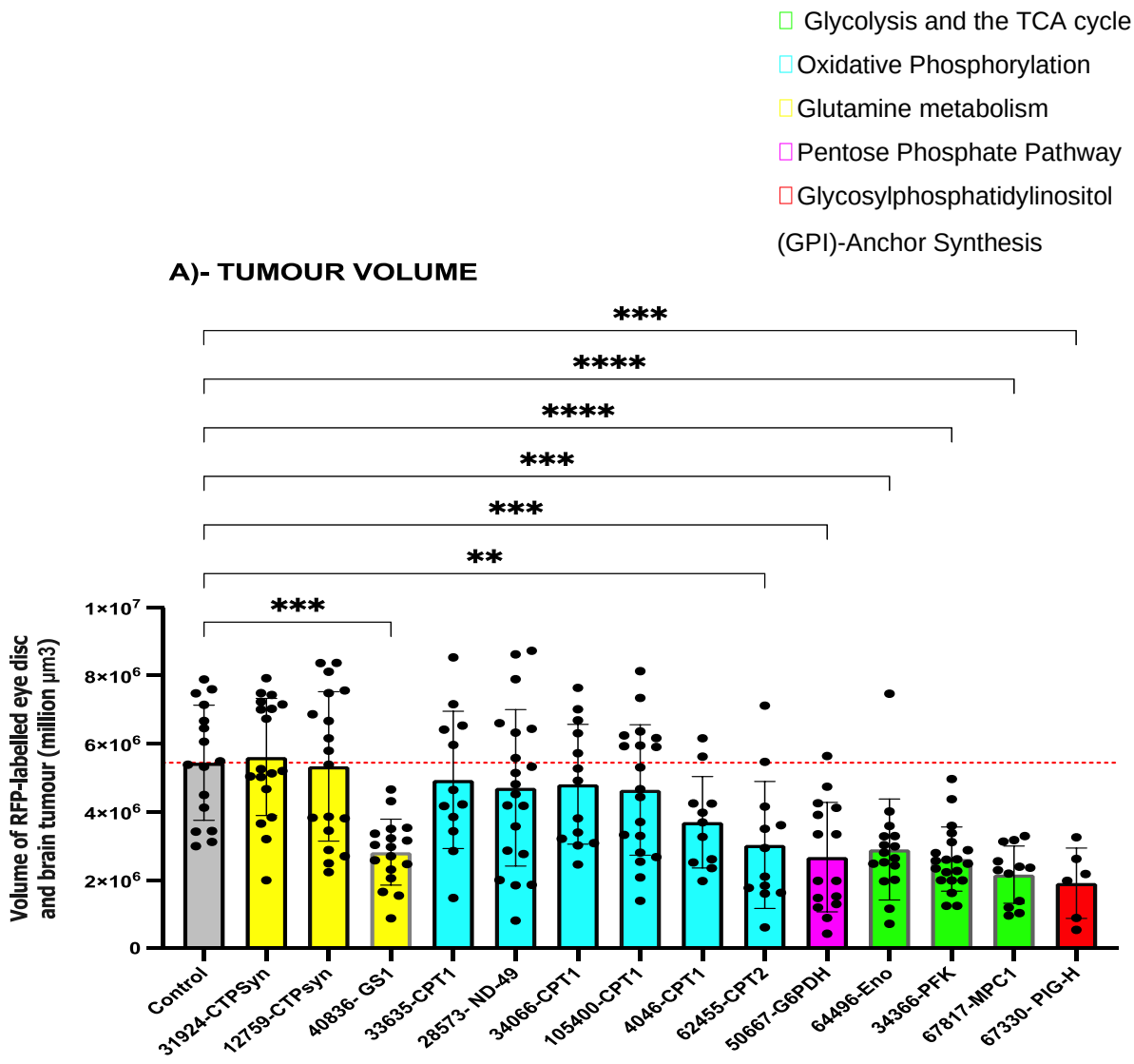
Glycolysis and the TCA cycle
Oxidative Phosphorylation
Glutamine metabolism
Pentose Phosphate Pathway
Glycosylphosphatidylinositol (GPI)-Anchor Synthesis
A)- TUMOUR VOLUME
***
****
****
***
***
**
***
Volume of RFP-labelled eye disc and brain tumour (million µm3)
1×10^7
8×10^6
6×10^6
4×10^6
2×10^6
0
Control
31924-CTPSyn
12759-CTPsyn
40836- GS1
33635-CPT1
28573- ND-49
34066-CPT1
105400-CPT1
4046-CPT1
62455-CPT2
50667-G6PDH
64496-Eno
34366-PFK
67817-MPC1
67330- PIG-H

B)- MMP1 INTENSITY

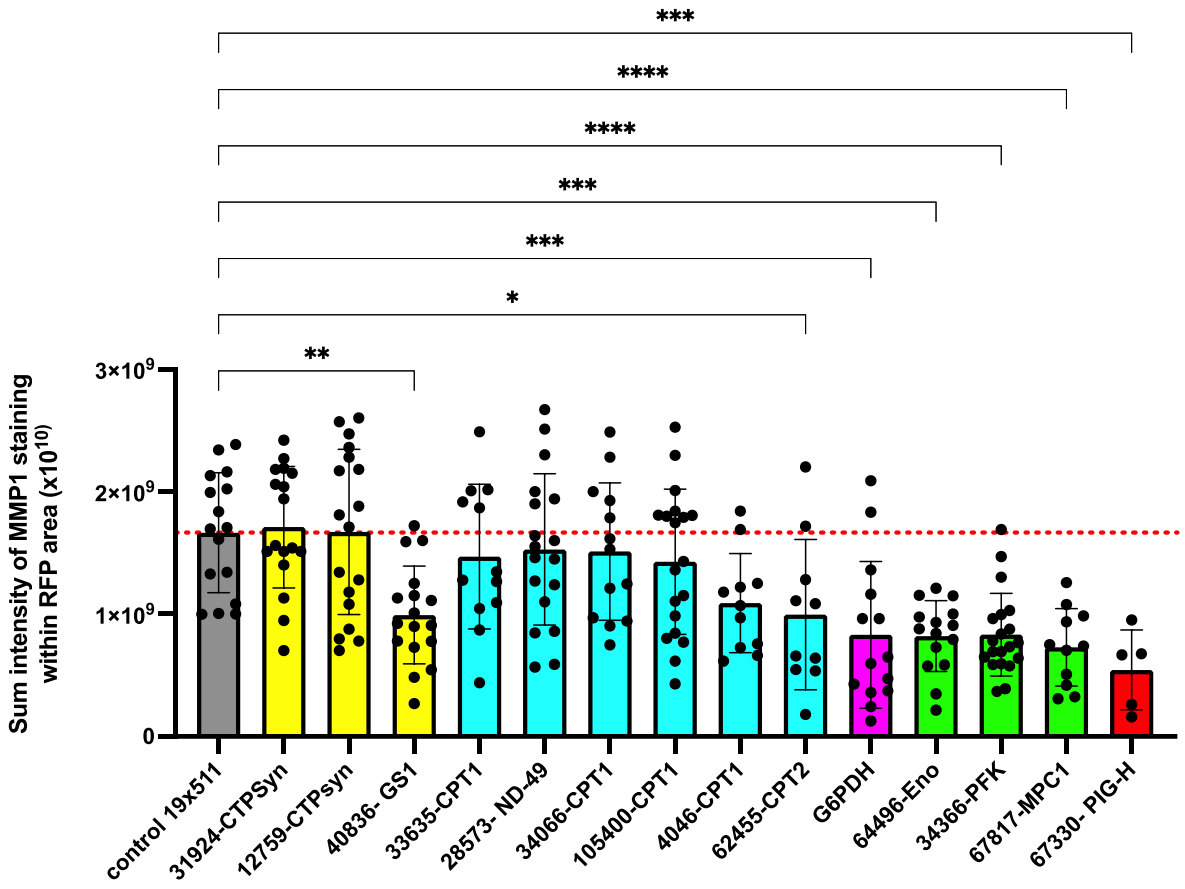

C)- HAEMOCYTES NUMBERS

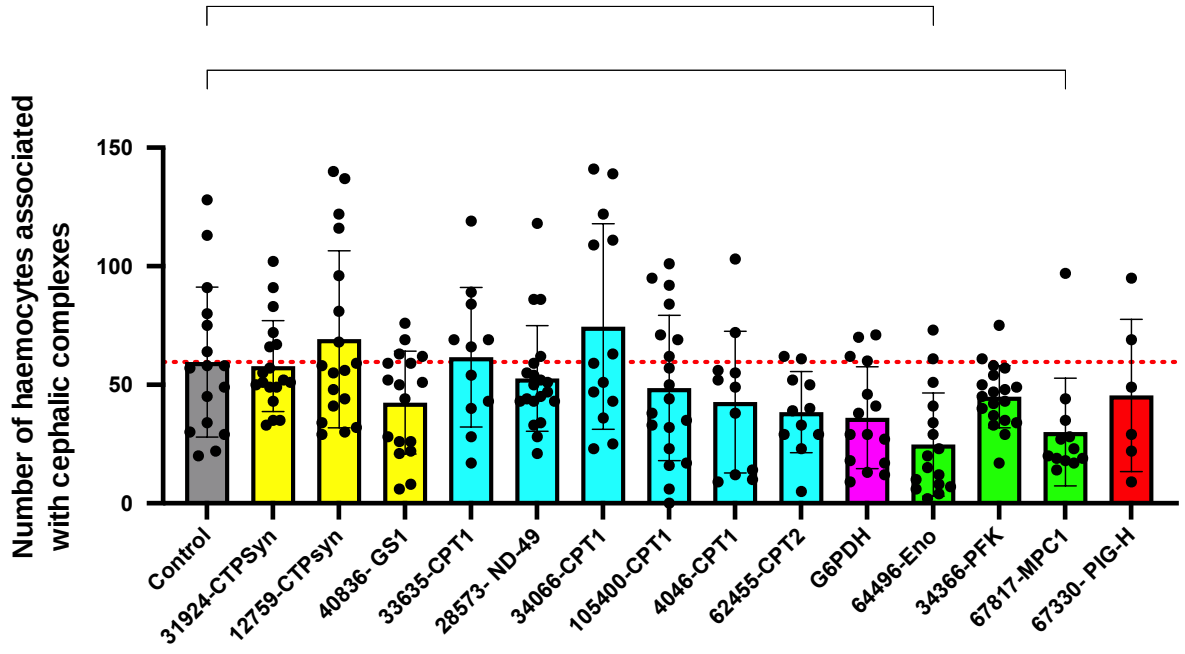

Figure 18.3.1. : Effect of perturbing haemocyte-derived metabolic regulators in animals harbouring *Ras^{V12}/S100A4* tumours.

A) Plot showing RFP-labelled tumour volumes in the presence or absence of metabolic regulators driven RNAi knockdown in haemocytes. Each data point is the volume of RFP-segmented surfaces from images of individual cephalic complexes, including eye discs, optic lobes and brain (n>10). B) Intensity of MMP1 antibody staining derived from images of the same samples as A. C) Quantification of number of GFP-labelled haemocyte associated with the dissected cephalic complexes from the same samples as above .2.6. Confocal Fluorescence Microscopy Haemocytes were labelled with nuclear marker GFP-labelled. Bars, colour coded for different metabolic pathways (see Key, inset panel A), show mean +/-SEM. Dotted red line indicates the mean of the control. Genotype of the control (*eyFLP, UAS-GFP; Lo-S100A4,Lo-Ras^{X2}; **he-GAL4**,A>lexA.* Genotype of the metabolic RNAi lines (*eyFLP, UAS-GFP; Lo-S100A4,Lo-Ras^{X2} ; **he-GAL4**,A>lexA /UAS-metabolic RNAi*). RNAi line number is as indicated, see Table 6. Metabolic regulators and metabolic pathways they are involved in. for more detailsTable 6. Metabolic regulators and metabolic pathways they are involved in. *, P < 0.05; **, P < 0.01; ***, P < 0.001; ****, P < 0.0001 by one-way ANOVA. A) Tumour volume was not significantly affected by RNAi lines for *CPT1*, *ND-49* and *CTPsyn* (one way ANOVA, P =0.999, 0.941 and 0.157, respectively*).* The other RNAi lines, *ENO*, *MPC1*, *PFK*, *G6PDH*, *PIG-H* and *GS1*, reduced the tumour volume significantly (P=0.0003, <0.0001, <0.0001, =0.00011, 0.00025 and 0.00017, respectively). B) MMP1 intensity was significantly reduced by RNAi lines for *CPT2-6245*, *G6PDH*, *Eno*, *Pig-H*, *PFK* and *MPC1*, (One way ANOVA, P=0.01, 0.004, 0.0003, 0.0004, <0.0001 respectively). C) *Eno* and *MPC1* RNAi significantly reduced haemocytes numbers: (One way ANOVA, P= 0.0039 , P= 0.04, respectively). Other lines did not have a significant effect.

Genes involved in oxidative phosphorylation pathway including (*CPT1*, *ND-49 and CTPsyn*) did not show a significant difference in tumour growth when knocked down in haemocytes. The most severe effects were seen with knockdown of genes involved in glycolysis and the TCA cycle including (*ENO*, *MPC1 and PFK*), reducing tumour volume by 0.5, 0.6 and 0.4-fold (one way ANOVA, P=0.0003, P<0.0001 and P<0.0001, respectively). We also saw a significant effect with knockdown of the other genes, *G6PDH*, involved in pentose phosphate pathway, *PIG-H* involved in Glycosyl phosphatidyl inositol (*GPI*)-Anchor Synthesis and *GS1* involved in glutamine synthesis (one way ANOVA, P=0.000109, P=0.000248 and P=0.000170, respectively). The MMP1 intensity and number of haemocytes observed in dissected samples were in

keeping with tumour sizes: when the tumour volume was reduced, the MMP1 expression and the number of haemocytes also decreased (**Figure 18.3.1.).**

3.3.2. Effect of perturbing metabolic regulators in tumour on growth of *Ras^{va12}/S100A4* tumours

Similar to the macrophages and metabolic regulator screening, we performed experiments to interrupt key metabolic pathways in cancer cells using Act (flip out)-Gal4 driver **(Figure 19.3.2.)**. *Act-Gal4* is expressed only in *Drosophila* eyes where we drive our tumour by using *ey (3.5) FLP*, site specific recombination in the eye. More details are escribed in Figure 11.2.1: Overview of approach used for induction of tumours alongside independent manipulation of the host tissue..

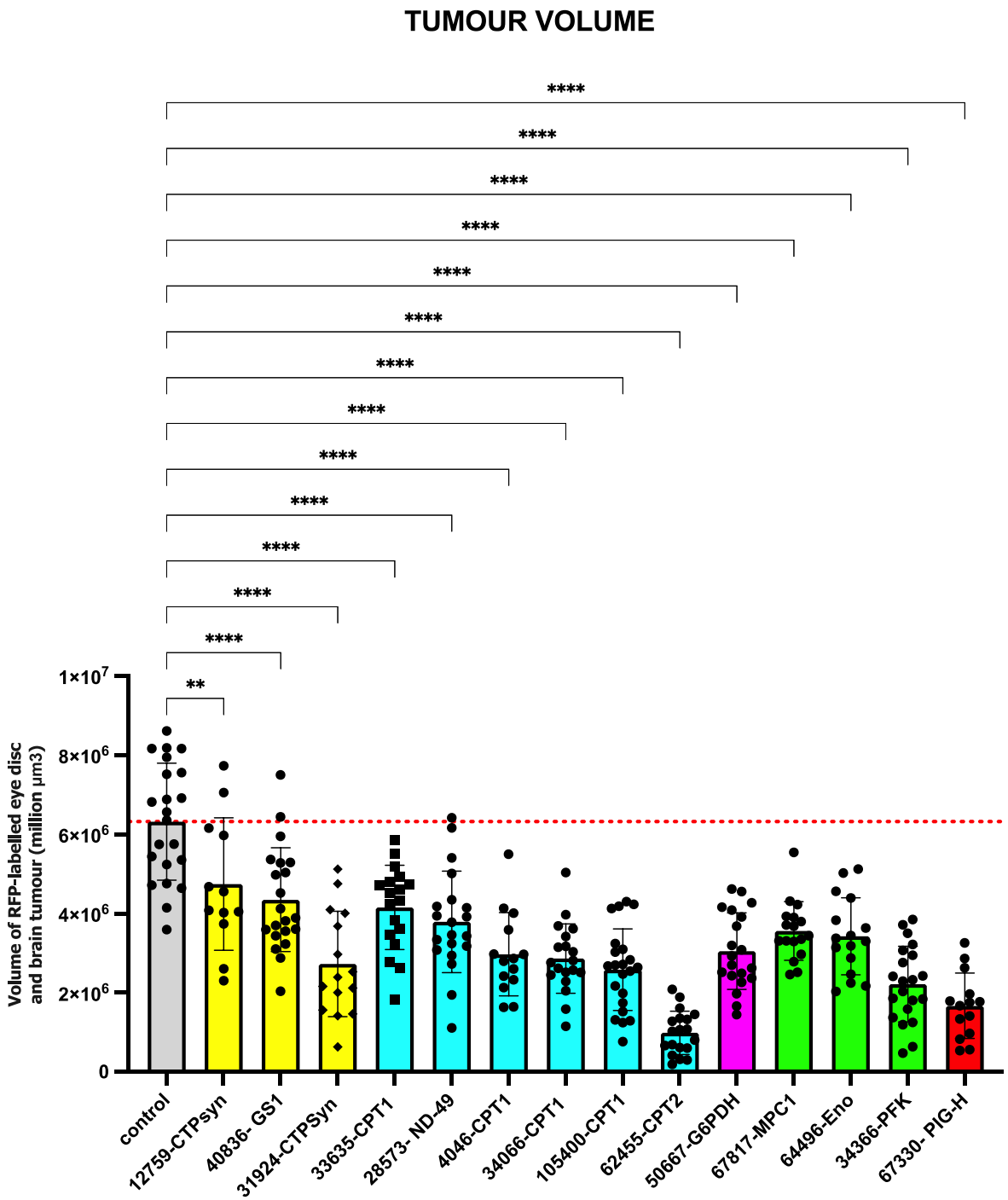

Figure 19.3.2. : Effect of perturbing cancer cells-derived metabolic regulators in animals harbouring *Ras^{V12}/S100A4* tumours.

Plot showing RFP-labelled tumour volumes in the presence or absence of metabolic regulators driven RNAi knockdown in cancer cells. Each data point is the volume of RFP-segmented surfaces from images of individual cephalic complexes, including eye discs, optic lobes and brain (n>10). Bars, colour coded for different metabolic pathways (see Key, inset panel A prescribed in Figure 18.3.1. :). The error bar indicates SEM. Dotted red line indicates the mean of the control. Significant differences in tumour volume compared to the control are indicated

with *. Genotype of the control (*eyFLP, UAS-GfP; Lo-S100A4,Lo-Ras^{X2} ; ; **Act>CD2>GAL4, A>lexA***). Genotype of the others with metabolic RNAi lines (*eyFLP, UAS-GfP; Lo-S100A4,Lo-Ras^{X2} ; **Act>CD2>GAL4, A>lexA**/ UAS-metabolic RNAi*). All metabolic-RNAi lines showed significant differences in tumour volume compared to the control, (One way ANOVA, **P=0,0011, **** P<0,0001).

The effect of RNAi in the tumour looks broadly similar to that of the haemocyte knockdown, except the effect of *CPT2* is notably stronger.

Foremost of the metabolic regulators we tested, *CPT2* strongly affected tumour growth when knocked down in either macrophages or tumour cells. Therefore, we attempted to validate these results by using other RNAi lines. Two additional lines were obtained (VRDC line 51900 and Bloomington Stock Center line 62455), that target non-overlapping regions of the *CPT2* sequence. Both RNAi lines have no OFF-target effects according to UP-Torr (see , Error! Reference source not found.). These showed a similar effect to the VDRC (inverted repeat) (**Figure 20.3.3.**).

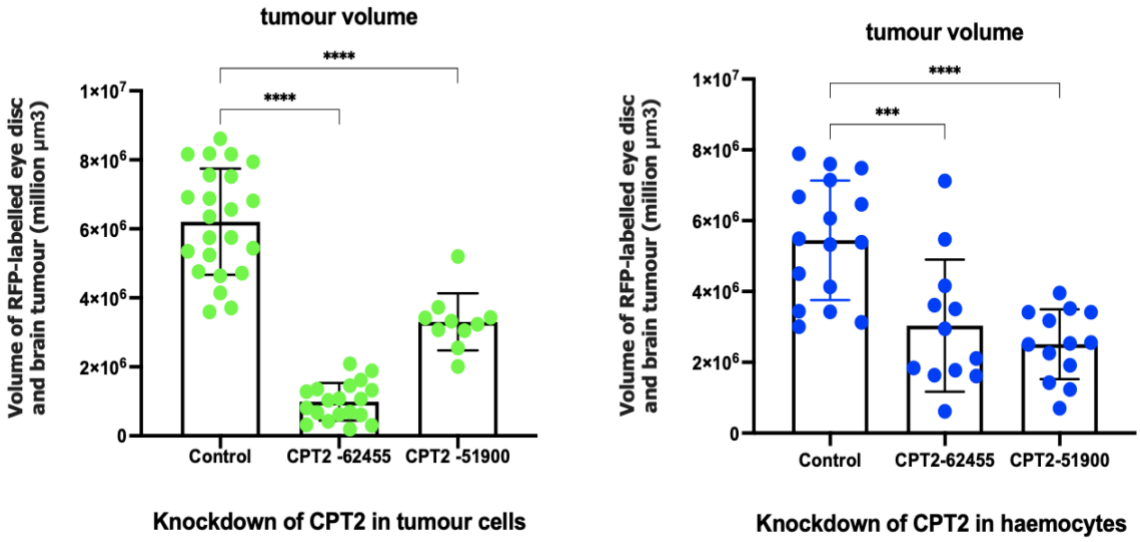

Figure 20.3.3. Volume of RFP-labelled tumours (*Ras^{va12}/S100A4*), in the presence or absence of driven *CPT2* knockdown in cancer cells and haemocytes.

Graphs shows plots of RFP-labelled tumour volumes when *CPT2* RNAi lines (62455 and 51900) were expressed in tumour cells and haemocytes. Each data point is the volume of RFP-segmented surfaces from images of individual cephalic complexes, including eye discs, optic lobes and brain (n>5). Knockdown of *CPT2* in cancer cells genotype (*eyFLP, UAS-GfP; Lo-S100A4,Lo-Ras^{X2} ;* ***Act>CD2>GAL4, A>lexA****/ UAS- CPT2^{IR}*). Knockdown of CPT2 in haemocytes genotype (*eyFLP, UAS-GfP; Lo-S100A4,Lo-Ras^{X2} ;* ***he-GAL4****,A>lexA /UAS- CPT2^{IR}*). Significant differences in tumour volume compared to the control are indicated with *. One way ANOVA test was performed for both tumour and haemocytes cells , **** P<0,0001, *** P=0,0023. The error bar indicates SEM.

We then followed these finding by looking at the JNK activity in both cancer models (haemocytes and tumour) to understand how *CPT2* interacts with JNK to reduce tumour volume. To do this we used *puc-lacZ,* a downstream reporter of JNK activity (see also **Chapter 2**.2.4. Studying JNK activity in *Drosophila*). We also monitored cell death with an anti-cleaved Caspase 3 antibody (Taylor et al., 2017).

3.3.3. CPT2 interactions with JNK activity to suppress tumour growth:

Combining our cancer models with *JNK* reporter resulted in progeny with genotypes described in Table 3. Genotypes of flies expressing Puc-lacZ. These larvae were then dissected and stained with β-gal and cleaved Caspase-3 antibodies to visualize and quantify *JNK* activity and cell death.

First, we looked at the effects of *CPT2* knockdown in tumours. We observed elevated JNK activity and cell death causing tumour suppression (Figure 21. 3.4). In comparison, when we knocked down *CPT2* in haemocytes, there was no significant increase in either JNK activity or cell death (Figure 22.3.5.). This indicates that the mechanism by which haemocyte-derived *CPT2* suppresses tumour growth is different from that of tumour derived-*CPT2.*

Tumorous larvae +/-*CPT2*^{IR} in cancer cells, were dissected and stained with β-gal (A-11132) and Caspase 3 (9H19L2) antibodies to visualize the JNK activity and cell death, respectively. Stained cells were then quantified as described in section 2.6. Confocal Fluorescence Microscopy

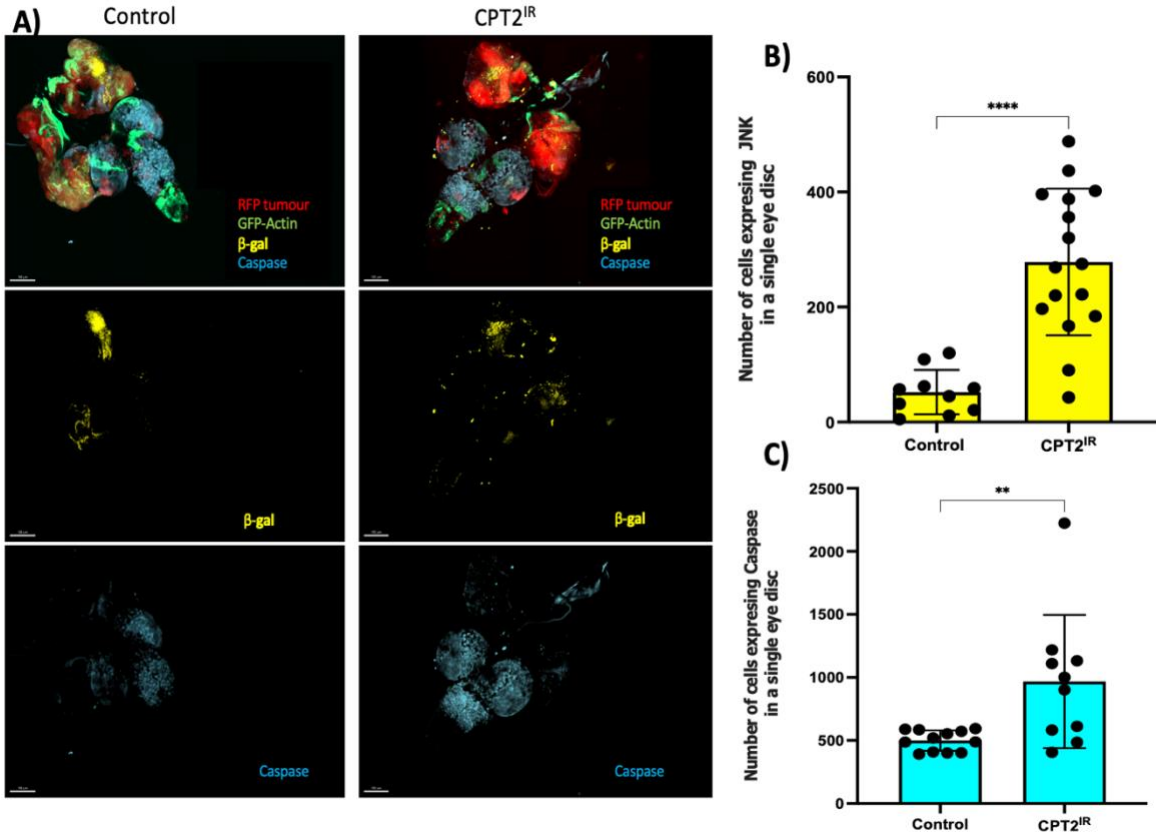

Figure 21.3.4. Tumourous cells expressing JNK and cell death in the presence or absence of driven *CPT2* knockdown in cancer cells.

A) Representative images comparing β-gal and cell death distribution in tumourous imaginal discs +/- *CPT2*^{IR} in cancer cells.100 µm scale is shown. B and C are quantifications of the number of cells, +/- *CPT2*^{IR} in cancer cells, expressing JNK and cleaved Caspase-3, respectively. Genotype of the control (*eyFLP, UAS-GfP; Lo-S100A4,Lo-Ras*^{X2} *; act-GAL4,A>lexA; puc-lacZ*). Genotype of *CPT2*^{IR} *(eyFLP, UAS-GfP; Lo-S100A4,Lo-Ras*^{X2} *; act-GAL4,A>lexA / UAS-CPT2 RNAi; puc-lacZ).* T test was performed to compare JNK activity and cell death in cells +/-*CPT2*^{IR} ,**** P<0.0001 and **P<0.0065. The error bar indicates SEM. Each data point is the number of cells expressing β-gal,(graph B) and caspase,(graph C) within the RFP-segmented surfaces from images of individual cephalic complexes, including eye discs, optic lobes and brain, (n>10). Quantification method of these cells was explained in 2.6. Confocal Fluorescence Microscopy

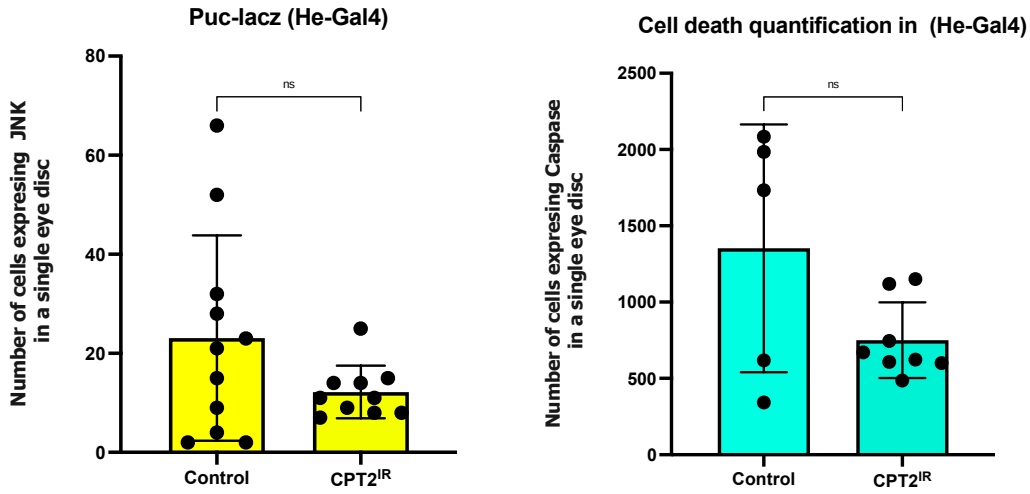

Figure 22.3.5. Quantifications of the number of tumourous cells expressing β-gal and cell death in the presence or absence of driven *CPT2* knockdown in haemocytes.

Quantifications of the number of cells, +/-*CPT2*^{IR} in haemocytes , expressing JNK and cleaved Caspase-3 within the RFP-labelled cells. Genotype of the control (*eyFLP, UAS-GfP; Lo-S100A4,Lo-Ras*^{X2} *; he-GAL4,A>lexA; puc-lacZ).* Genotype of *CPT2*^{IR} (*eyFLP, UAS-GfP; Lo-S100A4,Lo-Ras*^{X2} *; he-GAL4,A>lexA / UAS-CPT2 RNAi; puc-lacZ).* Both genotypes in each graph were stained with β-gal and cleaved Caspase-3 antibodies. The error bar indicates SEM. T test was performed to compare JNK activity and cell death in cells +/-*CPT2*^{IR} ,P=0.124 and P=0.071, respectively. ach data point is the number of cells expressing β-gal and caspase within the RFP-segmented surfaces from images of individual cephalic complexes, including eye discs, optic lobes and brain (n>5). Quantification method of these cells was explained in 2.6. Confocal Fluorescence Microscopy

The graphs (22.3.5) shows *CPT2* knockdown in haemocytes has no significant effect on JNK activity or cell death. The error bars are quite large and therefore we were unable to demonstrate an effect, but the large error bars may explain this. It is, therefore, suggested to have another biological replicates to confirm these findings.

3.3.4. Effect of *CPT-2* knockdown in haemocytes or tumour cells on tumour invasion and lipid droplet accumulation.

Cancer metabolism is shaped by interaction with TME as well as nutrient and oxygen availability (Anastasiou, 2017). *CPT2* has a key role in fatty acid oxidation, therefore we tested the effect of *CPT2* knockdown on lipid droplet availability (**Figure 23.3.6**).

Tumorous larvae with *CPT2^{IR}* were dissected and stained with LipidTOX antibody to visualize the lipid droplets. Lipid droplets were then quantified as described in section 2.6. Confocal Fluorescence Microscopy

A)-

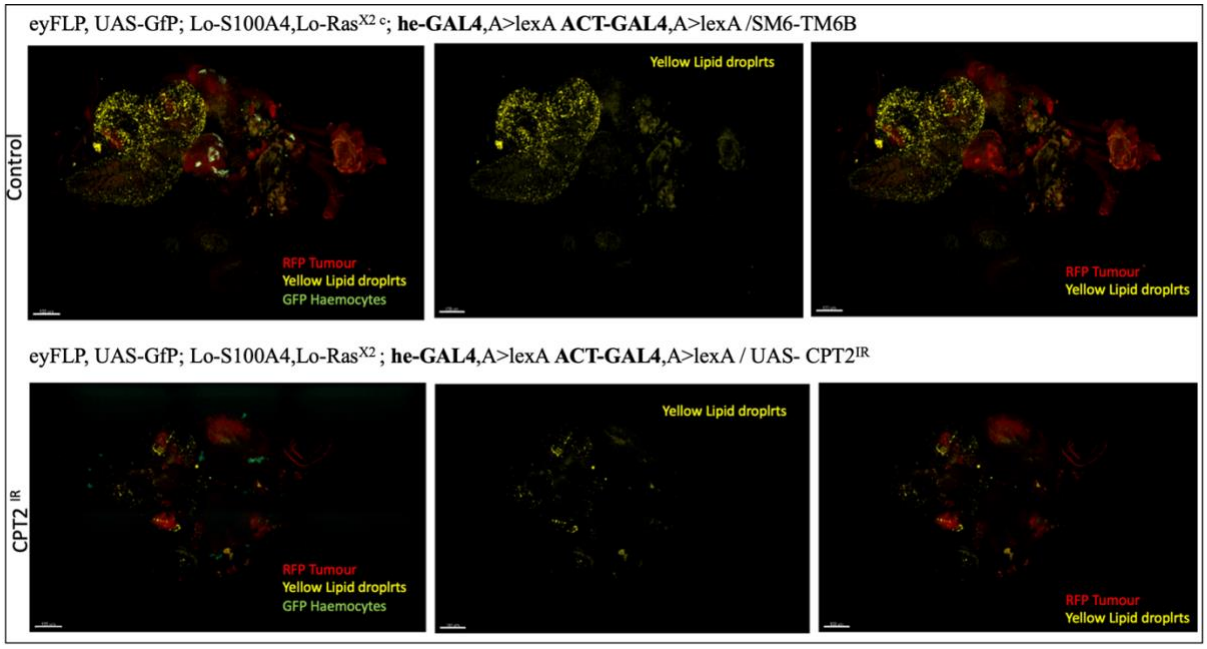

B)-

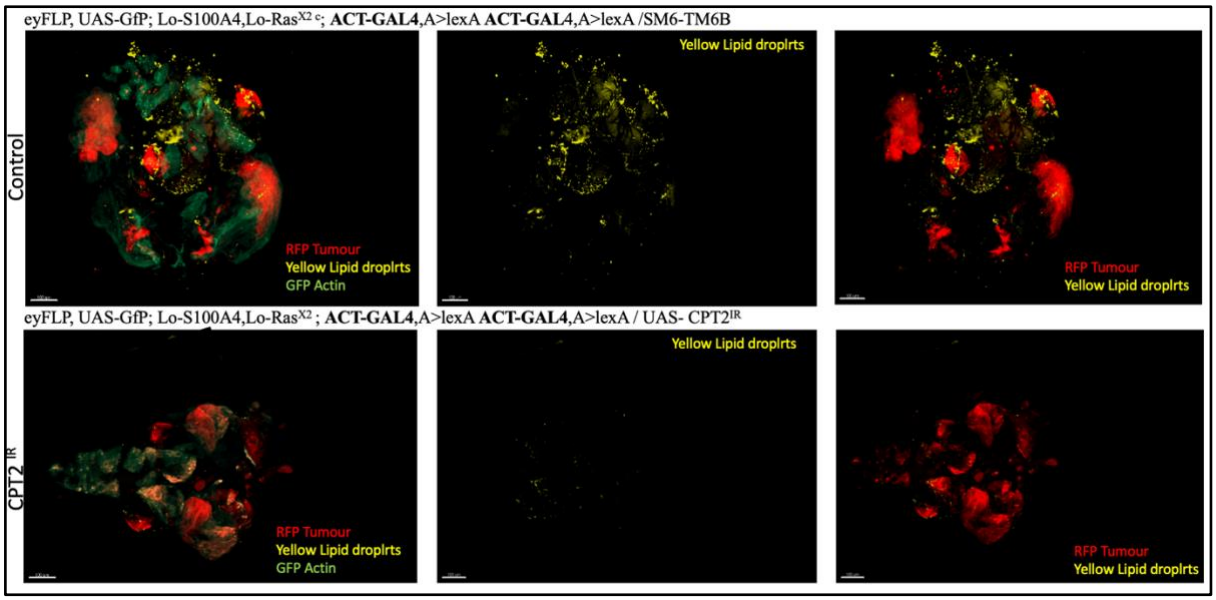

Figure 23.3.6. Representative image of lipid droplets distribution in *RAS^{v12}/S100A4,* in the presence or absence of driven CPT2 knockdown in (A) haemocytes and (B) cancer cells.

A) Knockdown of *CPT2* in GFP-labelled haemocytes (green) using *He-Gal4* driver. **B)** Knockdown of *CPT2* in GFP-labelled cancer cells (green) using *Act-Gal4* driver. In the control, lipid droplets accumulate in the brain and in the optic lobe, where RFP-labelled tumours (red) have started to invade, perhaps working to help the tumour cells survive. When *CPT2* was knocked down in cancer cells or haemocytes, less lipid droplets (yellow) were observed, 100µm scale is shown.

Knockdown was sufficient to limit the lipid droplet production as seen in the figures above and is correlated with tumour growth suppression in both cancer models.

3.4. Discussion

3.4.1 Involvement of the glycolysis pathway in Ras/S100A4 tumour cells

Genes involved in the FAO pathway including our key gene (*CPT2*) are critical for cancer cells and might affect the support of energy production in cases of

acidosis and reduced glycolysis. Data from the fly Ras/S100A4 model shows that knocking down these metabolic genes in macrophages did not affect the tumour growth. However, tumours were sensitive to disruption of *ENO, MPC1, PFK, G6PDH, GS1* and *PIG-H* enzymes.

Tumours attract haemocytes by secreting MMP1 (Bilder et al., 2000). It is known that large population of haemocytes result in smaller tumour. This is because haemocytes secret *Eiger/TNF*, which activates JNK signalling to eliminate polarity deficient cells via apoptosis (Bilder et al., 2000). Interestingly, measurements of haemocyte numbers, broadly tracked with the tumour sizes and MMP1 expression level; when the tumour was large and the MMP1 expression high, the number of haemocytes increased, and vice versa. This finding raises an interesting question whether tumours are reduced in size because metabolically impaired hemocytes fail to be recruited to the tumour (and are not able to have a pro-malignancy effect) or whether the balance of anti-/pro-malignancy effects on the tumour is altered so they are functionally more anti-tumour. One possible explanation for this is that during the inflammatory response, macrophages require elevated phagocytic cell activity to generate sufficient ATP (Galván-Peña and O'Neill, 2014, Liberti and Locasale, 2016) (Liberti and Locasale, 2016). Glycolysis is the one way to generate ATP without requiring oxygen, which is important for the hypoxic cancer cells to continue growing. Expressing RNAi constructs targeting either glycolysis or the TCA cycle, which produce ATP, supressed tumour growth in our study. This indicates that interrupting the development of the pro-inflammatory phenotype might affect the metabolic reprogramming shift in macrophages and therefore cancer cells did not have sufficient supply of ATP from macrophages (Galván-Peña and O'Neill, 2014). This may limit tumour source of ATP molecule provided by macrophages and thus the tumour volume was reduced. Furthermore, it is known that activated macrophages are heavily dependent on glycolysis to start inflammatory response

(Ciana and Eva, 2018). However, the literature is a little conflicted about the role of glycolysis in tumour-associated macrophages, a fact which may be due to context-dependent responses to immune cell signaling and inflammation.

3.4.2. Oxidative phosphorylation pathway

As mentioned before, activated M2 macrophages rely on the oxidative phosphorylation pathway and not glycolysis. Oxidative phosphorylation starts with the transport of cytosolic Acyl-CoA to mitochondria via CD36 and *CPT1*, then conversion to Malonyl-CoA with the help of *CPT2* (Ciana and Eva, 2018). This step is crucial for macrophage-associated cancer; as cells undergo acidosis and cannot perform glycolysis, they rely more on the oxidative phosphorylation pathway to generate ATP. Knockdown of *CPT1* and *CPT2* suppressed tumour growth presumably by disrupting this process. This would suggest that increasing fatty-acid oxidation in inflammatory macrophages could have beneficial anti-inflammatory effects.

Our identification of an innate tumour interaction with the tumour microenvironment in flies based may provide new ideas how such cancer treatments could be further improved in human patients.
It is important to note that false negative results may arise due to inefficient depletion of target transcripts. So, it is recommended to further validate the findings, for example by using additional RNAi lines as we have done for *CPT2*. Alternatively, RT-PCR/Western blots can be used to confirm a reduction in expression levels in the knockdown lines.

3.4.3. *CPT2*

It is clear that lipid metabolism meditate cellular functions by controlling energy homeostasis (Beloribi-Djefaflia et al., 2016). *CPT2* specifically has been proven to be a key part in these metabolic pathways as it serves an essential role in FAO process (Lin et al., 2018). Tumours create an oxidative stress environment and require more nutrients to be able to invade and grow (Anastasiou, 2017). This is clear in our control samples where the lipid droplet (energy source) accumulated in the larval brain, where cancer cells started to invade and undergo oxidative stress. To extends these findings, it would be interesting to stain with a hypoxia probe to correlate hypoxic stress, lipid droplet and *CPT2* with tumour growth in *Drosophila* tumorous larvae.

It is known, in mammals, that hypoxia induces lipid droplets in breast cancer and glioblastoma (Bensaad et al., 2014). It is intriguing that, in both mammals and *Drosophila*, inhibiting CPT2 by genetic manipulation has been reported to affect lipid droplet formation, increase reactive oxygen species (*ROS*) toxicity and impairs cell proliferation (Bensaad et al., 2014). It will therefore be important in future to determine whether lipid droplets also play antioxidant roles in cancer contexts.

Moreover, it has been reported that lipid droplet formed in niche glia, in *Drosophila*, during oxidative stress, inhibit the oxidation of polyunsaturated fatty acids and limit the levels of *ROS*. This protects glia and neuroblasts from peroxidation chain reactions that can damage many types of macromolecules (Bailey et al., 2015). This raises the possibility that *CPT2* contributes to the biogenesis of tumour lipid droplets during oxidative stress.

In humans, CPT2 dysfunction directly affects β-oxidation of long-chain FAs in mitochondrial matrix leading to variety of lipid metabolic diseases: for example, rhabdomyolysis, neonatal *CPT2* deficiency, hepatocellular carcinoma (HCC), non-alcoholic fatty liver disease (NAFLD) and obesity reviewed by (Wang et al., 2016). Another study showed that *CPT2* mutated fibroblasts lead to decrease

production of FAO and adenosine triphosphate, which leads to fibroblasts apoptosis (Xiao et al., 2015). In addition, *CPT2* mutation has significant effects on cancer progression such as HCC. Studies *in vivo* have shown low expression of *CPT2* might lead to abnormal elevated hepatic lipid accumulation to promote malignant transformation of hepatocytes in liver of rats (Gu et al., 2017).
FAO provides ATP, NADH, NADPH, flavin adenine dinucleotide (FADH2), all of which provide survival advantages for cancer. NADH and FADH2 enter the electron transport chain to produce ATP and NADPH which protect cancer cells from metabolic stress and hypoxia (Carracedo et al., 2013).

It is proven that FAO is a major source of biological energy and many cancer types has shown elevated activity of FAO, such as, triple negative breast cancer, ovarian cancer HCC, glioma and prostate cancer (PC) (reviewed by Wang et al., 2016). *CPT2* activity is largely involved in energy production and FAO (Yao et al., 2011). However, the relationship between *CPT2* activity and lipid accumulation has not been reported in cancers, especially in HCC (White et al., 2012) and NAFLD (Purohit et al., 2010). Our study indicates that knockdown of *CPT2* in tumours and TME induced the suppression of FA β-oxidation as less lipid droplet were generated. It will be interesting to examine further the relationship between FA β-oxidation JNK activity and tumour survival in the future.

Together our findings and other studies showed that *CPT2* is an interesting metabolic target for cancer therapy. These findings prompted us to investigate whether *CPT2* could be a biomarker of progression of early breast lesions in humans.

3.5. Human tissue study looking at CPT2 expression level in breast cancer patients

3.5.1. Introduction

Cancer is responsible for millions of deaths worldwide every year. For this reason, lots of effort has been put towards diagnosis of cancer at early stages to treat and prevent certain types of cancers. The potential for prevention to reduce the global cancer burden has never been greater and is now recognized by a variety of discipline some of which diagnostic or therapeutic devices or drugs. Ductal Carcinoma *In Situ* (DCIS) diseases, for example, could be identified by screening and treatment before they develop into invasive breast cancer (reviewed by Sanati, 2019).

In this chapter we aimed to extend our analysis of CPT2, by examining its involvement in DCIS progression into invasive breast cancers. Breast cancer has been chosen as a cancer to translate the *Drosophila* findings, partly because there are similarities in epithelial overgrowth in flies and humans and because *S100A4* is a prognostic factor in breast cancer (Ismail et al., 2017). Also, breast cancer is a cancer in which the precursor lesion is identified by screening and in which there is clinical interest in finding treatments and in trying to identify which patients with *in-situ* disease will progress (reviewed by Sanati, 2019). We were particularly interested in in DCIS because some DCIS cases will progress to invasive cancer if left untreated. There is also no good way to know for certain which DCIS lesions will become invasive cancer. Patients with DCIS are therefore routinely treated, despite possible adverse effects. Therefore, it would be beneficial to identify biomarkers that help us identify which DCIS will progress to invasive cancer and thus need treatment. We tested the role of *CPT2*

in DCIS, as a potential biomarker to validate and extend our analysis in *Drosophila.*

General breast tumour types are DCIS and Lobular Carcinoma *In Situ* (LCIS, also known as lobular neoplasia and both are not a true tumour but an indicator of increased risk for developing invasive cancer, (reviewed by Bane, 2013). DCIS recognised by is changes in the cells lining the breast ducts and the absence of cell spreading into the nearby breast tissue **(Figure 24.3.7.).** It is therefore called a noninvasive or pre-invasive breast cancer. One-third, and possibly more, of DCIS cases will progress to invasive cancer if left untreated. Currently, there is no good way to know for certain which DCIS lesions will become invasive cancer and which ones will not. Women with DCIS therefore are routinely treated with a choice of breast-conserving surgery (BCS) or mastectomy, and radiation, which given after BCS. If the DCIS is progesterone receptors(PR) +/ estrogen receptor (ER)+ medications such as Tamoxifen or an aromatase inhibitor might be given after the surgery (reviewed by Bane, 2013).

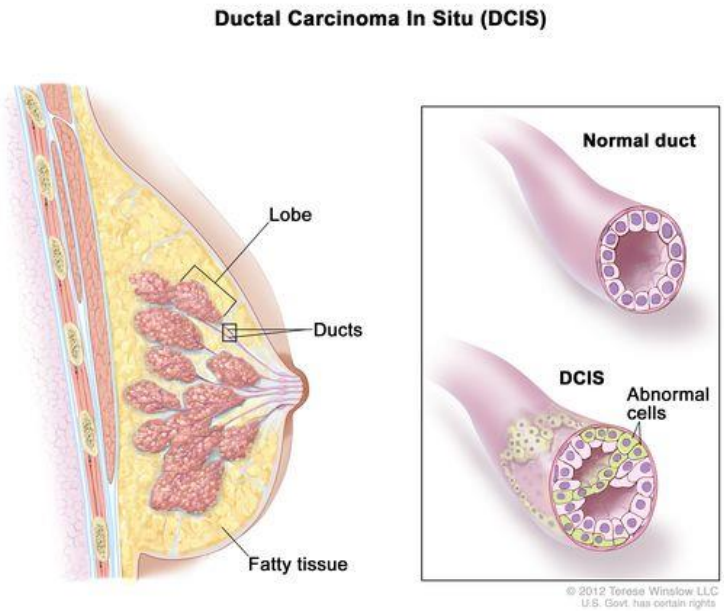

Figure 24.3.7. Ductal carcinoma in situ (DCIS)

Abnormal cells are found in the lining of a breast duct. These cells known as DCIS are considered the earliest form of breast cancer. DCIS is noninvasive, having not spread out of the milk duct. It is usually found during a mammogram done as part of breast cancer screening or to investigate a breast lump, reviewed by (Bane, 2013). It is unknown what causes DCIS, however there are several risk factors including, increased age, history of benign breast disease, such as atypical hyperplasia and family history of breast cancer. Image reproduced from (National cancer institute, 2022)

Breast cancer is divided into 4 different molecular subtypes, according to the presence or absence of biological markers: progesterone receptors (PR+/PR-), estrogen receptors (ER+/ER-), and human epidermal growth factor receptor 2 (HER2+/HER2-).

Luminal A, which are the most common tumours, tend to be PR+ and/or ER-, and HER2- and are identified as slow-growing and less aggressive than other subtypes. **Luminal B** tumours are also PR+ and/or ER+ but can be is distinguished by either expression of HER2 or high cancer cell division. **Basal-like phenotype,** also known as "triple negative," tumour is PR-, ER-, and HER2- **HER2 enriched** (HER2+) tumours overexpress HER2 and do not express hormone receptors (PR- and ER-) (reviewed by Bane, 2013, Sanati, 2019).

For the study reported here, we identified 2 cohorts of patients:

Cohort 1 represents 32 patients from different areas in England, we gathered set of patients in that group who had DCIS. Cohort 1 are patients from both Merseyside and the surrounding regions who presented in the era before breast screening when the diagnosis of DCIS was rare. The value of this cohort is that patients were not exposed to pharmacological treatments, because suitable therapies were not available at the time biopsies were taken.

Cohort 2 represents a screening population of patients who were screened and potentially treated for DCIS, where it was detected. Unfortunately, this cohort was not ready to be analysed during my PhD due to Covid-19, therefore the data presented are only from cohort 1.

3.5.2. Results:

To determine association of CPT2 with patient outcome in DCIS patients belonging to cohort 1, we divided the patients into 3 categories :

1- DCIS progression to invasion
2- DCIS recurrence
3- DCIS recurrence or progression to invasion

Based on these categories, we analysed CPT2 staining of patient biopsies according to method described in section 2.7.4. Statistical analysis:

First, we validated our antibody CPT2 (SN06-70; Thermo Fisher). We used paraffin-embedded human lung tissue. CPT2 is expressed in all human tissue (Britton et al., 1995), but the lung tissue was one of the tissue types the manufacturer recommended **(Figure 25.3.8).**

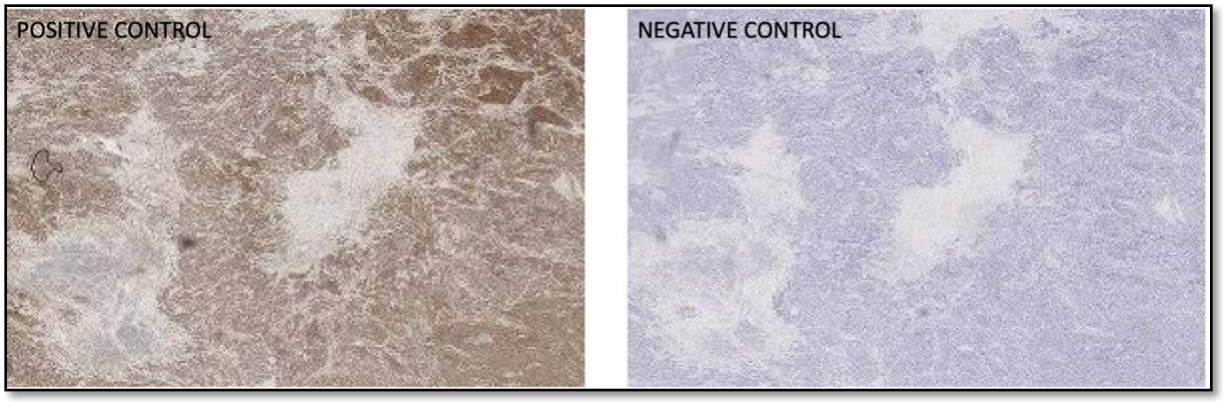

Figure 25.3.8. CPT2 in paraffin-embedded human Lung tissue.

On the left side, tissue stained with 1:50 CPT2 (SN06-70) antibody and on the right is another tissue without the antibody but treated in every other respect the same as the positive control.

We trialled different concentrations of antibody (1:50, 1:100 and 1:200); a concentration of 1:50 was selected as providing the best signal after review by pathologist Dr.Vijay Sharma.
Preparation of samples and staining are described in section 2.7.2. Immunohistochemistry:

3.5.2. OUTCOME DCIS RECURRENCE

To assess the overall survival outcome of 32, Cohort 1, patients diagnosed with DCIS, Kaplan-Meier survival analysis was performed, looking at recurrence, progression to invasion, and any form of recurrence or progression as endpoints (**Figure 26.3.1.).** The 1st quartile was found to be the best cut off to divide CPT-2 expression into low and high groups, see method 2.7.5. Kaplan-Meier survival analysis

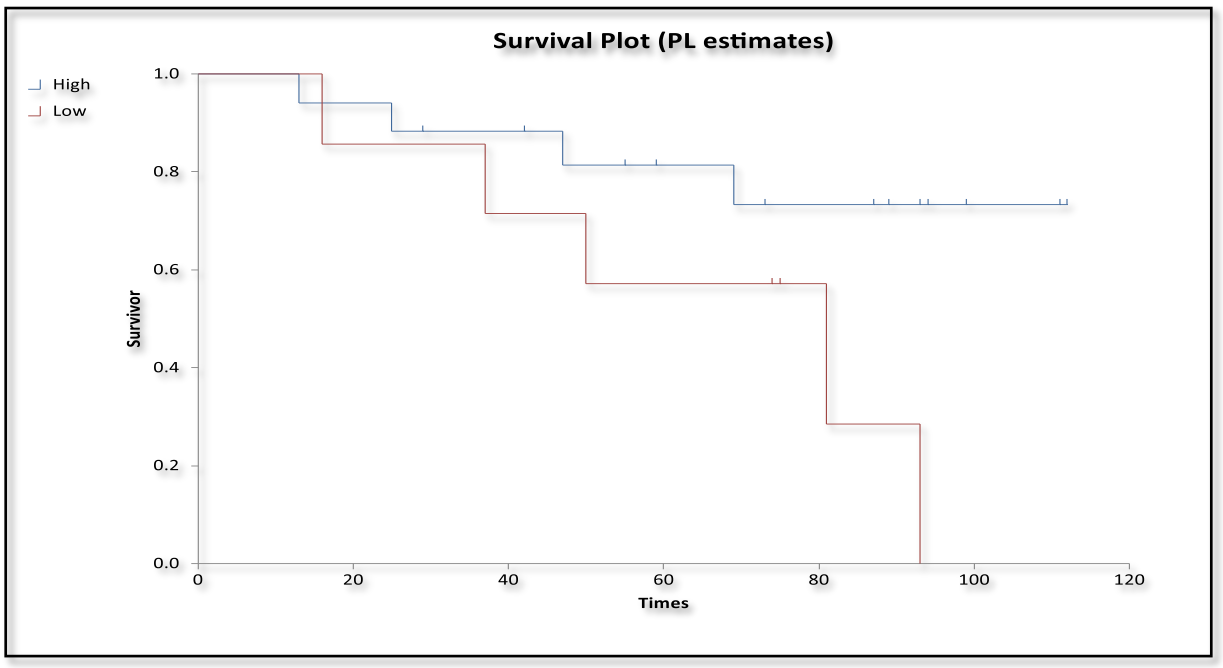

Figure 26.3.1. OUTCOME DCIS RECURRENCE.

High =high CPT2 expression , Low= low CPT2 expression . The scale of the x axis represents months. Each time the line go down (Red line) that means the patient got recurrence of DCIS at that time point. Patients with higher expression of CPT2 (blue line) showed less DCIS recurrence.Number of patients: 32.

High expression of CPT-2 prevented recurrence of DCIS (log-rank wilcoxon test , HR 0.29; P=0.045). High expression of CPT-2 had no effect on progression to invasion, data not shown. The effect was lost when the endpoints of recurrence and progression were grouped. The findings show that CPT-2 has a protective effect at the *in-situ* stage in preventing recurrence of *in-situ* disease. Only data that show an effect are presented which is for group with DCIS recurrence. There was no difference in CPT-2 expression between the pure DCIS, recurrence, and progression groups, confirmed by ANOVA, P = 0.9566. The finding highlights the complexity of this marker. Below a representative image of our staining (**Figure 27.3.1.).**

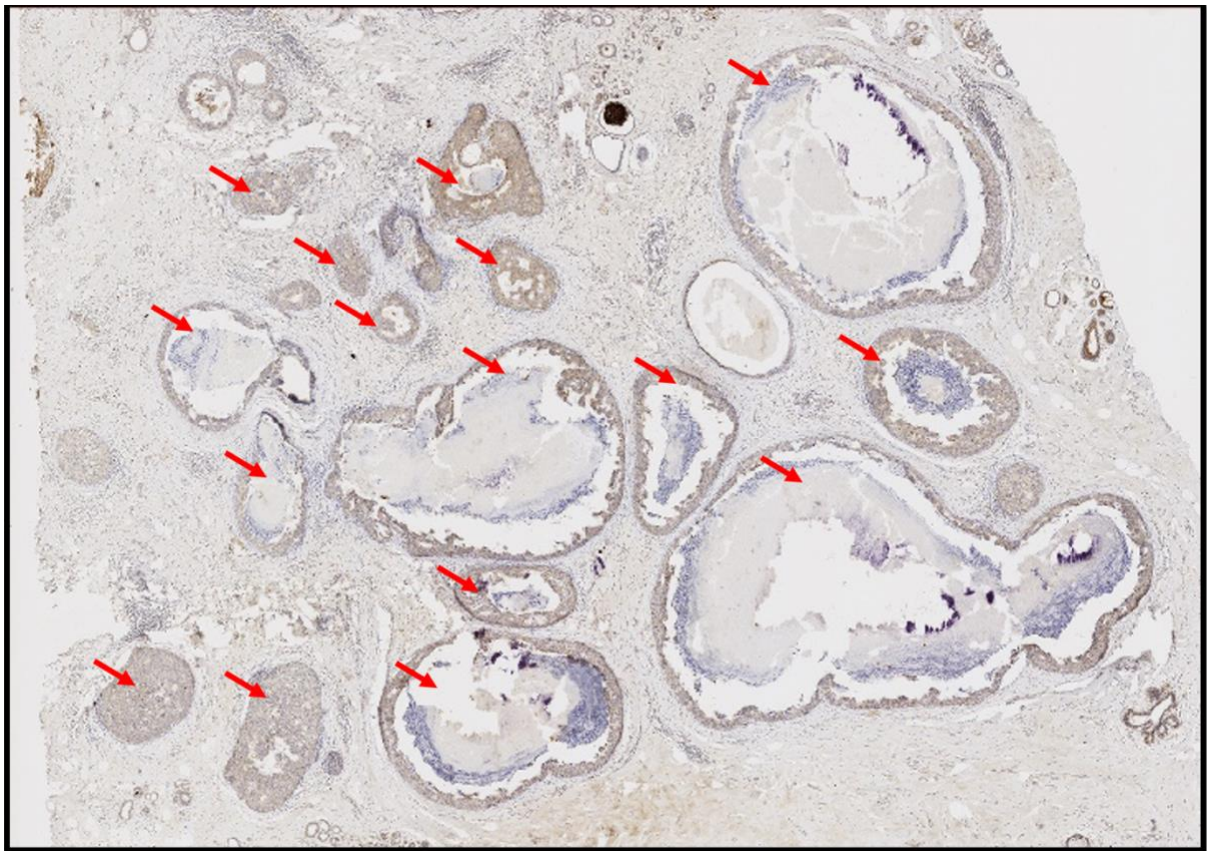

Figure 27.3.1. Immunohistochemical analysis of CPT2 in paraffin-embedded human breast cancer tissue using a CPT2 Monoclonal antibody (SN06-70).

Brown colour represents cells expressing CPT2. Blue is Hematoxylin and eosin which stains cell nuclei and the cytoplasm. DCIS (where the breast duct cells have abnormal cell growth) are red arrowed. Only brown staining within the DCIS was measured for quantitation purposes.

Originally, we had planned to test the correlation between level of *S100A4* expression and breast cancer patient outcome. However, due to covid-19 and staff shortages it was not possible to complete this analysis. In addition, the generation of Cohort 2 samples is still ongoing.

3.6. The potential role of CPT2 as a biomarker of breast cancer progression – a bioinformatic analysis

We wanted to look at a bigger data set to help extend our finding beyond the limited DCIS data we collected above. Therefore, we took a bioinformatic approach looking at correlation of *CPT2* expression level with overall survival of different cancers, the correlation between mutation in *CPT2* and cancers, between *CPT2* and JNK and immune cells and between CPT2 and treatment responses. Different platforms were used to run these correlations, described in 2.8. Bioinformatics: Online Method These are freely available online datasets in which RNA gene array, sequencing and proteomic data have been linked to clinical data, including follow-up data, allowing the prognostic effect of gene expression or mutation to be quickly and easily tested at both RNA and protein level. The cut-off for high and low expression was defined as the median expression in the dataset, and overall survival compared between high and low expressing tumours using Kaplan-Meier analysis.

The role of *CPT-2* as a predictor of treatment response was assessed by looking at ROC curves using the ROC-plotter tool, the treatment response outcomes being complete pathological response (to measure short term effects) and 5 year relapse-free survival (to measure long term effects). The response to endocrine therapy, HER-2 therapy and chemotherapy was assessed in the breast cancer subtypes to which these therapies are given.

The impact of immune compartments on the prognostic effect of CPT-2 was assessed using the KM Plotter tool by splitting the data both by enrichment or depletion of a particular immune compartment and simultaneously splitting the data by either stage or mutation burden. With these data in hand, it was possible to determine whether the prognostic effect of CPT-2 at a particular stage was

dependent on the enrichment or depletion of a particular immune compartment. This information was then tabulated.

Network analysis was performed using the Oncomine tool. Clustering of CPT-2 with genes in pathways involved in the major cancer hallmarks was determined by entering the defined lists of genes for each pathway into the tool along with CPT-2. The output provides details of which genes in the pathways cluster with CPT-2 as well as details of the subgroups in which the clustering occurs. These data were tabulated and summarised to reveal the overall patterns.

3.6.1. CPT2– prognostic effects

At the level of RNA expression, CPT-2, measured by either microarray or RNA sequencing, has no significant predictive or prognostic effect on overall survival. However, specifically at low mutational burden, CPT-2 has a poor prognostic effect. CPT-2 has a good prognostic effect on relapse-free survival, which is limited to luminal A cancers (Ioannis et al., 2017). At the protein level, there is a poor prognostic effect on overall survival when CPT-2 is measured using quantitative liquid chromatography and mass spectroscopy (P 0.0027), but no effect is seen when CPT-2 is measured by immunohistochemistry (supplementary data – **Table 10.**).

-Guidance on reading the graphs/data, which is available online, to decide good or poor prognostic effects:

To call a gene prognostic, the logrank p-value needs to reach significance, defined as less than 0.05. The HR value is examined to determine the size and clinical significance of the effect, and the graph is examined to determine the direction of

the effect (it is a poor prognostic marker if the high expressor line goes below the low expressor line, and a good prognostic marker if the high expressor line goes above the low expressor line) (**Figure 28.3.2**).

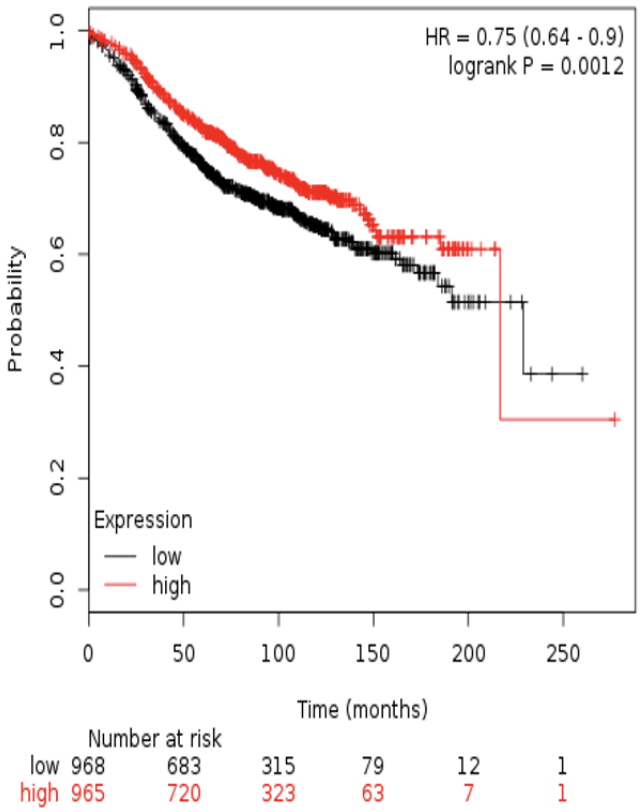

Figure 28.3.2. Correlation between CPT2 RNA expression level with overall survival ratio of Luminal A breast cancer patients.

High expressor line in RED. Low expressor line in BLACK. CPT2 level measured by RNA Microarray in patients with Luminal A breast cancer. CPT2 was found to be a good prognostic effect for these patients' overall survival rate.

Note. We have summarized and presented our data in tables; original graphs similar to (Figure 28.3.2.) are in a supplementary PPT, **Appendix I**.

Overall survival measured for different breast cancer subtypes by using RNA Microarray (Gatza et al., 2014) **(Table 10.).**

Table 9. Overall survival measured for different breast cancer subtypes

Detailing hazard ratios (HR), p value and outcomes of overall survival data in breast carcinomas showing the predictive and prognostic effects of CPT2 expression at mRNA and protein level, and of CPT2 mutations. Data obtained from the KM plotter (Eastel et al., 2019), G2O and the Human Protein Atlas.

Molecular level	Source	Subgroup	Method	HR	P value	Outcome
mRNA	KM plotter	Treated patients	RNA microarray	0.68	9.1e-07	NS
mRNA	KM plotter	Untreated patients	RNA microarray	0.81	0.047	Poor
mRNA	KM plotter	All breast carcinomas	RNA Seq and RNA Microarray	-	-	Ns
mRNA	KM plotter	Luminal A	RNA microarray	0.75	0.0012	Good
mRNA	KM plotter	Luminal B	RNA microarray	0.89	0.23	NS
mRNA	KM plotter	HER-2 positive	RNA microarray	0.68	0.69	Poor
mRNA	KM plotter	Basal phenotype	RNA microarray	0.78	0.055	Poor
mRNA	KM plotter	Low mutational burden	RNA microarray	1.78	0.02	Poor
mRNA	KM plotter	High mutational burden	RNA microarray	0.73	0.3	NS
DNA alterations	KM plotter	All breast carcinomas	DNA Seq	3.29	0.013	Poor
mRNA Metagene associated with mutation	G2O	All breast carcinomas	DNA Seq and RNA microarray	-	-	NS
Protein	Human Protein Atlas	All breast carcinoma	Immunohistochemistry	-	-	NS
Protein Expression	Human Protein Atlas	All breast carcinoma	Quantitative Liquid Chromatography / Mass	2.9	0.0027	Poor

3.6.2. CPT-2 Overall survival in other cancer types

CPT-2 at protein level has **a good prognostic effect** in Renal and Colorectal Cancer. CPT2 at RNA level also has a good prognostic effect on other cancer types (**Table11.).**

Table 10.*CPT2* prognostic effect in different cancer types.

Data obtained from the KM plotter datasets in which RNA gene array, sequencing and proteomic data have been linked to clinical data, including follow-up data, allowing the prognostic effect of gene expression to be quickly and easily tested at both RNA and protein level (Eastel et al., 2019).

Molecular level	**Cancer type**	**P value**	**Prognostic effect**
Protein Expression	Renal cancer	1.5	Good
Protein Expression	Colorectal Cancer	0.00035	Good
mRNA	Oesophageal adenocarcinoma	0.0015	Good
mRNA	Oesophageal squamous cell carcinoma	0.0029	Good
mRNA	Kidney Clear Cell Renal Cell carcinoma	3.1	Good
mRNA	Kidney Papillary Renal Cell carcinoma	9.7	Good
mRNA	Lung Adenocarcinoma	0.0058	Good
mRNA	Pancreatic ductal adenocarcinoma	0.035	Good
mRNA	Stomach Adenocarcinoma	0.031	Good
mRNA	Thyroid carcinoma	0.035	Good

3.6.3. Correlation between mutation in CPT2 and cancers

In breast cancer, about 1.6% of tumours harbour mutations in CPT-2 most of which are amplifications, data generated from cBioPortal (Cerami et al., 2012, Gao et al., 2013). No significant effect of mutation on prognosis was observed.

The metagene (the pan-genome pattern of changes in gene expression) associated with CPT-2 mutation also had no significant prognostic effect.

3.6.4. Correlation Between CPT-2 and JNK

To explore conservation of potential mechanisms, we examined correlation between levels of CPT2 and JNK at protein levels in human breast cancers **(Table 12.).**

Table 11.Correlation Between CPT-2 and JNK

Correlation between levels of CPT2 and JNK at protein levels in human breast cancers.

	CPT-2 and JNK
Pearson's correlation	-0.2397 (p<1e-04)
Spearman correlation	-0.2851 (p<1e-04)
N number	4929

There is an inverse correlation between the expression of CPT-2 and JNK, confirming that the effect we observed in the *Drosophila* model can also be observed in human breast cancers.

Unfortunately, the database we used does not include information on the correlation between CPT-2 and JNK in normal tissue. Therefore, this would be a good basis for further studies. The correlation could be determined using immunohistochemistry in normal tissues in a subsequent study, for example.

3.6.5. Correlation Between CPT-2 and different pathways

In our network analysis we examined how CPT-2 clusters with gene concepts for pathways involved in the major cancer hallmarks, including immune regulation, and epigenetic regulation using the Oncomine platform. The gene itself is subject to regulation by methylation, but clusters with pathways involved in acetylation, ubiquitination, chromatin remodelling and repair, hydroxymethylation and citrullination. CPT-2 clustered with genes involved in the key hallmarks of cell proliferation and apoptosis (Table 13).

Table 12.CPT2 and immune and epigenetics related pathways.

Summary table showing clustering of CPT2 with genes in the listed concepts covering immune and epigenetics pathways. The cohort in which the clustering occurred is listed. The table specifies whether the clustering occurred in the context of gene overexpression or under expression. The clustering occurred across all invasive carcinomas unless otherwise specified; if clustering occurred in a specific subgroup, this is specified. PR: Progesterone receptor, HER-2: Human epidermal receptor-2.

Concept	**Expression**	**Clustering subgroup**	**Cohort**
ANTIGEN PRESENTATION	Under expressed		TCGA
APOPTOSIS	Overexpressed		TCGA
CELL PROLIFERATION			DESMEDT
AUTOPHAGY			DESMEDT and CURTIS
COSTIMULATORY SIGNALLING	Under expressed	HER-2 positive	CURTIS
EPIGENETICS - CHROMATIN REMODELLING AND REPAIR	Overexpressed		BITTNER
EPIGENETICS - HISTONE ACETYLATION	overexpressed		TABCHY , BITTNER and HATZIS
EPIGENETICS - HISTONE DEUBIQUITINATION	Under expressed		MIYAKE
EPIGENETICS - HISTONE CITRULLINATION	Under expressed		DESMEDT
EPIGENETICS - HISTONE UBIQUITINATION	Overexpressed		CURTIS and BITTNER
IMMUNE CELL ADHESION AND MIGRATION	Under expressed	Invasive lobular carcinoma	CURTIS

MATRIX REMODELLING AND METASTASIS			MIYAKE
TGF B SIGNALLING	Under expressed		MIYAKE
cytotoxicity	Under expressed	PR positive	
EPIGENETICS - DNA Hydroxymethylation	Under expressed	HER-2 positive	CURTIS
EPIGENETICS - DNA Hydroxymethylation	Overexpressed		TCGA

3.6.6. Summary of Immune System interaction with CPT-2 depending on different cancer stages and depending on mutation burden

We used bioinformatic information on overall survival of patients and correlate it with their diagnostic details including stage of cancer (Table 14) and mutation occurred in different immune cells (Table 15) .

CPT2 interaction with immune system has no effect on cancer stage 1 and for stage 4 there was no sufficient data available. The correlation between CPT2 and cancer stage 2 and 3 are described below (**Table 14**).

Table 13.Summary of immune system interaction with CPT-2 depending on cancer stages 2 and 3.

		Stage 2	**Stage 3**
Good Prognosis	Effect dependent on enrichment of	CD4+ memory T cells	Mesenchymal stem cells Natural Killer T-cells
	Effect dependent on depletion of	Mesenchymal stem cells Natural Killer T-cells	
Poor prognosis	Effect dependent on enrichment of	Eosinophils Natural Killer T-cells	
	Effect dependent on depletion of	CD4+ memory T cells	Mesenchymal stem cells Natural Killer T-cells

Table 14.Summary of Immune System Interaction with CPT-2 depending on mutation burden.

		Low mutation burden	High mutation burden
Good Prognosis	Effect dependent on enrichment of		Regulatory T-cells
	Effect dependent on depletion of		
Poor prognosis	Effect dependent on enrichment of	Basophils B-cells CD4+ memory T-cells Macrophages Regulatory T-cells Type 2 T-helper cells	
	Effect dependent on depletion of	CD8+ T-cells Mesenchymal stem cells Type 1 T-helper cells	B-cells Regulatory T-cells

When the overall survival data are split by stage, CPT-2 has no prognostic effect. However, when the data are further split according to the enrichment or depletion of immune compartments, an intriguingly complex pattern emerges. At stage 2, CPT-2 has a good prognostic effect when there is enrichment of CD4+ T-cells and depletion of mesenchymal stem cells and natural killer cells. At the same stage, CPT-2 has a poor prognostic effect when there is enrichment of eosinophils and natural killer T-cells, and depletion of CD4+ T-cells. At stage 3, the effects of the immune compartments switch. Now a good prognostic effect is seen when there is enrichment, rather than depletion, of mesenchymal stem cells and natural killer T-cells. Depletion of these compartments at stage 3 produces a poor prognostic effect, the opposite to what is seen at stage 2. When the data are split by mutation burden, the poor prognostic effect is seen to be dependent on the enrichment of a number of immune compartments, including macrophages, and the depletion of other compartments. The effect of macrophage enrichment is equivalent to our finding in the flies. The effect of regulatory T cells and B-cells on the prognostic effect of CPT-2 switches between low and high mutation burden. These data show that the prognostic effect of CPT-2 is complex and depends on the stage, mutation burden and the enrichment and depletion of

immune compartments. The prognostic effect of the interaction of CPT-2 with immune compartment enrichment and depletion switches as breast cancer progresses. There is no effect at stage 1, and the effects which emerge at stage 2 switch to the opposite effect at stage 3, likely reflecting a complex shift of the entire regulatory network as breast cancer progresses.

To further examine the immune modulatory effects of CPT-2, we looked at 1100 breast cancer patients for whom data was available on the TISIDB platform (http://cis.hku.hk/TISIDB/browse.php?gene=CPT2). The data showed weak but significant inverse correlations between the level of CPT2 protein expression and immune cell infiltration of the tumour and the expression of immunomodulator genes and chemokines. Interestingly, CPT-2 protein levels are inversely correlated with the expression of both immunostimulator and immunoinhibitory genes, which reflects the complexity of the effects seen in our other data. CPT-2 expression was higher in the lymphocyte-depleted immune subtype. The expression of CPT-2 did not change across different stages overall. Finally, our network analysis showed the CPT-2 clusters with gene concepts involved in antigen presentation, costimulatory signalling and immune cell adhesion and migration in the context of underexpression of these genes. These data show that CPT-2 is involved in modulating immune infiltration and regulation in human breast tumours, which correlates with our findings in flies. However, the effect is stage, mutation burden and immune-compartment-specific, and shifts as breast cancer progresses.

3.6.7. Correlation between CPT-2 and treatment response

Table 15. CPT-2 correlation with treatment response

Gene	Treatment	Response Measure	Luminal A	Luminal B	HER-2 positive	Triple Negative
CPT-2	Endocrine therapy	Complete pathological response	Sensitiser (Fold change 1.9; p=1.2e-03)	Sensitiser (Fold change 3.3; p=7.1e-03)	N/A	N/A
CPT-2	Endocrine therapy	5-year RFS	No effect	No effect	N/A	N/A
CPT-2	Anti-HER-2 therapy	Complete pathological response	N/A	No effect	No effect	N/A
CPT-2	Anti-HER-2 therapy	5-year RFS	N/A	No effect	No effect	N/A
CPT-2	Chemotherapy	Complete pathological response	Resistance (Fold change 1.5; p=5e-09)	No effect	Resistance (Fold change 1.3; p=3.8e-03)	No effect
CPT-2	Chemotherapy	5-year RFS	No effect	Sensitiser (Fold change 1.4; p=2.9e-03)	No effect	No effect

There are complex effects of CPT-2 on treatment response. In the short term, as measured by complete pathological response, CPT-2 confers a strong increase in sensitivity to endocrine therapy in luminal A and B cancers but a more modest increase in resistance to neoadjuvant chemotherapy in luminal A and HER- 2 positive breast cancers. These effects are lost over the long term, as measured by 5-year relapse-free survival. However, CPT-2 does produce a modest long-term sensitising effect to neoadjuvant chemotherapy in luminal B breast cancers. These findings further reflect the complex nature of the role CPT-2 plays in breast cancer progression.

Chapter 4: Amino Acid Requirements for Tumour Growth and Invasion in *Drosophila*

4. Introduction

4.1. Non- essential amino acid metabolism in cancer cells

It is well established that cancer cells change their metabolic pathways in order to fulfil their demand for certain nutrients to sustain proliferation. Amino acids are one of the nutrients required for cancer progression (Hosios et al., 2016a, Johnson et al., 2018). Amino acids are known to contribute to the production of carbon-based biomass and as a source of nitrogen for nucleotides, hexosamines which are essential for rapid cell proliferation (Commisso et al., 2013, Johnson et al., 2018). There are 20 amino acids and they divided into two subgroups, based on dietary necessity: essential amino acids (EAAs) and non-essential amino acids (NEAAs) (**Table 17)** EAAs are those that "cannot be synthesized by the animal organism, out of materials ordinarily available to the cells, at a speed commensurate with the demands for normal growth" (Borman and Wood, 1946).

Table 16.Amino acid groups

Essential amino acid	Non-essential amino acid
(L-phenylalanine)	(L-alanine)
(L-histidine)	(L-cysteine)
(L-lysine)	(L-aspartate)
(L-methionine)	(glycine)

(L-arginine)	(L-asparagine)
(L-threonine)	(L-proline)
(L-valine)	(L-glutamine)
(L-tryptophan)	(L-serine)

In cancer cells, cell division requires many cellular components, building blocks such as Acetyl-Co-A, ribose sugar for nucleotide synthesis, amino acids for protein synthesis and lipids for bio-membrane synthesis (Fadaka et al., 2017). Thus, cancer cells elevate consumption of amino acids and use some for energy and the rest for biomass to support biosynthesis and expansion (Fadaka et al., 2017). Metabolic alteration is also triggered in stromal cells to synthesise amino acids. Glutamine for example, is synthesized from multiple sources such as exosome endocytosis, macropinocytosis of extracellular fluid and *de novo* glutamine synthesis, in order to meet the tumour requirements for glutamine (Bott et al., 2015). Several inhibitors targeting glutamine metabolism have been developed, the most clinically relevant one being CB-839, which inhibits the activity of glutaminase, the enzyme responsible for converting glutamine to glutamate (Gross et al., 2014). Co-targeting of glutaminase in tumour cells and glutamine synthetase in stromal cells has been shown to lead to a reduction in tumour weight and metastasis (Yang et al., 2016). Further, there is a link between amino acid metabolism and oncogene-mediated cancer signalling; for example, reprograming of glutamine metabolism is regulated by oncogenic *KRAS* and the oncogenic transcription factor *c-MYC (c-MYC*) (Son et al., 2013, Yang et al., 2009). Proline metabolism is also regulated by c-MYC (Wei et al., 2012). Other amino acids reported to correlate with cancer progression include asparagine, which reported to govern breast cancer metastasis (Bensaad et al., 2014, Knott et al., 2018). Reduction in serine levels have been reported to severely impair tumour proliferation by inducing tumor protein *P53*- dependent metabolic remodelling, which leads to oxidative stress in cancer cells (Maddocks et al.,

2017). *P53* is a tumour suppressor gene which represses the activity of phosphoglycerate dehydrogenase (PHGDH), an enzyme involved in serine synthesis and it is upregulated in different cancer types (DeNicola, 2011). These studies demonstrate that a complex network links signal transduction with amino acid metabolism and therefore it is important to understand this interaction to develop cancer therapy targeting amino acid metabolism.

4.1.2. Targeting NEAA metabolism for the therapeutic treatment of cancer

Currently, treatment options of cancer mostly target the underlying genetic causes and the molecular signalling pathways that are affected. However, developing novel strategies targeting amino acids metabolism is desirable (López-Lázaro, 2015) and might involve the development of drugs to specifically target metabolic enzymes (Shukla et al., 2012) or remove amino acids from the TME (Schulte et al., 2018).

Since cell survival requires adequate levels of nutrients including the 20 amino acids, one non-pharmacological strategy of cancer treatment is to restrict uptake of specific nutrients (López-Lázaro, 2015). In the clinic, patients with advanced cancer can be given chemically-defined diets (parenteral diets) via intravenous injection (Muscaritoli et al., 2012). Ideally, giving patients diet depleted of carbohydrates or amino acids, which tumours are known to be addicted to, would induce stress, impair tumour proliferation and ultimately improve survival rates. A study using a mouse cancer model has confirmed the effectiveness of this approach, showing that dietary restriction of serine resulted in reduced tumour size and enhanced survival rates (Maddocks et al., 2017). However, apart from parenteral diets, amino acids taken from daily meals inevitably enter patients' digestive systems and are exchanged into blood circulation and often transmitted to nourish cancer cells (López-Lázaro, 2015). Therefore, the Rabin medical

centre trialled giving patients with advanced cancer parenteral diets via intravenous injection without oral or enteral feeding. This improved their survival rate (LLC, 2018).

Additionally, synthesis or consumption of amino acids are dependent on complex interaction between diet consumption, gene expression programs and local secretion/ consumption rates in the tumour and tumour microenvironment (Pan et al., 2016, Kamphorst et al., 2015). It is reported that tumours may be able to synthesize *de novo* serine and reduce the effectiveness of the dietary restriction of serine uptake (Sullivan et al., 2019). Certain tumour types, for example melanoma and breast cancer in mice, are unable to acquire serine from their microenvironment. However, regions with limited serine could acquire a fitness advantage by upregulating PHGDH enzyme, which catalyzes the first step in serine synthesis. Therefore, it is critical to identify appropriate approaches for specific tumour types to successfully target serine or other NEAA metabolism (Sullivan et al., 2019). These studies together show the challenges with targeting amino acid metabolism for the therapeutic treatment of cancer.

In our study, we plan to investigate the requirements of NEAAs in cancer progression and dissemination by feeding flies that are harbouring genetically-defined tumours a chemically-defined food lacking individual NEAA. Although this experiment will allow us to determine which amino acids are required for tumour growth, it is unable to inform us about the differential requirements in the tumour itself compared to the TME. Therefore, our next step will be to systematically knock down selected transporters of NEAAs in the tumour and surrounding cells including haemocytes, glial, neural and fat cells. Amino acid transporters are emerging as effective drug targets for the treatment of cancer. For instance, chemical inhibition of the glutamine transporter *ASCT2*, leads to starvation phenotypes including attenuated tumour proliferation, elevated apoptosis, and upregulated oxidative stress, collectively contributing to anti-

tumour responses (Schulte et al., 2018). This study represents a novel therapy targeting amino-acid transport in cancer metabolism.

Using tumours that utilize evolutionarily conserved pathways to promote metastatic dissemination, our findings will guide studies in human cancer patients. Critically, a comprehensive understanding of the NEAA requirements for successful invasion to occur may offer new therapeutic strategies targeting NEAA metabolism.

4.2.Result

Method of how to make chemically defined food are described in the method section 2.9. Chemically-defined media method:

4.2.2. Chemically defined food restrains larval and tumour growth

Exogenous NEAA are thought to be an essential requirement for cancer cell growth and dissemination, despite the ability of cancer cells to synthesize NEAAs for themselves (Dang, 2019). Nevertheless, the requirement for NEAAs during cancer progression *in vivo* remains poorly understood. To address this, we have systematically tested the effect of chemically-defined diets lacking specific NEAAs on tumour growth in a fly Ras^{Val12}/ $scrib^{-/-}$ cancer model. First, we compared the effect of rearing flies on complete chemically defined food (CDF) with normal food (NF). The chemically-defined food is sufficient to support development over multiple generations, but at a reduced rate (Piper et al., 2014). It is reported that flies that developed on NF were ~18% bigger than those on chemically defined food, and the average time for development from egg to the appearance of the first pupa on chemically-defined media was considerably longer than on NF (Piper et al., 2014). These findings are consistent with our observation that larvae growing on ALL diet were smaller than larvae on NF, as shown below (**Figure 29.4.1.).**

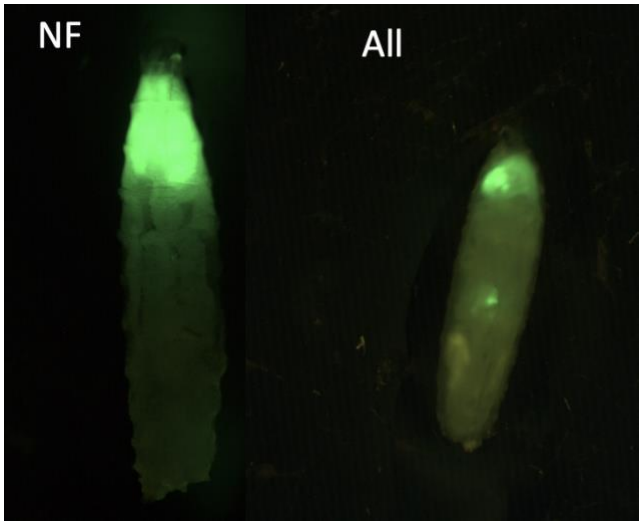

Figure 29.4.1.Images of whole larvae growing on NF and CDF.

GFP-labelled *Ras^{V12} /scrib$^{-/-}$* cells in eye-brain complexes. Images were acquired of larvae (aged 11 days) by fluorescence stereomicroscope with a digital camera (Leica).

3D optical images of eye discs and brains from *Ras^{Val12}/ scrib$^{-/-}$* larvae (at day 12) grown on All or NF were captured by confocal microscopy and the volume of GFP-labelled eye disc and brain tumours were measured. Compared to NF, there was a 7.8-fold reduction in mean tumour volume on the All diet (student t test, P <0.0001), **(Figure 30.4.2.).** This was accompanied by a 1.9-fold reduction in MMP1 staining intensity (student t test, P<0.0001), **(Figure 30.4.2**.). Together, these observations show that the chemically-defined food affects the growth of tumourous and normal tissue alike. Consequently, all subsequent comparisons with modified chemically-defined diets were made against the All diet.

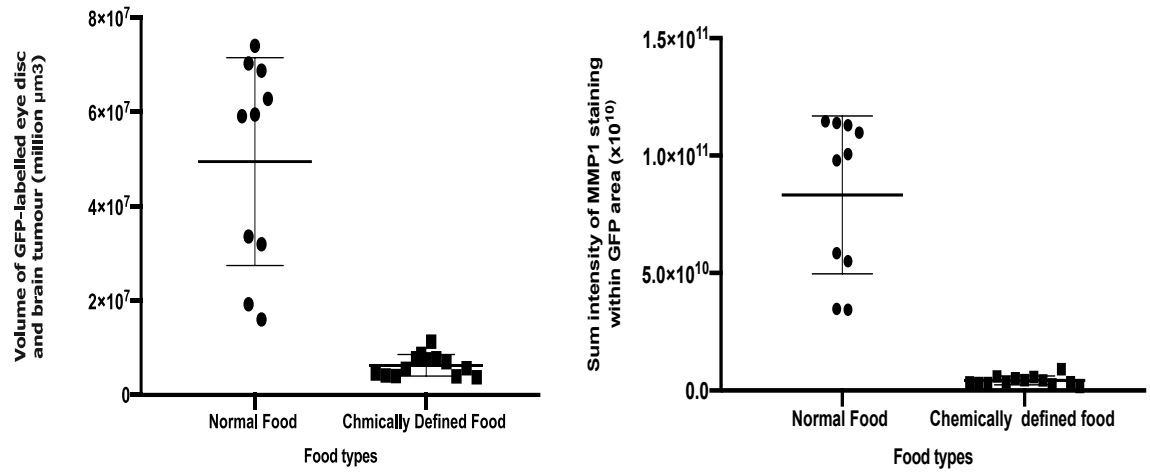

Figure 30.4.2. Tumour volume and MMP1 intensity within tumours *Ras^{Val12}/ scrib$^{-/-}$*, grown on normal food vs chemically defined food.

The error bar indicates SEM. Each data point is the measurement of total volume of GFP-labelled cells, segmented surfaces from images of individual cephalic complexes, including eye discs, optic lobes and brain, (n>10).Volume of GFP-labelled eye disc and brain tumours of chemically defined food were compared to volume of GFP-labelled eye disc and brain tumours of NF, there was a 7.8-fold reduction in mean tumour volume, (student t test, P <0.0001). This was accompanied by a 1.9-fold reduction in MMP1 staining intensity, (student t test, P<0.0001).

Note. Further study is required to test removal of individual NEAAs on non-tumourous larvae (Wild type).

4.2.3. Removal of Asn, Gly and Tyr from the diet strongly suppresses *Ras^{Val12}/ scrib$^{-/-}$* tumour growth

The larvae growing on food lacking all NEAAs showed significant reduction in tumour growth when compared to larvae growing on media complete with all EAAs and NEAAs (one-way anova, p <0.0001). For media lacking individual NEAAs, the most significant tumour reduction was associated with media lacking asparagine, glycine and tyrosine and serine. Media lacking aspartate, alanine, proline and cysteine showed no significant differences in tumour size, compared to the control diet (CDF) (**Figure 31.4.3**.).

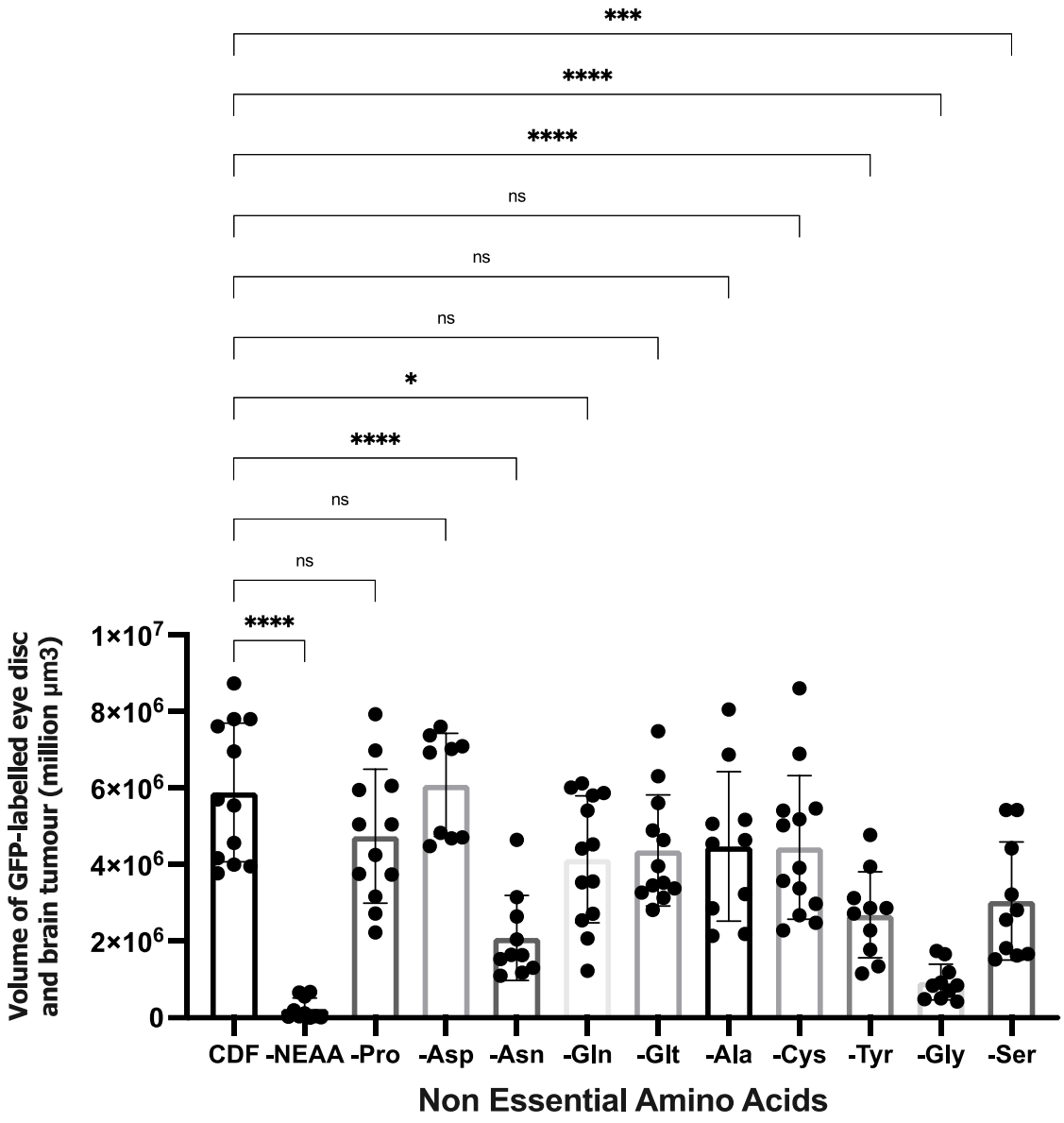

Figure 31.4.3. Volume of GFP-labelled tumours *Ras^{Val12}/ scrib$^{-/-}$* grown on different diets.

Significant differences in tumour volume of each diet lacking individual NEAA compared to the chemically defined food (CDF) are indicated with *, (One-way ANOVA was performed ,(NEAA, P<0.0001, Pro, P=0.368, Asp, P= 0.996, Asn P<0.0001, Gln, P=0.035, Glt, P= 0.0498, Ala P=0.199, Cys P= 0.130, Tyr, P=0.003, Gly, P<0,0001 and ,Ser, P=0.0002). The error bar indicates SEM. Each data point is the measurement of total volume of GFP-labeled cells, segmented surfaces from images of individual cephalic complexes, including eye discs, optic lobes and brain, (n>10).

4.2.4. Reduced tumour growth is accompanied by loss of MMP1 expression

In *Ras*^{Val12}/ *scrib*$^{-/-}$ tumours, activation of JNK leads to upregulation of MMP1, which drives local invasion by degrading the basement membrane (Wu et al., 2017, Tapon, 2003). When we examined MMP1 intensity by immunofluorescence we observed a correlation between tumour size and MMP1 expression levels, with asparagine, glycine and tyrosine restriction having the greatest reduction in tumour size and MMP1 expression relative to the control (CDF) (**Figure 32.4.4.).**

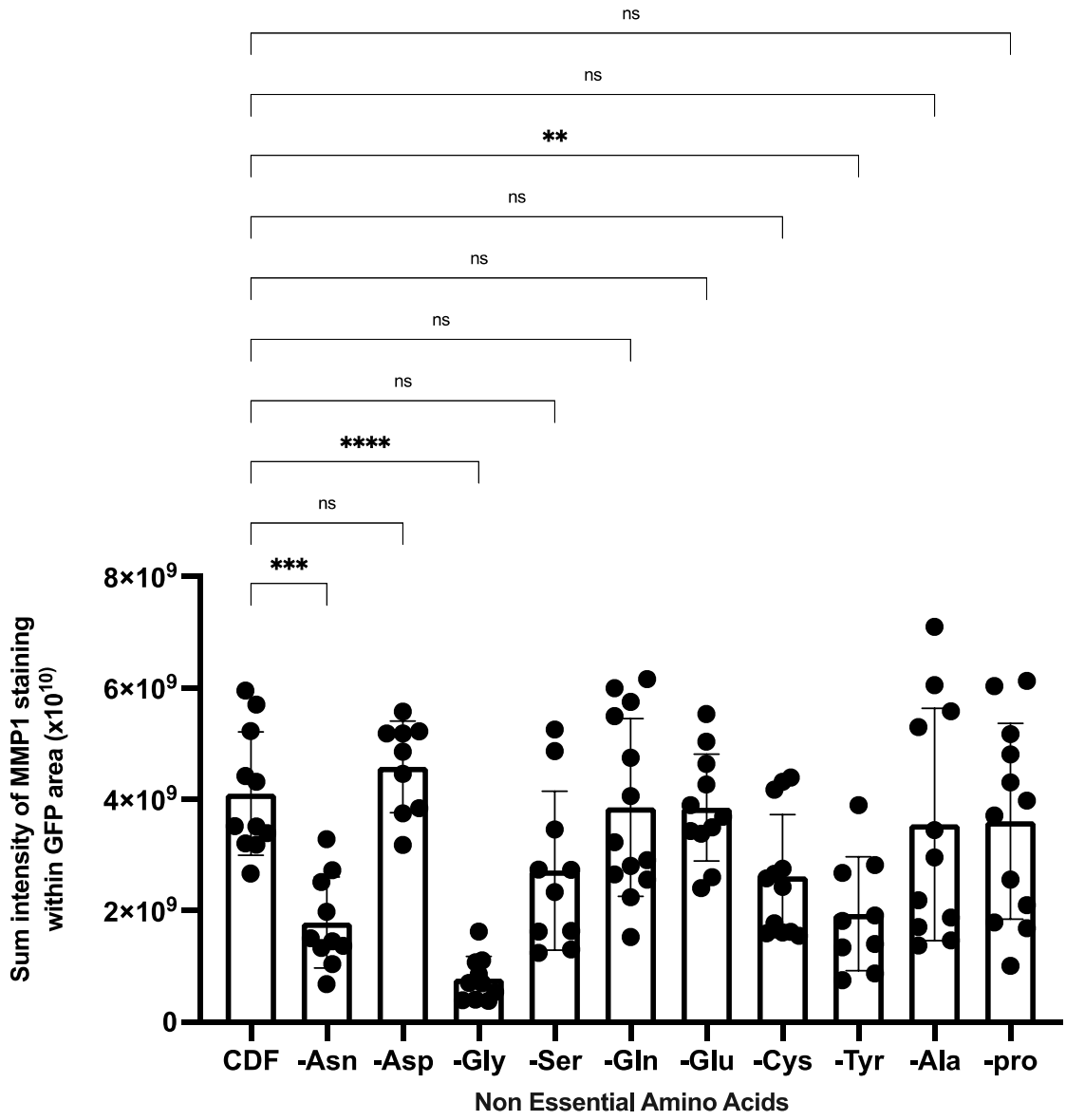

Figure 32.4.4. Quantification of MMP1 intensity within GFP-labelled tumours *Ras^{Val12}/ scrib$^{-/-}$*, grown on different diets.

Significant differences in MMP1 intensity of each diet lacking NEAAs compared to the chemically defined diet (CDF) are indicated with *. (One-way ANOVA was performed (Asn, P= 0.0009, Asp p=0.977, Gly, P<0,0001, Ser, P= 0.116, Gln, P=0.999, Glu, P= 0.999, Cys P= 0.0569, Tyr, P=0.003, Ala P=0.930 and Pro P=0.957). The error bar indicates SEM. Each data point is the measurement of MMP1 intensity within GFP-labeled cells, segmented surfaces from images of individual cephalic complexes, including eye discs, optic lobes and brain, (n>10).

Images of representative GFP-labelled eyes and brains tumours for each treatment are shown below (**Figure 33.4.5.**).

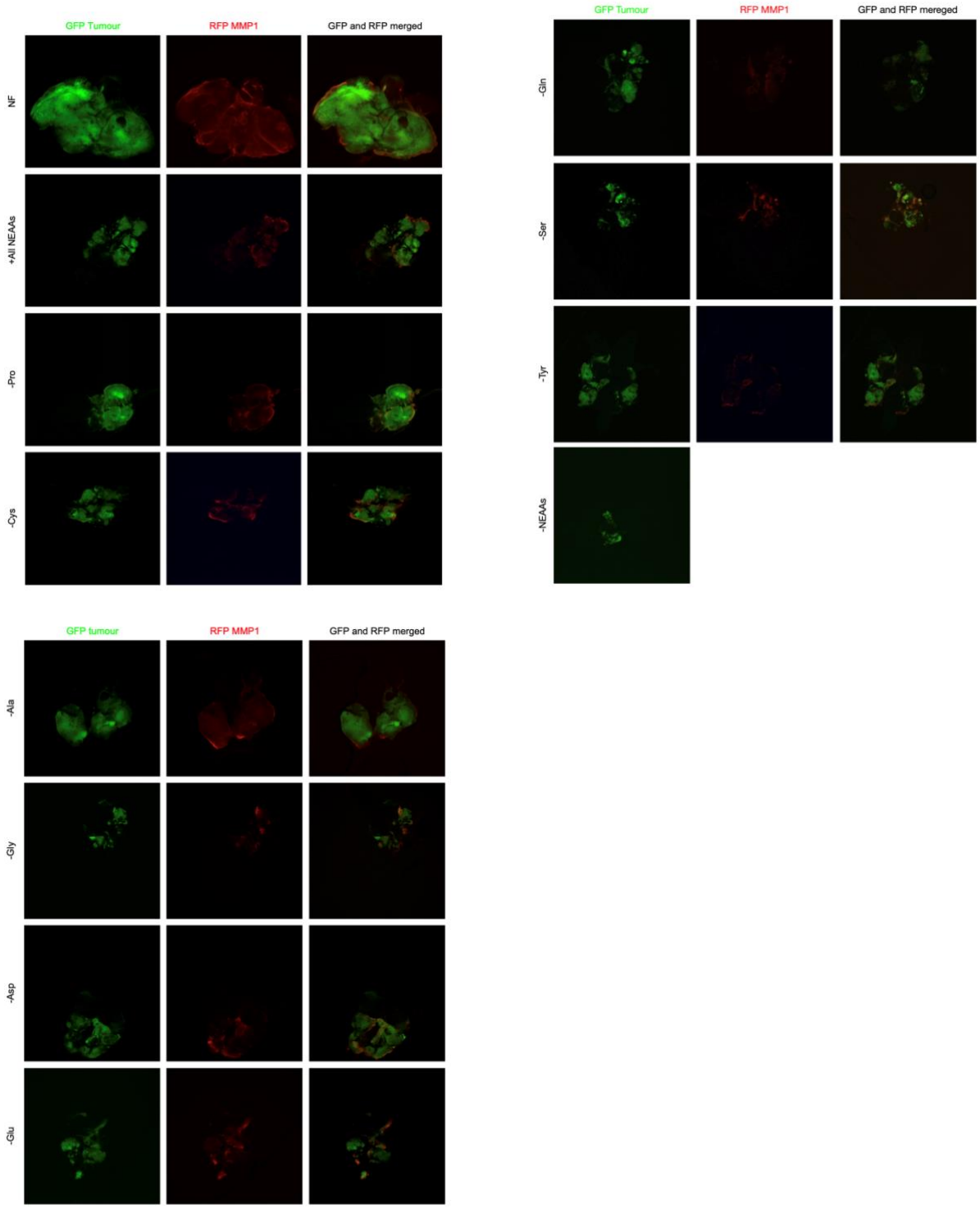

Figure 33.4.5. Brain and eyes discs from 3rd instar larvae showing the effect of amino acid deficient diets on tumour size and MMP1 expression.

Shown are GFP-labelled *Ras*^{Val12}/ *scrib*$^{-/-}$ tumours (in green), MMP1 (in red) and images where the two signals are merged. NEAA treatments are indicated on the left side of each image. Scale bar, 100 μm.

4.2.5. Scoring tumour invasion into the brain of *Ras^{Val12}/ scrib$^{-/-}$*

In our tumour model, cancer cells start to invade from eye disc into the optic lobe and into the ventral nerve cord. To determine effects of dietary intervention on tumour cell invasion into the brain we assigned individual cephalic complexes to one of four categories (Figure 34.4.6.A) allowing us to quantify the invasion phenotype in brains of 12-day old larvae with and without treatment (Figure 34. 4.6.B).

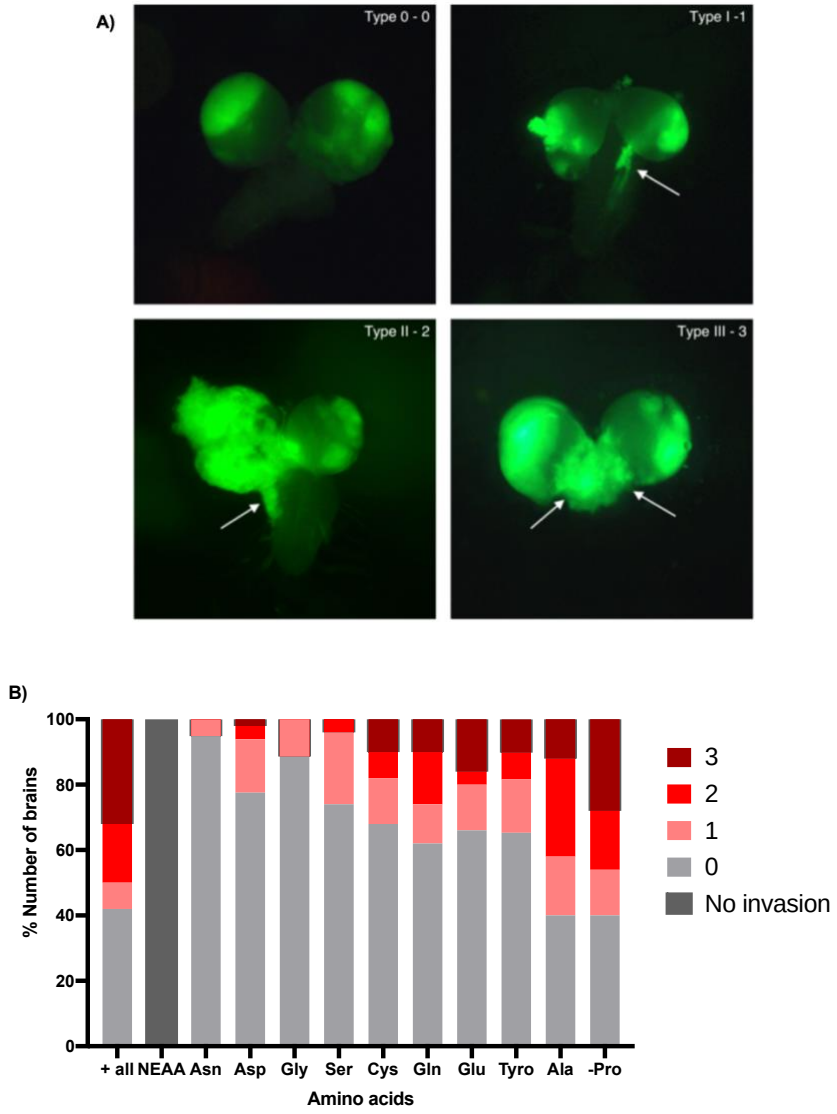

Figure 34.4.6.Dietry prevention and invasion.

(A) Dissemination of GFP from its original site of eye antennal discs to VNCs was scored on a scale of 0 to 3 for larvae grown on chemically defined media. (Stage 0) represents GFP localization in the optic lobes, (stage I) GFP disseminate to one side of the VNC, (stage II) on one side of VNC and overgrowth of one optic globe, and (stage III) optic lobe overgrowth and more extensive GFP distribution in the VNC (arrowed). **(B)** Average stage score of metastasis was determined for each experimental condition and the stacked bar chart illustrates percentage of brains assigned to each of the four categories described (A). Number of brains were (n = 50) for all amino acid treatments except Asn (n = 39), Gly (n = 44), NEAAs (n = 17), Asp (n = 49), Tyr (n = 49).

Dietary depletion of Asn, Gly, Tyr, Ser, Tyr and Asp suppresses tumour invasion. In the presence of all NEAA we observed invasion in 32% of larvae with the mean extent of invasion being (1.40). However, 42% of the animals showed no dissemination into the ventral nerve cord (stage 0), probably because the chemically-defined food, in general, delayed larvae growth, when compared to growth of larvae growing on NF. Tumours in larvae from NF grew massively by day 12 and as eyes discs and optic globes fused together and became undifferentiated, therefore, we could not score invasion in brain for larvae growing on NF. On media lacking all NEAAs, we found no tumour invasion to the brain, consistent with the greatly diminished growth of larvae on this food.

The lack of individual NEAAs affected the severity of invasion to different extents. Asparagine, glycine and serine and aspartate significantly limited the invasion compared to the All-inclusive diet (one-way Anova, p= <0.0001), whereas the absence of alanine and proline had no significant effect on the degree of invasion compared to complete synthetic diet (all) (one way Anova, p= 0.9688 and >0.9999, respectively).

Cysteine and tyrosine also significantly reduced the severity of invasion (One-way Anova, p= 0.0017, p= 0.0038, p= 0.0271, p= 0.0132), but to a lesser extent than asparagine, glycine, serine and aspartate.

4.3. Discussion

4.3.1. Glycine and asparagine:

Glycine and asparagine deprivation in our study severely impaired tumour progression, as measured by degree of tumour growth, induction of MMP1 expression and extent of local invasion into the brain.

Glycine is important for cancer cells as it is utilized for *de novo* purine nucleotide biosynthesis in rapidly proliferating cells (Jain et al., 2012). Further, glycine provides one-carbon units by one-carbon metabolism, a critical pathway for cancer cells as it is involved in nucleotide biosynthesis, protein translation, nicotinamide adenine dinucleotide phosphate (NADPH) regeneration and redox homeostasis (Maddocks et al., 2017).Glycine, therefore, is an important source for one carbon metabolism and insufficient uptake impairs tumour progression and invasion. A study on cancer cell lines reported that rapidly proliferating cells rely on glycine consumption. Deprivation of extracellular glycine and silencing glycine-synthesizing enzyme *serine hydroxyl methyl transferase enzymes (SHMT2*), slowed proliferation process in these cell lines and the proliferation was rescued by adding glycine to the medium (Jain et al., 2012). There is also an association between mortality in breast cancer patients and the expression of mitochondrial glycine biosynthesis pathway (Jain et al., 2012), indicating that glycine metabolism is highly associated with the invasiveness and progression of cancer. Another study showed linkage between the glycine metabolism enzyme, glycine decarboxylase (GLDC), to tumorigenesis as it induces changes in glycine, serine metabolism and glycolysis and lead to changes in pyrimidine metabolism to regulate the proliferation of cancer cells (Zhang et al., 2012). Glycine is a substrate of GLDC enzyme which is reported to be critical for tumour initiating cells in non-small cell lung cancer (NSCLC), upregulated in multiple cancer types, and correlated with poor survival in lung cancer patients (Zhang et al.,

2012). In addition, the glycine related metabolite sarcosine, an N-methyl derivative of glycine, increased during prostate cancer progression to metastasis (Sreekumar et al., 2013). These studies highlight the important roles of glycine metabolism in cancer progression and invasion and may therefore be targeted for therapeutic benefit.

Asparagine on the other hand, was clinically reported decades ago as a NEAA metabolic therapeutic target in acute leukemia patients. Asparaginase has been used to degrade asparagine in the plasma, and result in selectively killing leukemic cells because normal cells can survive and synthesize asparagine properly, whereas leukemic cells deficient of *asparagine synthase enzyme (ASNS*), cannot synthesize asparagine (Jaccard et al., 2009). The clinical utility of asparaginase clarify that asparagine is crucial for tumour growth. Moreover, asparagine has recently been reported to govern breast cancer metastasis (Knott et al., 2018), suggesting that dietary restriction and chemical inhibition of asparagine uptake and synthesis might be effective approach for treating breast cancer metastasis.

4.3.2. Serine and tyrosine:

Serine has a crucial role in biosynthesis reactions including folate-dependent reaction (Labuschagne et al., 2014), by providing one carbon units to support synthesis of purine and thymidine (lane and Fan ,20150). One carbon units derived from folate-dependent reaction can be also used to generate S-adenosylmethionine (SAM), a methyl donor, which supports methylation and synthesis of DNA, RNA, phospholipid, protein and polyamine, reviewed by (Luo et al., 2019). Serine can be also used to make glycine (Maddocks et al., 2017) and cysteine (DeNicola et al., 2015). It is reported that some tumours rely on *de*

novo serine synthesis and others on exogenous serine to support their growth (Labuschagne et al., 2014), reflecting the importance of serine in cancer progression. Given these biosynthetic roles of serine, tumours are sensitive to dietary serine withdrawal (Maddocks et al., 2017, Labuschagne et al., 2014).
Our data from *Drosophila*, shows that serine deprivation reduces tumour growth, which agrees with other *in vitro* and *in vivo* studies (Gravel et al., 2014).
Tyrosine restriction also showed an effect on tumour growth and dissemination. There is limited information about tyrosine functional biology in cancer cells, however, it is known to be involved in protein synthesis, reviewed by (Choi and Coloff, 2019). There is a drug (SM-88), developed based on tyrosine role in protein synthesis, and it is under clinical trials (Inc, 2020). SM-88 is absorbed by the cancer cell as a functional tyrosine, but it interrupts protein synthesis processes, after uptake (Inc, 2020, Pharma, 2021).

4.3.3. Glutamine and glutamate:

Cancer cells are able to preserve nitrogen for anabolic reactions and sustain their rapid proliferation (Coloff et al., 2016). Glutamine and glutamate are essential for these mechanisms because they provide nitrogen for the biosynthesis of other molecules including nucleotides and hexosamines and other NEAAs. Glutamine and glutamate also provide carbon in the form of *α-ketoglutarate (αKG*) by glutamate dehydrogenase (GLUD1) enzyme activity to support the biosynthetic functions of the tricarboxylic acid (TCA) cycle (Hosios et al., 2016b, Coloff et al., 2016, Yang et al., 2014).In addition, glutamine and glutamate are crucial for the synthesis of other amino acids, for example, glutamate is utilized to generate aspartate, serine, alanine and proline, which in turn are used for synthesizing glycine, asparagine, arginine and cysteine, reviewed by (Choi and Coloff, 2019). Several studies demonstrate cancer addiction to these amino acids as cancer cells

alter their metabolic pathway to overcome insufficient uptake of glutamine and glutamate from the diet, reviewed by (Jie et al., 2019).

Although we limited the glutamine uptake through dietary intervention in our studies, it has been reported that cancer cells are able to find other sources of the glutamine and are able to synthesise glutamine by glutamine synthesis (GLS) process, which requires glutamate and ammonia to function (Yang et al., 2016). Additional sources of glutamine are the proteolytic and macropinocytosis degradation of extracellular proteins (Commisso et al., 2013). In addition, metabolic alteration in stromal cells is triggered to provide and synthesize glutamine from multiple sources such as exosome endocytosis, and *de novo* glutamine synthesis, in order to meet the tumour requirements for glutamine (Bott et al., 2015). Moreover, it is reported that the oncogenic c-Myc regulates glutamine metabolism reprograming by increasing the expression of amino acid transporters and GLS, which results in more glutamine catabolism and increased sensitivity to glutamine withdrawal (Yang et al., 2009). Cancer cells also have a distinguishable pathway of acquiring glutamine, for example in human pancreatic ductal adenocarcinoma (PDAC), glutamine-derived aspartate is transported into the cytoplasm by aspartate transaminase to convert it into oxaloacetate. This subsequently increases the NADPH /$NADP^+$ ratio, which can potentially maintain the cellular redox state (Son et al., 2013). Thus, glutamine acquisition from the diet is not necessary for cancer progression, reviewed by (Jie et al., 2019).

The numerous sources of glutamine and glutamate available to cancer cells, and the variety of pathways by which theses amino acids are utilized, indicates the great challenges in producing therapies targeting their metabolism.

4.3.4. Aspartate, proline, cysteine and alanine:

Tumour cells were not significantly impaired by proline, alanine, cysteine and aspartate deprivation, indicating that other means of proline, alanine, cysteine and aspartate synthesis can satisfy the requirements in these cells.

Nevertheless, **Aspartate** has been shown to be essential for cancer proliferation as it is utilized to generate asparagine and to synthesis purine and pyrimidine nucleotides (Coloff et al., 2016). Aspartate is involved in the electron transport chain as it transfers electrons between the cytosol and mitochondria via the malate–aspartate (Birsoy et al., 2015), and it is found to be at low concentration in the cytosol among proteinogenic amino acids (Cantor et al., 2017). It is therefore, not transported efficiently into most cancer cells (Birsoy et al., 2015), suggesting that cancer cells rely on aspartate biosynthesis for their proliferation. Thus, it may be important to target enzymes involved in aspartate synthesis to impair tumour proliferation.

Proline is important for bioenergetics, stress protection, osmoregulation, and control of apoptosis in cancer cells (Tanner et al., 2018). In addition, proline is important for the variability of extracellular matrix structures because its cyclic shape and it is therefore participating in forming complex proteins such as collagen. Macropinocytosis resulted from collagen degradation therefore considered as another source of proline for cancer cells (Krane, 2008). Proline synthesis and degradation is regulated by the oncogenic *c-MYC* signalling pathway, indicating that proline metabolism is reprogrammed in cancer cells (Wei et al., 2012).

The variable sources of proline and metabolic changes in its synthesis and degradation, reported in the above studies, suggest that cancer cells reprogramed proline metabolism to overcome insufficient uptake. Moreover, a study conducted on a large panel of cancer cell lines showed that proline deprivation specifically reduces clonogenic potential of cancer cells (Sahu et al., 2016).

However, our result used an *in vivo* cancer model which may give more indication about the requirements for proline in the context of an intact TME.

Alanine's role in tumour progression is not understood compared to other NEAAs, however, it has been reported that alanine synthesis is correlated with proliferation (Coloff et al., 2016). In addition, in cancer cells, the extracellular matrix of the metastatic niche is shaped by hydroxylating collagen. It is found that alanine aminotransferase, converts pyruvate and glutamate to α-ketoglutarate, which is an important source for the hydroxylation of collagen and the preparation of the metastatic niche in breast cancer (Elia et al., 2019). This indicates that nutrients such as alanine could be important in cancer cells growth and metastasis. Interestingly, alanine secretion from stromal cells has been reported to promote cell survival in pancreatic cancer, and it is utilized in TCA cycle of the cancer cells (Sousa et al., 2016). This again indicates the importance of studying NEAAs role using *in vivo* cancer models and indicate the complex interaction between cancer cells and TME metabolism.

Cysteine is one of the amino acids that has been heavily studied in cancer cells (Combs and DeNicola, 2019). Cellular stress associated with sustained proliferation and increased demand of nutrients including cysteine, is caused by oncogenic transformation which produce signals to activate pathways and meet the requirement of cysteine from extracellular sources and *de novo* generation (Ioannis et al., 2017). Oncogenic *KRas* and *PI3K* signaling pathways, for example, are reported to activate the transcriptional regulator of cysteine (Nef2/ and its repressor protein Keap1), and thus controlling the downstream of cysteine metabolism (Lien et al., 2016, DeNicola, 2011). *Keap1/Nrf2* regulates the *reactive oxygen species (ROS), ROS* which cased cellular stress and are suppressed by oncogenes. Therefore, the oncogenes *K-Ras* increase the transcription of *Nrf2* to lower these *ROS* (DeNicola, 2011). Elevated glutathione

biosynthesis is important for *PI3K* activities, including initiation of tumour spheroids and resistance to oxidative stress, and thus *PI3K* activate *NRF2* to upregulate the *GSH* biosynthetic genes (Lien et al., 2016).

Cysteine can be acquired through multiple pathways, other than the diet uptake, it can be synthesised from *de novo* transsulfuration (Belalcázar et al., 2014, Leikam et al., 2014).

Cysteine is involved in tripeptide antioxidant glutathione (GSH) synthesis and cysteinase enzyme used as a drug and impaired the GSH synthesis, resulting in tumour growth suppression, in mice model (Cramer et al., 2017). Further, lymphocytic leukaemia (CLL) cells from patients, which have limited cysteine and thus limited GLS synthesis, can import cysteine from bone marrow stromal cells and release it to the TME to be up taken by CLL cells to promote GSH synthesis and survival (Zhang et al., 2012). This interaction between stromal and cancer cells indicates that that cancer cells may recruited cells in the TME to survive insufficient cysteine uptake.

4.4. Conclusion: Dietary intervention has been proposed to be a new therapeutic strategy in cancer, however, it is central to understand how tumour cells respond and adapt to NEAAS starvation for optimized therapeutic intervention.

Chapter 5: A non-autonomous requirement for glycine in tumour growth

5.1. Introduction

To increase amino acid uptake in cancer cells, amino acid transporters are often upregulated. For example, solute carrier (SLC) SLC7A5, SLC1A5, SLC7A11, and SLC6A14 found to be highly expressed in cancer, reviewed by (Bhutia et al., 2015). Therefore, logically, it is crucial to identify transporters that are functionally important to cancer cell survival and tumour progression so that suitable inhibitors can be developed for therapeutic intervention (Bhutia et al., 2015).

There are 11 SLC transporter gene families in humans, classified according to similarity of their amino acids sequence such as (primary structure), transporter mechanism (coupled, uniporter, exchanger, facilitated transporter and active transporter) and coupling icons such as (H^+, Na^+, K^+, Cl^-) reviewed by (Bhutia et al., 2015).

To complement and extend our analysis of amino acid restriction in the diet, we decided to focus our efforts on understanding the role of glycine because tumour cells were particularly sensitive to its loss in our system. To do this, we investigated the effect of knocking down the glycine transporter (*glyT*, *CG5549*) (**Table 18.**) genetically in cancer cells and the TME using the dual expression cancer models we had developed in chapter 2.

Table 17.Summary information about the Glycine transporter, compiled from Flybase (https://flybase.org/reports/FBgn0034911).

Molecular function	Temporal Expression Profile
neurotransmitter transmembrane transporter activity; neurotransmitter: sodium symporter activity; glycine: sodium symporter activity. It is involved in the biological process described with sodium ion transmembrane transport; glycine imports across plasma membrane; regulation of circadian rhythm; glycine transport; neurotransmitter transport.	Temporal profile ranges from a peak of low expression to a trough of no expression detected. Peak expression observed within 18–24-hour embryonic stages, during early larval stages, during late pupal stages, in stages of adults of both sexes

5.2.Glycine transporters in *Drosophila*:

There are two glycine transporters in *Drosophila*, which belong to the SLC6 family: GlyT1 and GlyT2 (Aragón and López-Corcuera, 2003). It is also possible that some of the other transporters move glycine along with other amino acids such as the amino acid sensors, SLC7 transporters (Featherstone, 2011, Galagovsky et al., 2018). Deletion of SLC6 family of transporters has dramatic physiologic consequences in human, however, less is known about this family of transporters in *Drosophila melanogaster* (Thimgan et al., 2006). GlyT1 regulates glycine synaptic levels (Gomeza et al., 2003a) and GlyT2 supplies neurotransmitter for presynaptic vesicle refilling and promotes the recycling of synaptic glycine at inhibitory synapses (Rousseau et al., 2008).

CG5549 (GlyT2) encodes the major transporter of glycine in flies and is localised broadly in the central nervous system (CNS)(Aragón and López-Corcuera, 2003, Cristina et al., 2018) especially in optic neuropils and photoreceptors (Thimgan et al., 2006). It is highly similar to its mammalian orthologues, SLC6A5 and SLCA9 (Romero-Calderon et al., 2007) (Boudko et al., 2005). Transgenic RNAi lines capable of expressing inverted repeats (IR) for *CG5549* (*CG5549*^{IR}), were previously found by real-time qPCR to reduce the level of *CG5549* mRNA to ~30% of wild type in fly heads (Frenkel et al., 2017). Knockdown of GlyT2 in adult flies using *CG5549*^{IR} resulted in impaired rhythmicity of the central circadian pacemaker, implicating glycine uptake in regulating daily light-dark activity patterns (Frenkel et al., 2017).

5.3. Results

5.3.1 RNAi line characterization

In this chapter we are aimed to dissect where glycine uptake is required to support the growth of Ras-induced tumours. Transgenic RNAi lines for *CG5559* were selected with reference to the literature and following off-target searches using UP-TORR (Updated Targets of RNAi Reagents; www.flyrnai.org/up-torr), an online database of *in vivo* RNAi reagents from all the major public collections (Hu et al., 2013),(**Table 19**). These were then combined with our cancer models Ras^{Val12}*/ dlg* (tumour, haemocytes and neural cancer models) by fly breeding to generate a panel of "tester" strains **(**see Methods, Table 2. Genotypes of different cell types in TME**)**.

As explained in Chapter 2, Ras^{V12}*/scrib* tumours develop in a very similar way to those of Ras^{V12}*/dlg* and have a number of features in common. We also have looked at the eye phenotype associated with these RNAi lines according to (Pletcher et al., 2019), where the *eyes absent composite enhancer-GAL4* (*eya composite*-GAL4) driver was used to induce expression of RNAi during development of the eye imaginal disc .

Table 18.Transgenic RNAi lines and their off-target affect.

These lines encode inverted repeat constructs for the gene of interest. Both lines were obtained from the Japanese National Institute of Genetics (NIG).

UAS-RNAi, transgenic ID, SOURCE	**Eyes phenotype according to Pletcher *et al.*, (2019) paper**
5549R-1, NIG	Glossy, rough
5549R-2, NIG	Wild type (WT)

We used *5549R-1* and *5549R-2* RNAi lines ,which previously been characterized by real-time qPCR (Frenkel et al., 2017), to knockdown GlyT in three different TME compartments in our *Ras*^{Val12}*/ dlg* cancer model: **A)** tumour cells using a flip-out *Act-Gal4* driver; **B)** haemocytes using *he-Gal4* driver; **C)** neural cells using the pan-neuronal *nSyb-Gal4* driver **(Figure 35.5.1.)**.

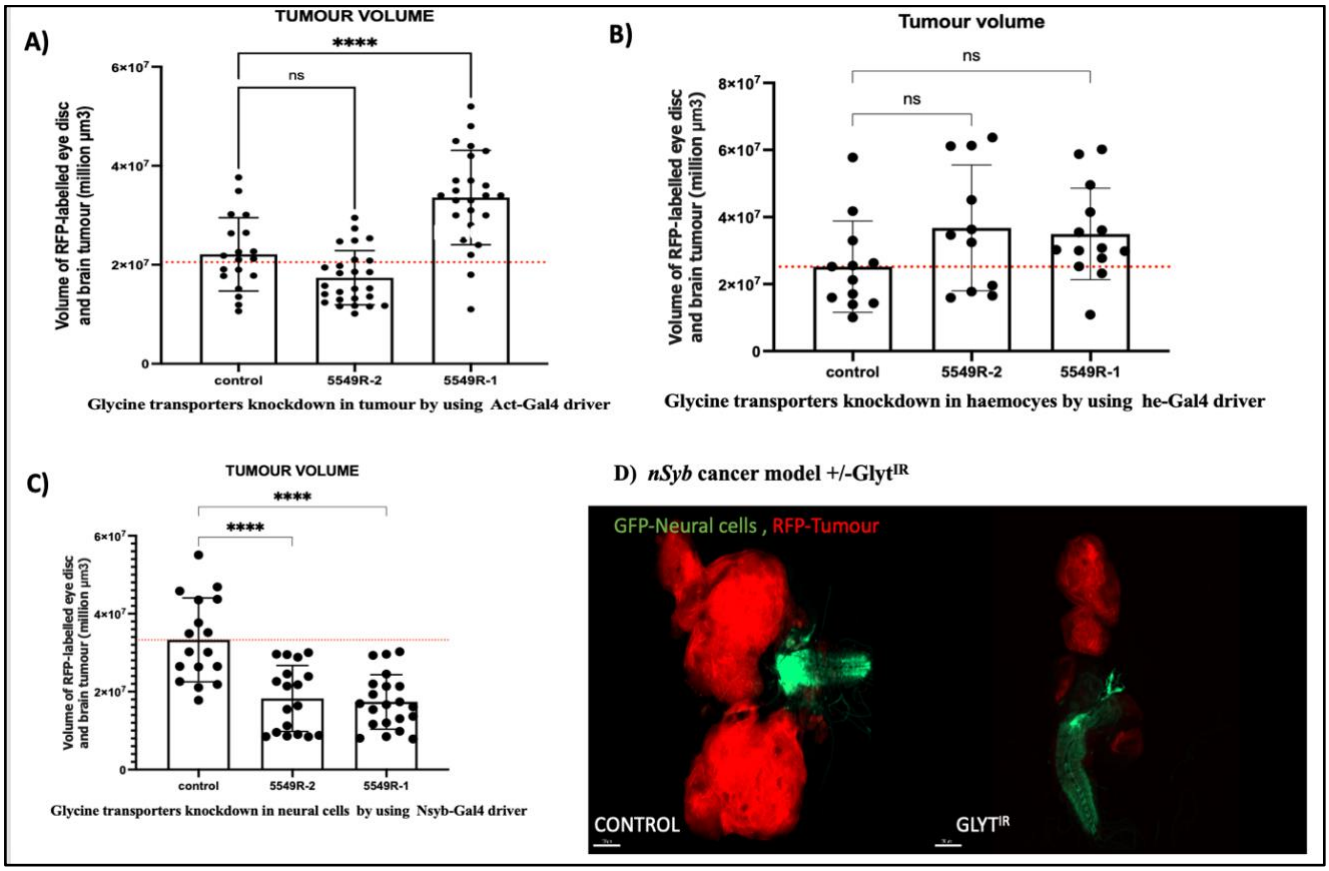

Figure 35.5.1. Volume of RFP-labelled tumours (*Ras*^{V12}*/dlg)* in the presence or absence of driven GlyT RNAi lines in different cells.

A-C, Effects of knocking down glyT using A) *Act-y-Gal4* driver (tumour cells), B) h*e-Gal4* driver (haemocytes cells); or C) *nSyb -Gal4 driver* (neural cells). Each data point is the measurement of total volume of RFP-labelled cells, segmented surfaces from images of individual cephalic complexes, including eye discs, optic lobes and brain, (n>10). The error bar indicates SEM. Significant differences in tumour volume compared to control in A,B and C are indicated with *. C)Knockdown of GlyT with either RNAi line using the pan neuronal *nSyb-Gal4* driver significantly reduced the tumour size by 1.8 and 1.9 fold, respectively (one way ANOVA was performed, **** P<0.0001, A) 5549R-2, P=0.078 , B) 5549R-2 P= 0.1338, 5549R-1 , P=0.196). Red line indicates the mean of the control. D) Image showing the differences between tumour size +/- GlyT knockdown in neural cells. 150 µm scale is shown. Genotype of the control: *ey(3.5)FLP, UAS-td-GFP, dlg*^{GFP}*/Y; Lo-Ras*^{V12}*, Lo-GFPi-*

mCherry/+; nSyb-GAL4, Act>LexA/UAS-GlyT^{IR}). Genotype of GlyT^{IR}: (*ey(3.5)FLP, UAS-td-GFP, dlg^{GFP}/Y; Lo-Ras^{V12}, Lo-GFPi-mCherry/+; nSyb-GAL4, Act>LexA/UAS-GlyT^{IR}*) .

Strikingly, knockdown of GlyT with either RNAi line using the pan neuronal *nSyb-Gal4* driver significantly reduced the tumour size by 1.8 and 1.9 fold, respectively (P<0.0001). No effect was seen when the RNAi lines were expressed in haemocytes with, *he-GAL4*. One line enhanced tumour growth when expressed in the tumour with *A>y>GAL4*.

CG5549/glyT is expressed in eye discs and is required for normal eye development (Pletcher et al., 2019) (**Table. 19**.) but is not required in eye-disc tumours for their growth. These data do not rule out the possibility that cancer cells require glycine, which they acquire through the action of other, less specific, amino-acid transporters. However, our data indicate that glycine transporter activity provided by *CG5549* is required in neural cells for tumour progression.

5.4. Exploring the oncogenic potential of glycinergic signalling in the brain: insights from the literature

5.4.1. Glycinergic signalling and the circadian clock:

In *Drosophila*, there are approximately 150 clock-neurons organized in groups based on their location and size: Ventrolateral neurons (small and large lateral neurons ventral), dorsolateral neurons (lateral neurons dorsal, lateral posterior neurons, and dorsal neurons 1–3 and three groups of dorsal neurons (Shafer et al., 2006). Less is known of how these neurons communicate in *Drosophila* (Shafer et al., 2006). However, it is known that glycine functions as an inhibitory

neurotransmitter (Frenkel et al., 2017). The absence of its transporter GlyT2, in mice, has shown to eliminate glycinergic neurotransmission inhibitory function (Gomeza et al., 2003b). Another study on fast neuronal communication in *Drosophila*, revealed that glycine is employed by the ventral lateral neurons (LNvs) and has a role in the central circadian pacemaker in the *Drosophila* brain (Frenkel et al., 2017). The circadian clock is a timekeeping mechanism that coordinates behavioural and physiological processes with cyclical changes occurring within the environment (Hegazi et al., 2019). Adult flies in which glyT is knocked down with $CG5549^{IR}$ in their heads, showed close to 1-hr lengthening of the free-running circadian period compared controls. Similar results on period length were noticed when the enzyme converting serine into glycine were disrupted (Frenkel et al., 2017). Therefore, this study strongly suggests that **glycinergic inhibition of specific targets is a cue that contributes to the synchronization of the circadian network.**

A subtle increase in light intensity at night can trigger arrhythmicity in the clock, *and it is been shown that flies with* $CG5549^{IR}$ became arrhythmic by (~80 %) while the control flies showed complex rhythms by 60-70 % , reinforcing the idea that glycinergic transmission is crucial for the stability of the activity patterns (Frenkel et al., 2017). These data show that **Glycine depletion also renders the circadian network susceptible to environmental changes.**

Note : We initially started looking at the involvement of circadian genes in cancer progression. Bioinformatic data was collected, similar to CPT2 project. These data were used to guide us on choosing the most critical circadian genes in human cancer as well as their orthologue in flies, data in supplementary (Circadian genes bioinformatics PPT, **Appendix II)** . We had trouble testing these genes in flies

due to the delays in placing and receiving orders. However, RNAi lines for *period* and *clock* genes were chosen for analysis.

Initial experiments were performed using our *Ras^{V12}/dlg* cancer model Knockdown of *period* in the tumour had no significant effect on tumour growth (One way ANOVA, P=0.3439) (**Figure 36.5.2**.). Future experiments will be focused on testing the effects of *period* and *clock* RNAi lines from Michael Rosbash (Zhao et al., 2003) in neuronal cells using *nSyb-GAL4.*

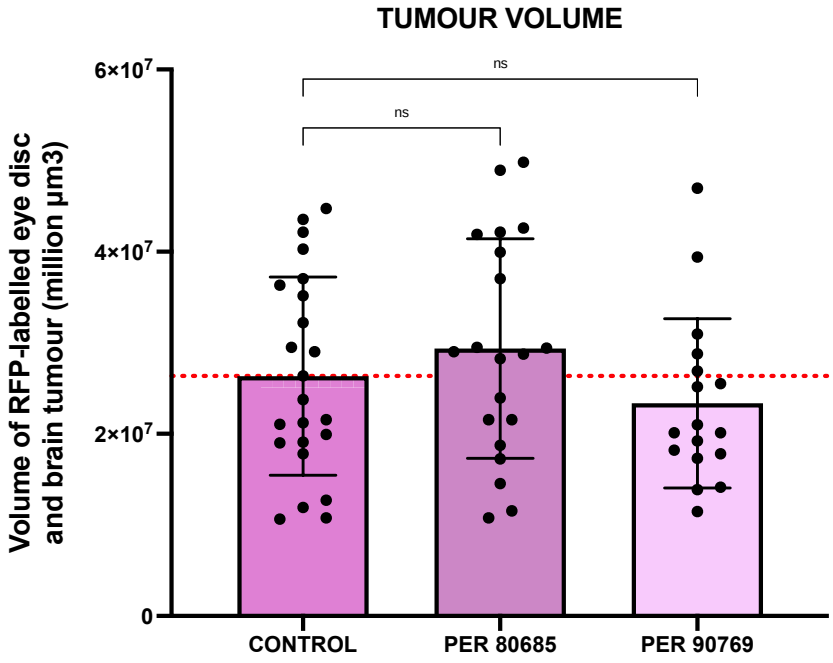

Figure 36.5.2. Volume of RFP-labelled cells (*Ras^{V12}/dlg)* in the presence or absence of driven *Per* knockdown in cancer cells.

The error bar indicates SEM. Red line represents the mean of the control. Each data point is the measurement of total volume of RFP-labelled cells, segmented surfaces from images of individual cephalic complexes, including eye discs, optic lobes and brain, (n>10). Tumour volume of RFP-labelled cells with *Per* knockdown was not significantly affected compared to the control, (One way ANOVA, *PER* 80685, P=0.9 and *PER* 90769 P= 0.8). Genotype of the control: *ey(3.5)FLP, UAS-td-GFP, dlg^{GFP}/Y; Lo-Ras^{V12}, Lo-GFPi-mCherry/+; Act>y-GAL4, Act>LexA/+). Per RNAi lines* Genotype: *ey(3.5)FLP, UAS-td-GFP, dlg^{GFP}/Y; Lo-Ras^{V12}, Lo-GFPi-mCherry/+; Act>y-GAL4, Act>LexA/UAS-Per^{IR}).*

Note: We were not able to generate data on period and clock knockdown in *nSyb-GAL4* in this thesis. It is, however, will be tested by Daimark's current post-doctor at University of Manchester .

5.4.2. Control of steroid hormone signalling by the clock:

Perturbation of the circadian clock, in the *Drosophila* prothoracic gland (PG), the major steroid hormone-producing organ, can have the effect of reducing steroid production and thus can block larval development (Di Cara and King-Jones, 2016). The steroid hormone Ecdysone is produced primarily in the PG and, when it is released into the hemolymph, is converted into an active form, 20-hydroxyecdysone (20E). 20E is the primary molting hormone, which binds to a nuclear receptor and initiates expression of various genes, which then leads to the morphological, behavioural and physiological changes associated with molting and metamorphosis (Yamanaka et al., 2013). Ecdysone initiates developmental transitions by controlling gene expression via its heterodimeric protein receptor, consisting of ecdysone receptor subunit (*EcR*) and ultraspiracle (*usp*) (Oro et al., 1990). The EcR/USP complex binds to ecdysone response element (*EcRE*) in the enhancers of specific target genes, leading to an increase in target gene transcription (Ashburner, 1973).

Ecdysone is regulated by prothoracicotropic hormone (*PTTH*), a neuropeptide hormone that is produced in the brain. *PTTH* upregulates the level of ecdysteroidogenic enzyme transcription in the PG through the *ERK/MAPK* signaling pathway (Yamanaka et al., 2013). *PTTH* is known to be controlled by circadian clocks (Ou et al., 2011). *PTTH'*s receptor, *Torso*, is highly specific to the PG (Ou et al., 2011). *PTTH* acts as a timer the metamorphosis and final body size of the *Drosophila* larva, but that it is not required metamorphosis (Ou et al., 2011).

In addition, *timeless*, a core component of *Drosophila* clocks, has been reported to be coupled with the circadian machinery to regulate steroid synthesis by *PTTH* and insulin signalling (Di Cara and King-Jones, 2016). Hence, Ecdysone production is controlled by *PTTH* which is controlled by the circadian clocks.

Taken together, these studies together indicate that, by blocking glycine transmitting into the brain, the circadian clock is disturbed, potentially affecting hormonal secretion.

5.4.3.Steroid hormone ecdysone mediates tumour suppression during metamorphosis in flies:

Developing eye-antennal imaginal discs cells homozygous mutant for Polyhomeotic (Ph) can overgrow and develop neoplastic tumours (Martinez et al., 2009). These tumorigenic *ph* mutant cells are transformed into nontumorigenic cells and eliminated during metamorphosis by ecdysone meditated signalling (Yanrui et al., 2018). Ecdysone regulates the expression of the microRNA *lethal-7 (let-7*), which when activated suppresses its target, the transcription factor *chronologically inappropriate morphogenesis* (*chinmo*). This facilitates differentiation, thereby suppressing tumour overgrowth (Yanrui et al., 2018).

It is worth noting that *let-7* has a consensus sequence that is identical from *Caenorhabditis elegans* to humans ; meaning it is controlling a conserved targets in regulating differentiation and proliferation (Büssing et al., 2008).

Moreover, in another study it has been shown that overexpression of *chinmo* in cooperation with Ras^{V12}, promotes JNK-independent epithelial tumour formation in the eye-antennal imaginal disc (Doggett et al., 2015). Retinal cell fates are marked by the expression of the differentiation factors *Embryonic lethal abnormal vision (Elav), Dachshund (Dac)*and *Eyes absent (eya),* which form the

core of the so-called retinal determination network (Tavsanli et al., 2004). Overexpression of *chinmo* blocks these factors in the eye disc priming cells towards transformation (Doggett et al., 2015). Moreover, *chinmo* overexpression also increases numbers of enteroblast like cells in the adult flies midgut, and induces intestinal neoplasia in the presence of Ras^{ACT} (Doggett et al., 2015). It is been reported in (Ras^{ACT}/N^{ACT}) driving tumorigenesis in the eye-antennal disc, *chinmo* is a *JNK-induced* gene and has an oncogenic function as it maintains progenitor-like states (Doggett et al., 2015). Its overexpression promotes stem cell proliferation, and, in response to JAK/STAT signaling, *chinmo* is expressed within the progenitor domain of the eye disc and required for eye disc growth and/or proliferation. Together, these data indicate that *Chinmo* could be an important STAT effector of progenitor cell maintenance in the eye-antennal disc tumors, downstream of JNK signalling. On the other hand, overexpression of the *let-7* cascade suppresses the overgrowth of brain tumours in *brain tumour* (*brat*) mutant flies (Yanrui et al., 2018). In *Drosophila*, *brat* gene mutations lead to the formation of malignant brain tumours. According to this study, brain tumours with chinmo overexpression continue to grow in adults flies, while overexpression of *let-7* suppressed the tumour growth (Yanrui et al., 2018). It is therefore suspected that *let-7* inhibits *brat* tumour growth by suppressing *chinmo*.

One or more *let-7* members downregulation has been observed in different human cancers (Shell et al., 2007). Functions of *let-7* family members in the human genome are more complicated and still remain elusive (Shell et al., 2007).

It is important to note that most of the *Drosophila* studies cited above have revealed conserved mechanisms and/or molecules used in mammals.

5.5. Glycinergic signaling to tumour hypothesis:

Insights from the literature summarised above led to the following hypothesis: Glycine transported into the brain via the *glyT(CG5549*) regulates the circadian clock; when glycinergic signalling and the circadian clock are disrupted, ecdysone is induced; ecdysone induces *let7* in the eye disc, reducing chinmo levels, and relieving inhibition of differentiation; this leads to increased differentiation and the suppression of tumour growth (Figure 37.5.3.).

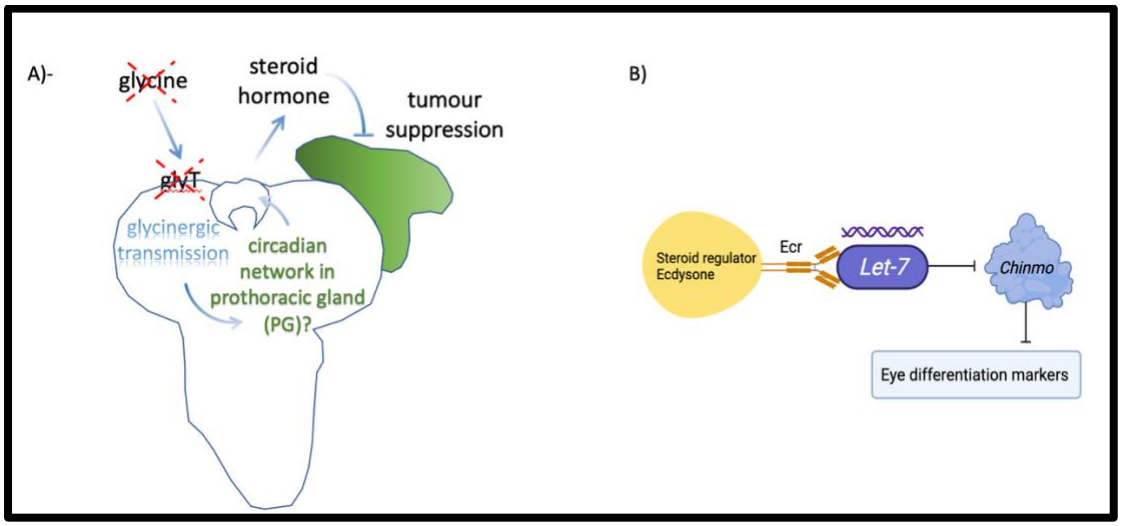

Figure 37.5.3. Graphical representation of our hypothesis .

Graphical representation of how GlyT knockdown might act in neural cells act non-autonomously to suppress tumour growth. A)- We propose that glycine transmission into the brain is suppressed by GlyT knockdown and therefore its inhibitory neurotransmitter function is blocked, affecting synchronization of the circadian network in PG. Steroid production is regulated in the PG and due to glycine depletion, we hypothesise that steroid production is upregulated, and this supresses tumour growth. **B)-** We further predict that tumour growth is supressed by increased *ecdysone (ECR)* inducing *let7* in the eye disc, reducing *chinmo* levels, and relieving inhibition of eye differentiation.

5.6. Experiments to test Glycinergic signaling to tumour hypothesis

5.6.1. Mass spectrometry study:

To show that this pathway is involved in our third-instar tumourous larvae, we first tested the possibility that circulating 20E was elevated following *glyT* knockdown in neuronal cells. Using metabolomics, we analyzed the circulating haemolymph from animals harbouring tumours ± neuronal-specific *glyT* knockdown. Previous studies have used liquid chromatography tandem mass spectrometry (LC-MS/MS) methods for measuring steroids, see (Keevil, 2013). Therefore, we adopted a similar approach, Method described in 2.10. Mass Spectrometry experimentMass spectrometry analysis was performed by Nigel Gotts in the Centre for Metabolomics research, Liverpool.

5.6.1.A. Result

Initial standard addition results showed that pooled control samples (*Ras/dlg* with *nSyb* alone) were estimated to contain **0.03-0.30 20E pg/uL** heamolymph, whereas the concentration of 20E in extracts from Ras/dlg, nSyb>glyT larvae was likely between **4.04-4.33 20E pg/uL** heamolymph. In view of very low biomass, it remains difficult to form firm conclusions from these data. However, these preliminary results indicate that 20-Hydroxyecdysone may be elevated in tumourous larvae in which glyT is knocked down in neuronal cells using nSyb-GAL4. Further repeats with increased biomass is required to validate these findings.

NOTE. Our samples were subject to careful optimisation, done by our collaborator Nigel Gotts (data not shown). Preliminary data was collected on 40 µL and 70 µL of haemolymph. An additional 100µl haemolymph was collected from animals harbouring tumours ± neuronal-specific glyT knockdown. However, due to this time consuming process , further study has been postponed until the quantity needed for replication is available.

5.6.2. Supplementing diet with 20E study

To test the potential for systemic 20E to suppress *Ras^{va12}/Dlg* tumour growth we fed larvae harbouring *Ras^{va12}/Dlg* tumours with the biologically active form of ecdysone 20-Hydroxyecdysone (20E, Steraloids Inc.). We grew larvae harbouring *Ras^{V12}/dlg* tumours (*ey(3.5)FLP, UAS-td-GFP, dlg^{GFP}/Y; Lo-Ras^{V12}, Lo-GFPi-mCherry/+; nSyb-GAL4, Act>LexA/+)* on food containing either 20E and ethanol. Tumorous 10 days old larvae were then dissected and imaged according to our method described in the method chapter 2. Analysis of RFP-tumour volume showed that larvae fed 20E had 1.9 fold reduction in tumour size compared to the control (t test, P<0.0001) **(Figure 38.5.5.).**

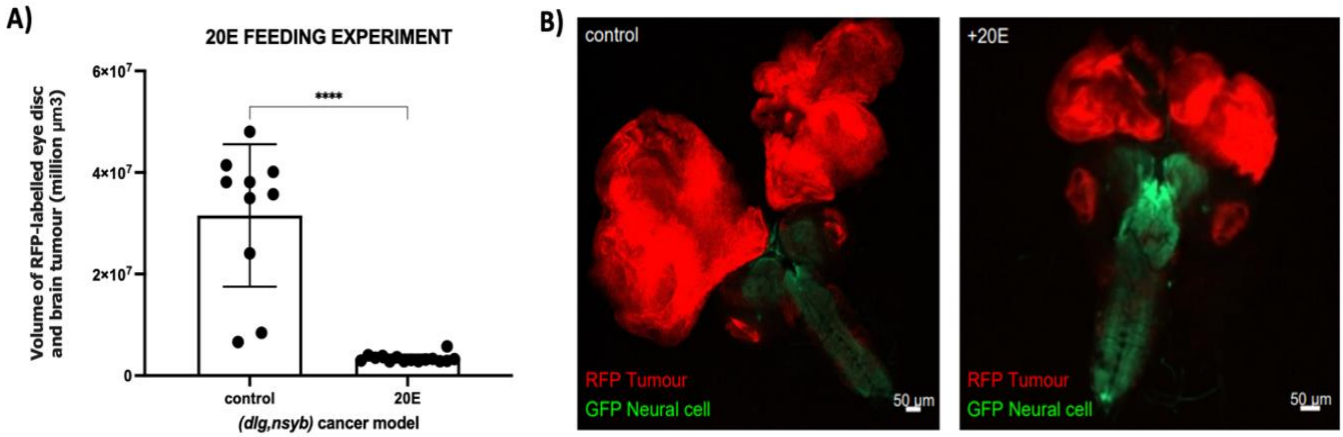

Figure 38. 5.5. Volume of RFP-labelled cells (*Ras^{V12}/dlg)* in larvae growing on food +/- 20E.

A) Volume of RFP-labelled tumours in larvae growing on food +/- 20E. Analysis of RFP-tumour volume showed that larvae fed 20E had 1.9 fold reduction in tumour size compared to the control (t test, P<0.0001). **B)** Image showing the differences between tumours models growing on food +/- 20E. Genotype: *ey(3.5)FLP, UAS-td-GFP, dlg^{GFP}/Y; Lo-Ras^{V12}, Lo-GFPi-mCherry/+; nSyb-GAL4, Act>LexA/+).* The error bar indicates SEM. 50 µm scale is shown. Each data point is the measurement of total volume of RFP-labelled cells, segmented surfaces from images of individual cephalic complexes, including eye discs, optic lobes and brain, (n>10).

This result supports the hypothesis that elevated ecdysone levels results in reduced tumour size.

5.6.3. Ectopic tumour-directed expression of the EcR suppresses tumour growth

As per the discussion earlier, *Drosophila* ecdysone (steroid hormone) controls the larval transition into the subsequent developmental stage by its receptor EcR (Davis et al., 2005). The EcR protein has three isoforms (*Ecr-A, Ecr-B1, and Ecr-B2*), each with distinct patterns of expression in larval and imaginal tissues suggesting that their responses confer with tissue specificity (Davis et al., 2005). *EcRB1* is a neuronal-specific ecdysone receptor isoform, regulated temporarily in the neuroblasts from the mid third instar larval stage (Syed et al., 2017). *EcR-A*, on the other hand, is expressed highly in the imaginal discs which differentiates to form the head of the adult fly during metamorphosis, as well as in larval tissues and imaginal histoblasts but at a low level (Talbot et al., 1993).
To explore whether ecdysone is likely to be acting directly on tumour tissue we next investigated the effect of modulating *Ecdysone Receptor (EcR*) levels in Ras^{V12}*/dlg* eye imaginal discs. We also looked at the potential role of downstream signalling via *let-7* and *chinmo*.
Effects of overexpressing ecdysone receptors *EcR*, or overexpression of *let-7* or knockdown of *Chinmo* in the eye discs of our cancer model Ras^{V12}*/dlg* using Act-Gal4 driver, activated by *ey-FLP*, are shown in **Figure 39.5.7.**

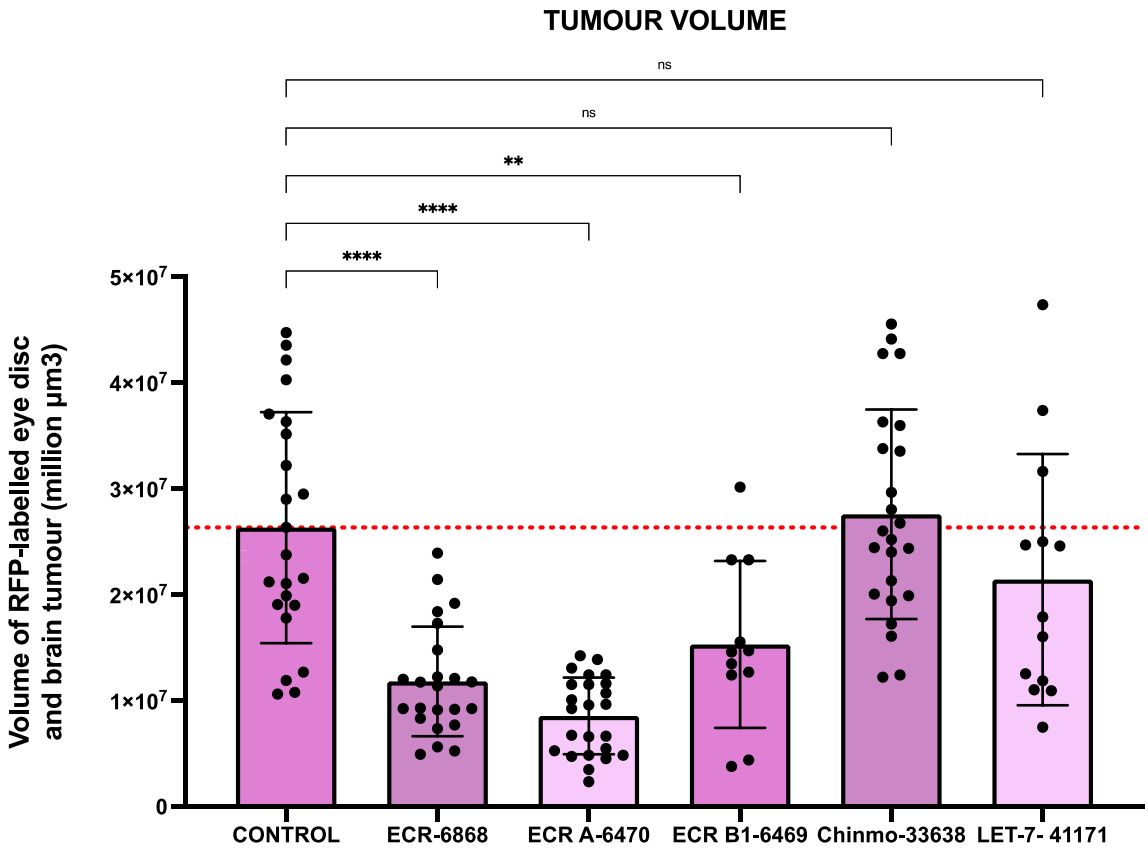

Figure 39.5.7. Volume of RFP-labelled tumours cells (*Ras^{V12}/dlg)* in the presence or absences of driven *Ecr, Chinmo and Let-7* knockdown in cancer cells.

The error bar indicates SEM. *UAS-Ecr* (Bloomington stock centre: BL-6868), UAS-EcRA (BL-6470), *UAS-EcRB1* (BL-6469),*UAS-RNAi-chinmo* (BL-33638), *UAS-let-7* (BL-41171). Red line represents the mean of the control. Each data point is the measurement of total volume of RFP-labelled cells, segmented surfaces from images of individual cephalic complexes, including eye discs, optic lobes and brain, (n>10). Significant differences in tumour volume compared to the control are indicated with *. One-way ANOVA was performed, **** P<0.0001, *ECR B1*, **P= 0.0027, *Chinmo* P=0.983 and *Let-7*, P= 0.509). Genotype of the control: *ey(3.5)FLP, UAS-td-GFP, dlg^{GFP}/Y; Lo-Ras^{V12}, Lo-GFPi-mCherry/+; Act>y-GAL4, Act>LexA/+). Genotype of the RNAi lines : ey(3.5)FLP, UAS-td-GFP, dlg^{GFP}/Y; Lo-Ras^{V12}, Lo-GFPi-mCherry/+; Act>y-GAL4, Act>LexA/UAS-RNAi).*

Although *chinmo* knockdown or *let-7* overexpression did not affect tumour growth, we found that ectopic expression of the ecdysone receptors in tumour cells suppressed tumour growth and phenocopied the effects of *nSyb>GlyT* knockdown or ecdysone supplementation. We used different Ecr isoforms, which have been reported to have different developmental roles. They all suppressed the

tumour, albeit to different extents. Again, this is consistent with the potential for ectopic ecdysone to suppress tumour growth.

To explore the role of other downstream pathways that might mediate the effect of Ecdysone in tumour cells, we turned to transcription factors, including Broad (*br*), which is an early target of ecdysone signalling and promotes cell differentiation to repress chinmo (Narbonne-Reveau and Maurange, 2019). As discussed previously, *chinmo* controls oncogenic transformation by blocking differentiation in the eye disc (Doggett et al., 2015). In *Drosophila,* the *broad complex* belongs to complex/Tramtrack/Bric-à-brac Zinc-finger (*ZBTB*) transcription factor family, and encodes a family of proteins each possessing a common core (BR-C "core") domain and one of four pairs of zinc fingers (*Br-Z1, Br-Z2, Br-Z3 and Br-Z4*) (Tzolovsky et al., 1999). BR-C has an amino-terminal motif, called the BTB or POZ domain, which is highly conserved and is involved in protein-protein interactions and in a large array of functions during development and malignancy, reviewed by (Lee and Maeda, 2012). The *broad* complex is essential for the morphogenesis of imaginal discs (Tzolovsky et al., 1999). We therefore tested *br* involvement in tumour suppression, by overexpression of either *br-Z1* or *br-Z3* transcripts in Ras^{V12}*/dlg* tumour cells (**Figure 40.5.8**.)

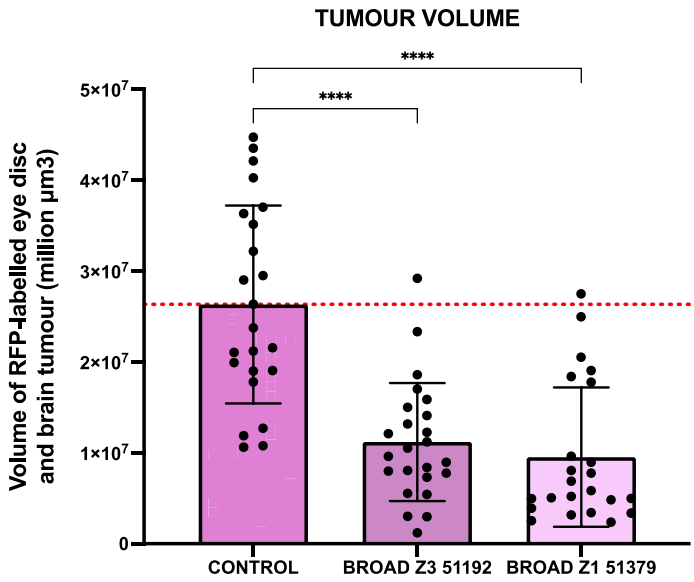

Figure 40.5.8. Volume of RFP-labelled tumours cells (*Ras^{V12}/dlg)* in the presence or absence of driven *Br* knockdown in cancer cells.

The error bar indicates SEM. Red line represents the mean of the control. Each data point is the measurement of total volume of RFP-labelled cells, segmented surfaces from images of individual cephalic complexes, including eye discs, optic lobes and brain, (n>10). Significant differences in tumour volume compared to the control are indicated with *. One-way ANOVA was performed , **** P<0.0001. Genotype of the control: *ey(3.5)FLP, UAS-td-GFP, dlg^{GFP}/Y; Lo-Ras^{V12}, Lo-GFPi-mCherry/+; Act>y-GAL4, Act>LexA/+).* Genotype of the *Br* RNAi lines*: ey(3.5)FLP, UAS-td-GFP, dlg^{GFP}/Y; Lo-Ras^{V12}, Lo-GFPi-mCherry/+; Act>y-GAL4, Act>LexA/UAS- Br ^{IR}).*

We found that overexpression of *br-Z1* and *br-Z3* isoforms in cancer cells (with Act>GAL4, expressed by *eyFlp*) significantly suppressed tumour growth.

5.7. Discussion:

In this chapter, we find that knockdown of the major glycine transporter, glyT2, in neurons acts to suppress growth of epithelial tumours in the developing eye imaginal disc. We hypothesise that these inter-tissue effects may be mediated by circuitry in the brain controlling the circadian clock because circadian neurobiology is a key target of glycinergic signalling in *Drosophila* (Frenkel et al., 2017). This raises the possibility that nutritional inputs mediate changes in the neuronal circadian clock, ultimately impacting on tumour growth and

progression, perhaps via steroid hormone production (Yanrui et al., 2018) which we know is under control of glycinergic neuronal circuits (Di Cara and King-Jones, 2016).

A key, but preliminary, observation in support of this idea is that elevated ecdysone could be detected in haemolymph from tumourous larvae harbouring *nSyb>GlyT*^{IR}. This result needs to be repeated to increase confidence in the finding and better quantify the effect. This could be done using a 20-Hydroxyecdysone ELISA assay, which is now commercially available, and may be more sensitive than the LC-MS/MS approach.

To test the potential of elevated ecdysone to suppress tumour growth, we performed 20E feeding experiments; we also tested the effect of EcR overexpression. Both approaches showed similar results.

It is been reported that feeding larvae with 20E restricts regenerative capacity of damaged tissues in the eye and wing (Halme et al., 2010). As ecdysone production is controlled by *PTTH* so one possible further study to do is to knockdown the neuropeptide *PTTH* in larvae harbouring tumours.

Furthermore, overexpression of *EcR* isoforms with different endogenous patterns of expression suppressed tumour growth, with *Ecr-B1* being the most effective. This is reminiscent of the ability of *EcRB*1 overexpression to suppress growth of *brat* mutant brain tumours (Doggett et al., 2015). It would therefore be interesting to examine whether the glyT2-ecdysone axis has a role in other tumour types.

These findings with our previous study on restricting glycine uptake from food shows that glycine uptake is involved in supporting tumour growth and that there is a potential link between diet, hormone levels and tumour growth promotion.

The downstream pathway by which ecdysone acts to suppress tumour growth remains to be fully delineated. As discussed earlier, *chinmo* is a positive target of JAK/STAT signaling in early eye discs and other tissues (Flaherty et al., 2010), and is under control of *let-7*. In the *Drosophila* wing, it has been reported that

misexpression of *br* isoforms in damaged cells affected *chinmo* expression; *br-Z1* caused *chinmo* repression in mid larvae stage 3 (L3), while *br-Z2* is cell lethal; *br-Z3* and *br-Z4* led to partial *chinmo* repression during early and mid L3. Knowing that *Chinmo* facilitates efficient regeneration, these studies indicate that *br* restricted regenerative response of *chinmo* in wing discs (Narbonne-Reveau and Maurange, 2019). Similarly, in our study, overexpression of *br-Z1* or *br-Z3* in tumourous cells restricted tumour growth, although it is not yet clear whether they act through a similar *chinmo*-dependent mechanism. Indeed, whilst ectopic *br-Z1* strongly suppressed tumour growth, when we manipulated levels of *chinmo* or *let-7* in our experiments, we did not see any significant effect on tumour volume. It will be interesting to see whether *br-Z1* expression is induced in tumours by ecdysone or in response to *nSyb>glyT*^{IR}.

In addition, it is known that *chinmo* and *br* belong to a family of Zinc finger and BTB domain containing (*ZBTB*) developmental transcription factors and are associated with a repressive activity which may translate at the chromatin factors. However, their mode of action is still poorly understood (Flaherty et al., 2010). Interestingly, in humans, *LAZ3*, a novel zinc-finger encoding gene shares amino-terminal homology with the *Drosophila broad*-complex genes and inappropriate expression of this gene *LAZ3* may have a direct role in the neoplastic process. For example, chromosomal translocation 3q27 in human lymphomas lead to disruption of *LAZ3* in two locations (Kerckaert et al., 1993). Moreover, The structural conserved features of *LAZ3* suggest it is a DNA-binding regulatory protein. Similarly, the *br*-complex genes in *Drosophila* act as transactivating factors in the hormone-dependent regulatory cascade which precedes metamorphosis. Taken together human studies on *LAZ3* and ours we suggest that *br* has a developmental transcriptional role in *Drosophila* as well as indicating that conserved factors involved in *ZBTB* are an attractive field that could contribute to cancer research and should be investigated. Especially that

the conserved zinc-finger family reported to have numbers of rearranged genes involved in leukaemia and lymphomas such as, T-cell acute lymphoblastic leukaemia acute leukaemia (Kerckaert et al., 1993).

Chapter 6: Conclusion and Perspective

- Our ultimate aim is to obtain a comprehensive list of gene candidates that can normally limit the spread of cancer cells in an intact animal. This has the potential to help develop ways to boost resistance of healthy tissues, preventing them from being overrun by cancer cells while other treatments acting on the cancer have time to have their effect, leading to better overall patient survival. Using the *Drosophila* dual expression systems *Gal4/UAS* system and *LexA*/ *Lexop* (Hales *et a*l.2015), we generated spatially-restricted, genetically-defined tumours, whilst simultaneously, but independently, manipulating the surrounding healthy tissue. This allowed us to interrogate the involvement of haemocytes and other components of the TME in tumour development and progression. Understanding the intricacies of these factors will ultimately expand our understanding of cancer progression and metastases and provide possible therapeutic strategies targeting this interaction. The advantages of the fly system over other systems include the precision of the genetic manipulation that can be achieved in a fly model.

- There are some limitations to these type of experiments, including the specificity and efficiency of the RNAi lines we have used. We also cannot eliminate the possibility that some genes are so abundant that RNAi is incapable of reducing their expression below a threshold level at which biological function becomes impaired. For our key genes we tried to overcome this problem by using more than one RNAi line, where each target different gene sequences and have been proven by other studies to be specific.

- We identified 10 metabolic regulators involved in cancer metabolism that suppress tumour growth when knocked down in cancer cells or

haemocytes. Of the genes we tested, *CPT2* knockdown was the most effective in reducing tumour growth in either cellular context. Targeting these metabolic regulators in cancer by using pharmacological agents may represent one therapeutic strategy. Indeed, there are number of inhibitors available in trails including Etomoxir (CPT1 inhibitor). However, a recent study reported that high concentrations of Etomoxir (200 μM) has an off-target effect by targeting complex I of the electron transport chain (Yao et al., 2018). Thus, the significant reduction in cell proliferation reported by (Camarda et al., 2016) in breast cancers and other cancers' patients, who treated were with 200 μM Etoximir, may not be because the drug inhibits its primary target (*CPT1*) but rather be due to a reduction in cell proliferation independent of FAO (Yao et al., 2018). Accordingly, the stability, efficiency and specificity of the agent should be considered in future clinical trials. Moreover, due to the uncertainty of these genes' roles in a complex disease such as cancer, it is suggested to use techniques to explore their cell-specific role. Our identification of an innate tumour interaction with the tumour microenvironment in flies may provide insight into potential gene targets and provide us ideas on how such gene-orientated cancer treatments could be further improved in human patients.

- DCIS is the in-situ phase of breast carcinoma development, prior to the development of invasion. Currently, there is no reliable way to know which instances of DCIS will become invasive cancer and which ones will not. Consequently, women with DCIS are routinely treated, despite the possible adverse effects of therapy. Therefore, we tried to identify whether *CPT-2* may be a suitable biomarker to stratify patients. By staining DCIS patient samples and correlating *CPT-2* levels with patient outcomes, we found that high levels of *CPT-2* prevented DCIS recurrence, but there was no

difference in *CPT-2* expression between the pure DCIS, recurrence, and progression groups. This finding highlights the complexity of this marker. Moreover, bioinformatic analysis revealed that *CPT-2* is involved in modulating immune infiltration and regulation in human breast tumours, which correlates with our findings in flies. However, the effect is stage, mutation burden and immune-compartment-specific, and shifts as breast cancer progresses. This highlights the complexities involved in finding biomarkers of progression of DCIS and other stages of breast cancer.

- It is well established that cancer cells change their metabolic pathways in order to fulfil their demand for certain nutrients to sustain proliferation. Amino acids are one of the nutrients required for cancer progression (Hosios et al., 2016a, Johnson et al., 2018). We have identified that the lack of certain individual NEAAs affected the tumour growth as well as the severity of invasion to different extents. Dietary intervention has been proposed to be a new therapeutic strategy in cancer. However, it is central to understand how tumour cells respond and adapt to NEAAS starvation for optimized therapeutic intervention.

- In parallel with genetic perturbation of the *Drosophila* TME, we also examined the effect of dietary interventions to test the effect of non-essential amino acid withdrawal. We found that the lack of Glycine from the *Drosophila* diet suppressed tumour growth the most compared to other NEAAs. We followed up this finding by knockdown of the glycine transporter (*GlyT*) in different TME compartments using our genetically developed *Drosophila* models. We found tumour growth and spread was suppressed by knocking down *GlyT* in neuronal cells but not in haemocytes or the tumour itself, phenocopying the loss of glycine in the diet. We

hypothesise that these effects may be mediated by circuitry in the brain controlling the circadian clock because it has previously been shown that circadian neurobiology is a key target of glycinergic signalling in *Drosophila*. Consequently, there is a possibility that nutritional inputs mediate changes in the neuronal circadian clock, ultimately impacting on tumour growth and progression, via steroid hormone production which we know is under control of these neuronal circuits. Excitingly, our preliminary MS findings confirmed that Ecdysone is upregulated in animals with neuronal *GlyT* knockdown. It will be essential to replicate and extend these studies. Further studies on the involvement of circadian genes in cancer development is also desirable.

- Based on our studies of possible signaling downstream of ecdysone, we find that *broad* overexpression in tumours phenocopies *GlyT* knockdown in neural cells. This raises the possibility of a signalling cascade triggered by glycine depletion leading to *broad*-induced differentiation and tumour suppression via 20E ecdysone. Analysis of 20E and tumour-derived *br* levels following perturbation of *GlyT* will help to support these ideas.

In summary, Glycine represents a metabolic vulnerability in rapidly proliferating cancer cells that could in principle be translated into human studies and be targeted for therapeutic benefit.

References

ANASTASIOU, D. 2017. Tumour microenvironment factors shaping the cancer metabolism landscape. *British Journal of Cancer,* 116**,** 277.

ARAGÓN, C. & LÓPEZ-CORCUERA, B. 2003. Structure, function and regulation of glycine neurotransporters. *European Journal of Pharmacology,* 479**,** 249-262.

ASHBURNER, M. 1973. Sequential gene activation by ecdysone in polytene chromosomes of Drosophila melanogaster: I. Dependence upon ecdysone concentration. *Developmental Biology,* 35**,** 47-61.

BAILEY, ANDREW P., KOSTER, G., GUILLERMIER, C., HIRST, ELIZABETH M. A., MACRAE, JAMES I., LECHENE, CLAUDE P., POSTLE, ANTHONY D. & GOULD, ALEX P. 2015. Antioxidant Role for Lipid Droplets in a Stem Cell Niche of Drosophila. *Cell,* 163**,** 340-353.

BANE, A. 2013. Ductal Carcinoma In Situ: What the Pathologist Needs to Know and Why. *International journal of breast cancer,* 2013**,** 914053-7.

BECKINGHAM, K. M., ARMSTRONG, J. D., TEXADA, M. J., MUNJAAL, R. & BAKER, D. A. 2005. Drosophila melanogaster--the model organism of choice for the complex biology of multi-cellular organisms. *Gravitational and Space Biology,* 18**,** 17.

BELALCÁZAR, A. D., BALL, J. G., FROST, L. M., VALENTOVIC, M. A. & WILKINSON, J. T. 2014. Transsulfuration Is a Significant Source of Sulfur for Glutathione Production in Human Mammary Epithelial Cells. *ISRN biochemistry,* 2013**,** 637897.

BELORIBI-DJEFAFLIA, S., VASSEUR, S. & GUILLAUMOND, F. 2016. Lipid metabolic reprogramming in cancer cells.

BENSAAD, K., FAVARO, E., LEWIS, C. A., PECK, B., LORD, S., COLLINS, J. M., PINNICK, K. E., WIGFIELD, S., BUFFA, F. M., LI, J.-L., ZHANG, Q., WAKELAM, M. J. O., KARPE, F., SCHULZE, A. & HARRIS, A. L. 2014. Fatty acid uptake and lipid storage induced by HIF-1α contribute to cell growth and survival after hypoxia-reoxygenation. *Cell reports (Cambridge),* 9**,** 349-365.

BHUTIA, Y. D., BABU, E., RAMACHANDRAN, S. & GANAPATHY, V. 2015. Amino Acid Transporters in Cancer and Their Relevance to "Glutamine Addiction": Novel Targets for the Design of a New Class of Anticancer Drugs.

BILDER, D., MIN, L. I. & PERRIMON, N. 2000. Cooperative Regulation of Cell Polarity and Growth by Drosophila Tumor Suppressors. *Science (American Association for the Advancement of Science),* 289**,** 113-116.

BIRSOY, K., WANG, T., CHEN, WALTER W., FREINKMAN, E., ABU-REMAILEH, M. & SABATINI, DAVID M. 2015. An Essential Role of the Mitochondrial Electron Transport Chain in Cell Proliferation Is to Enable Aspartate Synthesis. *Cell,* 162**,** 540-551.

BORMAN, A. & WOOD, T. R. 1946. The rôle of arginine in growth with some observations on the effects of argininic acid. *The Journal of biological chemistry,* 166**,** 585-594.

BOTT, A. J., PENG, I. C., FAN, Y., FAUBERT, B., ZHAO, L., LI, J., NEIDLER, S., SUN, Y., JABER, N., KROKOWSKI, D., LU, W., PAN, J.-A., POWERS, S., RABINOWITZ, J., HATZOGLOU, M., MURPHY, D. J., JONES, R., WU, S.,

GIRNUN, G. & ZONG, W.-X. 2015. Oncogenic Myc Induces Expression of Glutamine Synthetase through Promoter Demethylation.
BOUDKO, D. Y., KOHN, A. B., MELESHKEVITCH, E. A., DASHER, M. K., SERON, T. J., STEVENS, B. R. & HARVEY, W. R. 2005. Ancestry and progeny of nutrient amino acid transporters. *Proceedings of the National Academy of Sciences of the United States of America,* 102**,** 1360-1365.
BRISTOW, M. 2000. Etomoxir: a new approach to treatment of chronic heart failure. *Lancet,* 356**,** 1621.
BRITTON, C. H., SCHULTZ, R. A., ZHANG, B., ESSER, V., FOSTER, D. W. & MCGARRY, J. D. 1995. Human liver mitochondrial carnitine palmitoyltransferase I: characterization of its cDNA and chromosomal localization and partial analysis of the gene. *Proceedings Of The National Academy Of Sciences Of The United States Of America,* 92**,** 1984-1988.
BRUMBY, A., SECOMBE, J., HORSFIELD, J., COOMBE, M., AMIN, N., COATES, D., SAINT, R. & RICHARDSON, H. 2004. A genetic screen for dominant modifiers of a cyclin E hypomorphic mutation identifies novel regulators of S-phase entry in Drosophila. United States: GENETICS SOCIETY OF AMERICA.
BRUMBY, A. M. & RICHARDSON, H. E. 2003a. scribble mutants cooperate with oncogenic Ras or Notch to cause neoplastic overgrowth in Drosophila.
BRUMBY, A. M. & RICHARDSON, H. E. 2003b. scribble mutants cooperate with oncogenic Ras or Notch to cause neoplastic overgrowth in Drosophila. *The EMBO journal,* 22**,** 5769-5779.
BUREL, J.-M., BESSON, S., BLACKBURN, C., CARROLL, M., FERGUSON, R. K., FLYNN, H., GILLEN, K., LEIGH, R., LI, S., LINDNER, D., LINKERT, M., MOORE, W. J., RAMALINGAM, B., ROZBICKI, E., TARKOWSKA, A., WALCZYSKO, P., ALLAN, C., MOORE, J. & SWEDLOW, J. R. 2015. Publishing and sharing multi-dimensional image data with OMERO. *Mammalian Genome,* 26**,** 441-447.
BÜSSING, I., SLACK, F. J. & GROSSHAN, H. 2008. let-7 microRNAs in development, stem cells and cancer. *Trends in molecular medicine,* 14**,** 400-409.
CAMARDA, R., ZHOU, A. Y., KOHNZ, R. A., BALAKRISHNAN, S., MAHIEU, C., ANDERTON, B., EYOB, H., KAJIMURA, S., TWARD, A., KRINGS, G., NOMURA, D. K. & GOGA, A. 2016. Inhibition of fatty acid oxidation as a therapy for MYC-overexpressing triple-negative breast cancer. *Nature Medicine***,** 427.
CANTOR, J. R., ABU-REMAILEH, M., KANAREK, N., FREINKMAN, E., GAO, X., LOUISSAINT, J. A., LEWIS, C. A. & SABATINI, D. M. 2017. Physiologic Medium Rewires Cellular Metabolism and Reveals Uric Acid as an Endogenous Inhibitor of UMP Synthase. *Cell,* 169**,** 258-272.
CARL-JOHAN, Z., INES, A., MICHAEL, J. W., RUTH, P., EVA, K., ISTVAN, A., DAN, H. & KATHRYN, V. A. 2004. A Directed Screen for Genes Involved in Drosophila Blood Cell Activation. *Proceedings of the National Academy of Sciences of the United States of America,* 101**,** 14192.
CARRACEDO, A., CANTLEY, L. C. & PANDOLFI, P. P. 2013. Cancer metabolism: fatty acid oxidation in the limelight. *Nature Reviews. Cancer,* 13**,** 227-232.
CERAMI, E., GAO, J., DOGRUSOZ, U., GROSS, B. E., SUMER, S. O., AKSOY, B. A., JACOBSEN, A., BYRNE, C. J., HEUER, M. L., LARSSON, E., ANTIPIN, Y., REVA, B., GOLDBERG, A. P., SANDER, C. & SCHULTZ, N. 2012. The cBio cancer genomics portal: an open platform for exploring multidimensional cancer genomics data. *Cancer Discov,* 2**,** 401-4.

CHANG, C.-H., QIU, J., O'SULLIVAN, D., BUCK, M. D., NOGUCHI, T., CURTIS, J. D., CHEN, Q., GINDIN, M., GUBIN, M. M., VAN DER WINDT, G. J. W., TONC, E., SCHREIBER, R. D., PEARCE, E. J. & PEARCE, E. L. 2015. Metabolic Competition in the Tumor Microenvironment Is a Driver of Cancer Progression. *Cell,* 162**,** 1229-1241.

CHAVARRO, J. E., KENFIELD, S. A., STAMPFER, M. J., LODA, M., CAMPOS, H., SESSO, H. D. & MA, J. 2013. Blood Levels of Saturated and Monounsaturated Fatty Acids as Markers of De Novo Lipogenesis and Risk of Prostate Cancer.

CHOI, B.-H. & COLOFF, J. L. 2019. The Diverse Functions of Non-Essential Amino Acids in Cancer.

CIANA, D. & EVA, M. P.-M. 2018. Metabolic Modulation in Macrophage Effector Function. *Frontiers in Immunology*, 9.

COLOFF, JONATHAN L., MURPHY, J. P., BRAUN, CRAIG R., HARRIS, ISAAC S., SHELTON, LAURA M., KAMI, K., GYGI, STEVEN P., SELFORS, LAURA M. & BRUGGE, JOAN S. 2016. Differential Glutamate Metabolism in Proliferating and Quiescent Mammary Epithelial Cells. *Cell Metabolism,* 23**,** 867-880.

COMBS, J. A. & DENICOLA, G. M. 2019. The Non-Essential Amino Acid Cysteine Becomes Essential for Tumor Proliferation and Survival.

COMMISSO, C., DAVIDSON, S. M., SOYDANER-AZELOGLU, R. G., PARKER, S. J., KAMPHORST, J. J., HACKETT, S., GRABOCKA, E., NOFAL, M., DREBIN, J. A., THOMPSON, C. B., RABINOWITZ, J. D., METALLO, C. M., VANDER HEIDEN, M. G. & BAR-SAGI, D. 2013. Macropinocytosis of protein is an amino acid supply route in Ras-transformed cells. *Nature,* 497**,** 633-637.

CRAMER, S. L., SAHA, A., LIU, J., TADI, S., TIZIANI, S., YAN, W., TRIPLETT, K., LAMB, C., ALTERS, S. E. & ROWLINSON, S. 2017. Systemic depletion of L-cyst(e)ine with cyst(e)inase increases reactive oxygen species and suppresses tumor growth. Great Britain: Nature Publishing Group.

CRISTINA, B.-M., ALMUDENA, P., DAVID, A., HELENA, G. D. S., ENRIQUE, N., CARMEN, A. & BEATRIZ, L.-C. 2018. Modification of a Putative Third Sodium Site in the Glycine Transporter GlyT2 Influences the Chloride Dependence of Substrate Transport. *Frontiers in Molecular Neuroscience,* 11.

DANG, C. V. 2019. Essentiality of non-essential amino acids for tumour cells and tumorigenesis. *Nature metabolism,* 1**,** 847-848.

DAVIS, M. B., CARNEY, G. E., ROBERTSON, A. E. & BENDER, M. 2005. Phenotypic analysis of EcR-A mutants suggests that EcR isoforms have unique functions during Drosophila development. *Developmental biology,* 282**,** 385-396.

DENICOLA, G. M. 2011. Oncogene-induced Nrf2 transcription promotes ROS detoxification and tumorigenesis. Great Britain: Nature Publishing Group.

DENICOLA, G. M., CHEN, P.-H., MULLARKY, E., SUDDERTH, J. A., HU, Z., WU, D., TANG, H., XIE, Y., ASARA, J. M., HUFFMAN, K. E., WISTUBA, I. I., MINNA, J. D., DEBERARDINIS, R. J. & CANTLEY, L. C. 2015. NRF2 regulates serine biosynthesis in non-small cell lung cancer. *Nature Genetics***,** 1475.

DENKO, N. C. 2008. Hypoxia, HIF 1 and glucose metabolism in the solid tumour. *Nature Reviews Cancer***,** 705.

DI CARA, F. & KING-JONES, K. 2016. The Circadian Clock Is a Key Driver of Steroid Hormone Production in Drosophila. *Current Biology,* 26**,** 2469.

DIANNE, M. D., PAULA, K. & IAN, D. 2017. Mutants for Drosophila Isocitrate Dehydrogenase 3b Are Defective in Mitochondrial Function and Larval Cell Death. *G3: Genes, Genomes, Genetics***,** 789.

DIETZL, G., CHEN, D., SCHNORRER, F., SU, K.-C., BARINOVA, Y., FELLNER, M., GASSER, B., KINSEY, K., OPPEL, S., SCHEIBLAUER, S., COUTO, A., MARRA, V., KELEMAN, K. & DICKSON, B. J. 2007. A genome-wide transgenic RNAi library for conditional gene inactivation in Drosophila. *Nature,* 448**,** 151-156.

DOGGETT, K., TURKEL, N., WILLOUGHBY, L. F., ELLUL, J., MURRAY, M. J., RICHARDSON, H. E. & BRUMBY, A. M. 2015. BTB-Zinc Finger Oncogenes Are Required for Ras and Notch-Driven Tumorigenesis in Drosophila. *PLoS ONE,* 10**,** 1-29.

DU, M., WANG, G., ISMAIL, T. M., BARRACLOUGH, R., DAIMARK, B. H., RUDLAND, P., CRICK, R. & NIXON, G. 2018. Proteolysis-targeting chimera (PROTAC) compounds to degrade S100A4 and inhibit breast cancer metastasis. *Annals of oncology : official journal of the European Society for Medical Oncology,* 29**,** ix20.

EASTEL, J. M., LAM, K. W., LEE, N. L., LOK, W. Y., TSANG, A. H. F., PEI, X. M., CHAN, A. K. C., CHO, W. C. S. & WONG, S. C. C. 2019. Application of NanoString technologies in companion diagnostic development. *Expert Rev Mol Diagn,* 19**,** 591-598.

ELIA, I., ROSSI, M., STEGEN, S., BROEKAERT, D., DOGLIONI, G., VAN GORSEL, M., BOON, R., ESCALONA-NOGUERO, C., TORREKENS, S., VERFAILLIE, C., VERBEKEN, E., CARMELIET, G. & FENDT, S.-M. 2019. Breast cancer cells rely on environmental pyruvate to shape the metastatic niche. *Nature: International weekly journal of science,* 568**,** 117.

ENOMOTO, M. & IGAKI, T. 2011. Deciphering tumor-suppressor signaling in flies: Genetic link between Scribble/Dlg/Lgl and the Hippo pathways. *Journal of Genetics and Genomics,* 38**,** 461-470.

ENOMOTO, M., KIZAWA, D., OHSAWA, S. & IGAKI, T. 2015. JNK signaling is converted from anti- to pro-tumor pathway by Ras-mediated switch of Warts activity. *Developmental Biology,* 403**,** 162-171.

ERIKA, L. P., MAYA, C. P., CHIH-HAO, C. & RUSSELL, G. J. 2013. Fueling Immunity: Insights into Metabolism and Lymphocyte Function. *Science,* 342**,** 210.

FADAKA, A., AJIBOYE, B., OJO, O., ADEWALE, O., OLAYIDE, I. & EMUOWHOCHERE, R. 2017. Biology of glucose metabolization in cancer cells. *Journal of Oncological Sciences,* 3**,** 45-51.

FARESE JR, R. V. & WALTHER, T. C. 2009. Lipid Droplets Finally Get a Little R-E-S-P-E-C-T. *Cell,* 139**,** 855-860.

FEATHERSTONE, D. E. 2011. Glial solute carrier transporters in drosophila and mice. *Glia,* 59**,** 1351-1363.

FEI, F., QU, J., ZHANG, M., LI, Y. & ZHANG, S. 2017. S100A4 in cancer progression and metastasis: A systematic review.

FLAHERTY, M. S., SALIS, P., EVANS, C. J., EKAS, L. A., MAROUF, A., ZAVADIL, J., BANERJEE, U. & BACH, E. A. 2010. chinmo Is a Functional Effector of the JAK/STAT Pathway that Regulates Eye Development, Tumor Formation, and Stem Cell Self-Renewal in Drosophila. *Developmental cell,* 18**,** 556-568.

FRENKEL, L., MURARO, N. I., BELTRÁN GONZÁLEZ, A. N., MARCORA, M. S., BERNABÓ, G., HERMANN-LUIBL, C., ROMERO, J. I., HELFRICH-FÖRSTER, C., CASTAÑO, E. M., MARINO-BUSJLE, C., CALVO, D. J. & CERIANI, M. F. 2017. Organization of Circadian Behavior Relies on Glycinergic Transmission. *Cell Reports,* 19**,** 72-85.

FUNG, J. 2018. Available at: https://medium.com/@drjasonfung/the-paradox-of-cancers-warburg-effect-7fb572364b81 (accessed on 12/3/2019).

GAGLIO, D., METALLO, C. M., GAMEIRO, P. A., HILLER, K., DANNA, L. S., BALESTRIERI, C., ALBERGHINA, L., STEPHANOPOULOS, G. & CHIARADONNA, F. 2011. Oncogenic K-Ras decouples glucose and glutamine metabolism to support cancer cell growth. *Molecular Systems Biology,* 7**,** 523-523.

GALAGOVSKY, D., DEPETRIS-CHAUVIN, A., MANIÈRE, G., GEILLON, F., BERTHELOT-GROSJEAN, M., NOIROT, E., ALVES, G. & GROSJEAN, Y. 2018. Sobremesa L-type Amino Acid Transporter Expressed in Glia Is Essential for Proper Timing of Development and Brain Growth. *Cell reports (Cambridge),* 24**,** 3156-3166.e4.

GALVÁN-PEÑA, S. & O'NEILL, L. A. J. 2014. Metabolic reprograming in macrophage polarization. *Frontiers in immunology,* 5**,** 420.

GAO, J., AKSOY, B. A., DOGRUSOZ, U., DRESDNER, G., GROSS, B., SUMER, S. O., SUN, Y., JACOBSEN, A., SINHA, R., LARSSON, E., CERAMI, E., SANDER, C. & SCHULTZ, N. 2013. Integrative analysis of complex cancer genomics and clinical profiles using the cBioPortal. *Sci Signal,* 6**,** pl1.

GATENBY, R. A. & GILLIES, R. J. 2004. Why do cancers have high aerobic glycolysis? Great Britain: Nature Publishing Group.

GATZA, M. L., SILVA, G. O., PARKER, J. S., FAN, C. & PEROU, C. M. 2014. An integrated genomics approach identifies drivers of proliferation in luminal-subtype human breast cancer. *Nature genetics,* 46**,** 1051-1059.

GERALD, M. R. & ALLAN, C. S. 1982. Genetic Transformation of Drosophila with Transposable Element Vectors. *Science,* 218**,** 348.

GOMEZA, J., HÜLSMANN, S., OHNO, K., EULENBURG, V., SZÖKE, K., RICHTER, D. & BETZ, H. 2003a. Inactivation of the Glycine Transporter 1 Gene Discloses Vital Role of Glial Glycine Uptake in Glycinergic Inhibition. *Neuron,* 40**,** 785-796.

GOMEZA, J., OHNO, K., HÜLSMANN, S., ARMSEN, W., EULENBURG, V., RICHTER, D. W., LAUBE, B. & BETZ, H. 2003b. Deletion of the Mouse Glycine Transporter 2 Results in a Hyperekplexia Phenotype and Postnatal Lethality. *Neuron,* 40**,** 797-806.

GONZALEZ, E. A., GARG, A., TANG, J., NAZARIO-TOOLE, A. E. & WU, L. P. 2013. A Glutamate-Dependent Redox System in Blood Cells Is Integral for Phagocytosis in Drosophila melanogaster. *Current Biology***,** 2319.

GRAVEL, S. P., ST-PIERRE, J., TOPISIROVIC, I., HULEA, L., TOBAN, N., POLLAK, M., BIRMAN, E., BLOUIN, M. J., ZAKIKHANI, M. & ZHAO, Y. 2014. Serine deprivation enhances antineoplastic activity of biguanides. *Cancer Research,* 74**,** 7521-7533.

GROSS, M. I., DEMO, S. D., DENNISON, J. B., CHEN, L., CHERNOV-ROGAN, T., GOYAL, B., JANES, J. R., LAIDIG, G. J., LEWIS, E. R., LI, J., MACKINNON, A. L., PARLATI, F., RODRIGUEZ, M. L. M., SHWONEK, P. J., SJOGREN, E. B., STANTON, T. F., WANG, T., YANG, J., ZHAO, F. & BENNETT, M. K. 2014. Antitumor Activity of the Glutaminase Inhibitor CB-839 in Triple-Negative Breast Cancer.

GROTH, A. C., FISH, M., NUSSE, R. & CALOS, M. P. 2004. Construction of transgenic Drosophila by using the site-specific integrase from phage phiC31. *Genetics,* 166**,** 1775-1782.

GU, J.-J., YAO, M., YANG, J., CAI, Y., ZHENG, W.-J., WANG, L., YAO, D.-B. & YAO, D.-F. 2017. Mitochondrial carnitine palmitoyl transferase-II inactivity aggravates lipid accumulation in rat hepatocarcinogenesis. *World journal of gastroenterology : WJG,* 23**,** 256-264.

HALDER, G. & JOHNSON, R. L. 2011. Hippo signaling: growth control and beyond.

HALES, K. G., KOREY, C. A., LARRACUENTE, A. M. & ROBERTS, D. M. 2015. Genetics on the Fly: A Primer on the Drosophila Model System. *Genetics,* 201**,** 815-842.
HALME, A., CHENG, M. & HARIHARAN, I. K. 2010. Retinoids Regulate a Developmental Checkpoint for Tissue Regeneration in Drosophila. Great Britain: Elsevier Science B.V., Amsterdam.
HANAHAN, D. & WEINBERG, R. A. 2011. Hallmarks of Cancer: The Next Generation. United States: Elsevier Science B.V., Amsterdam.
HAO, Q., LI, T., ZHANG, X., GAO, P., QIAO, P., LI, S. & GENG, Z. 2014. Expression and roles of fatty acid synthase in hepatocellular carcinoma.
HÉCTOR, H. & STEPHEN, M. C. 2017. Drosophila as a Model to Study the Link between Metabolism and Cancer. *Journal of Developmental Biology***,** 15.
HEGAZI, S., LOWDEN, C., GARCIA, J. R., CHENG, A. H., LEVINE, J. D., CHENG, H. Y. M. & OBRIETAN, K. 2019. A symphony of signals: Intercellular and intracellular signaling mechanisms underlying circadian timekeeping in mice and flies. *International Journal of Molecular Sciences,* 20.
HENTGES, K. E. & JUSTICE, M. J. 2004. Checks and balancers: balancer chromosomes to facilitate genome annotation. *Trends in Genetics,* 20**,** 252-259.
HODGSON, J., PARVY, J.-P., YU, Y., VIDAL, M. & CORDERO, J. 2021. Drosophila Larval Models of Invasive Tumorigenesis for In Vivo Studies on Tumour/Peripheral Host Tissue Interactions during Cancer Cachexia. *International journal of molecular sciences,* 22**,** 8317.
HOSIOS, AARON M., HECHT, VIVIAN C., DANAI, LAURA V., JOHNSON, MARC O., RATHMELL, JEFFREY C., STEINHAUSER, MATTHEW L., MANALIS, SCOTT R. & VANDER HEIDEN, MATTHEW G. 2016a. Amino Acids Rather than Glucose Account for the Majority of Cell Mass in Proliferating Mammalian Cells. *Developmental Cell,* 36**,** 540-549.
HOSIOS, A. M., HECHT, V. C., DANAI, L. V., JOHNSON, M. O., RATHMELL, J. C., STEINHAUSER, M. L., MANALIS, S. R. & VANDER HEIDEN, M. G. 2016b. Amino acids rather than glucose account for the majority of cell mass in proliferating mammalian cells.
HU, Y., ROESEL, C., FLOCKHART, I., PERKINS, L., PERRIMON, N. & MOHR, S. E. 2013. UP-TORR: online tool for accurate and Up-to-Date annotation of RNAi Reagents. *Genetics,* 195**,** 37-45.
HUMBERT, P. O., GRZESCHIK, N. A., BRUMBY, A. M., GALEA, R., ELSUM, I. & RICHARDSON, H. E. 2008. Control of tumourigenesis by the Scribble/Dlg/Lgl polarity module. Great Britain: Nature Publishing Group.
INC, T. 2020. Available at: https://medium.com/@drjasonfung/the-paradox-of-cancers-warburg-effect-7fb572364b81 (accessed on 12/3/2019).
IOANNIS, P., XIAOMENG, W., THOMAS, C., CHRISTIAAN, L., DAVID, M., SHIRA, L. C., KENDRA, T., RAJAT, R., OLIVIER, E. P., MICHAEL, J. S., SCOTT, W. R., EVERETT, S. & RICHARD, F. L. 2017. Oncogene-Selective Sensitivity to Synchronous Cell Death following Modulation of the Amino Acid Nutrient Cystine. *Cell Reports,* 18**,** 2547-2556.
ISMAIL, T. M., BENNETT, D., PLATT-HIGGINS, A. M., AL-MEDHITY, M., BARRACLOUGH, R. & RUDLAND, P. S. 2017. S100A4 Elevation Empowers Expression of Metastasis Effector Molecules in Human Breast Cancer.
JACCARD, A., PETIT, B., GIRAULT, S., SUAREZ, F., GRESSIN, R., ZINI, J. M., COITEUX, V., LARROCHE, C., DEVIDAS, A., THIÉBLEMONT, C., GAULARD, P., MARIN, B., GACHARD, N., BORDESSOULE, D. & HERMINE, O. 2009. L-

Asparaginase-based treatment of 15 western patients with extranodal NK/T-cell lymphoma and leukemia and a review of the literature. *Annals of oncology,* 20**,** 110-116.
JAIN, M., NILSSON, R., SHARMA, S., MADHUSUDHAN, N., KITAMI, T., SOUZA, A. L., KAFRI, R., KIRSCHNER, M. W., CLISH, C. B. & MOOTHA, V. K. 2012. Metabolite profiling identifies a key role for glycine in rapid cancer cell proliferation. *Science (New York, N.Y.),* 336**,** 1040-1044.
JIE, J., SANKALP, S. & JI, Z. 2019. Starve Cancer Cells of Glutamine: Break the Spell or Make a Hungry Monster? *Cancers,* 11**,** 804-804.
JOHNSON, M. O., RATHMELL, J. C., STEINHAUSER, M. L., HOSIOS, A. M., HECHT, V. C., DANAI, L. V., MANALIS, S. R. & VANDER HEIDEN, M. G. 2018. Amino Acids Rather than Glucose Account for the Majority of Cell Mass in Proliferating Mammalian Cells.
KALYANARAMAN, B. 2017. Teaching the basics of cancer metabolism: Developing antitumor strategies by exploiting the differences between normal and cancer cell metabolism. *Redox Biology,* 12**,** 833-842.
KAMPHORST, J. J., NOFAL, M., COMMISSO, C., HACKETT, S. R., LU, W., GRABOCKA, E., VANDER HEIDEN, M. G., MILLER, G., DREBIN, J. A., BAR-SAGI, D., THOMPSON, C. B. & RABINOWITZ, J. D. 2015. Human Pancreatic Cancer Tumors Are Nutrient Poor and Tumor Cells Actively Scavenge Extracellular Protein.
KEEVIL, B. G. B. M. F. 2013. Novel liquid chromatography tandem mass spectrometry (LC-MS/MS) methods for measuring steroids. *Best Practice & Research Clinical Endocrinology & Metabolism,* 27**,** 663-674.
KERCKAERT, J. P., DEWEINDT, C., QUIEF, S., LECOCQ, G., TILLY, H. & BASTARD, C. 1993. LAZ3, a novel zinc-finger encoding gene, is disrupted by recurring chromosome 3q27 translocations in human lymphomas. *Nature Genetics,* 5**,** 66-70.
KIM, J. W. & DANG, C. V. 2006. Cancer's Molecular Sweet Tooth and the Warburg Effect. United States: AMERICAN ASSOCIATION FOR CANCER RESEARCH.
KING, R. C. & AKAI, H. 1982. *Insect ultrastructure,* New York : Plenum, 1982-1984.
KNOTT, S. R. V., WAGENBLAST, E., KHAN, S., KIM, S. Y., SOTO, M., WAGNER, M., TURGEON, M.-O., FISH, L., ERARD, N., GABLE, A. L., MACELI, A. R., DICKOPF, S., PAPACHRISTOU, E. K., D'SANTOS, C. S., CAREY, L. A., WILKINSON, J. E., HARRELL, J. C., PEROU, C. M., GOODARZI, H., POULOGIANNIS, G. & HANNON, G. J. 2018. Asparagine bioavailability governs metastasis in a model of breast cancer. *Nature (London),* 554**,** 378-381.
KRANE, S. M. The importance of proline residues in the structure, stability and susceptibility to proteolytic degradation of collagens. 2008 2008. Springer, 703.
KUMAR, J. P. 2001. Signalling pathways in Drosophila and vertebrate retinal development. *Nature Reviews. Genetics,* 2**,** 846-857.
LA MARCA, J. E. & RICHARDSON, H. E. 2020. Two-Faced: Roles of JNK Signalling During Tumourigenesis in the Drosophila Model.
LABUSCHAGNE, CHRISTIAAN F., VAN DEN BROEK, NIELS J. F., MACKAY, GILLIAN M., VOUSDEN, KAREN H. & MADDOCKS, OLIVER D. K. 2014. Serine, but Not Glycine, Supports One-Carbon Metabolism and Proliferation of Cancer Cells. *Cell Reports,* 7**,** 1248-1258.
LEE, S.-U. & MAEDA, T. 2012. POK/ZBTB proteins: an emerging family of proteins that regulate lymphoid development and function: POK/ZBTB protein in lymphoid development. *Immunological reviews,* 247**,** 107-119.

LEIKAM, C., HUFNAGEL, A., WALZ, S., KNEITZ, S., FEKETE, A., MÜLLER, M. J., EILERS, M., SCHARTL, M. & MEIERJOHANN, S. 2014. Cystathionase mediates senescence evasion in melanocytes and melanoma cells. *Oncogene,* 33**,** 771-782.

LIBERTI, M. V. & LOCASALE, J. W. 2016. The Warburg Effect: How Does it Benefit Cancer Cells? *Trends in Biochemical Sciences,* 41**,** 211-218.

LIEN, E. C., LYSSIOTIS, C. A., JUVEKAR, A., HU, H., ASARA, J. M., CANTLEY, L. C. & TOKER, A. 2016. Glutathione biosynthesis is a metabolic vulnerability in PI(3)K/Akt-driven breast cancer. *Nature Cell Biology***,** 572.

LIN, M., LV, D., ZHENG, Y., WU, M., XU, C., ZHANG, Q. & WU, L. 2018. Downregulation of CPT2 promotes tumorigenesis and chemoresistance to cisplatin in hepatocellular carcinoma. *OncoTargets and therapy,* 11**,** 3101-3110.

LLC, N. 2018. Findings from Rabin Medical Center Reveals New Findings on Diet and Nutrition (Home parenteral nutrition for advanced cancer patients: Contributes to survival?). NewsRX LLC.

LÓPEZ-LÁZARO, M. 2015. Selective amino acid restriction therapy (SAART): a non-pharmacological strategy against all types of cancer cells. *Oncoscience,* 2**,** 857-866.

LOWY, D. R. & WILLUMSEN, B. M. 1993. Function and regulation of ras. *Annual review of biochemistry,* 62**,** 851-891.

LUO, H., HANSEN, A. S. L., YANG, L., SCHNEIDER, K., KRISTENSEN, M., CHRISTENSEN, U., CHRISTENSEN, H. B., DU, B., ÖZDEMIR, E., FEIST, A. M., KEASLING, J. D., JENSEN, M. K., HERRGÅRD, M. J. & PALSSON, B. O. 2019. Coupling S-adenosylmethionine-dependent methylation to growth: Design and uses. *PLoS biology,* 17**,** e2007050.

MAAN, M., DUTTA, M., PETERS, J. M. & PATTERSON, A. D. 2018. Lipid metabolism and lipophagy in cancer. *Biochemical and Biophysical Research Communications,* 504**,** 582-589.

MADDOCKS, O. D., ATHINEOS, D., CHEUNG, E. C., LEE, P., ZHANG, T., VAN DEN BROEK, N. J., MACKAY, G. M., LABUSCHAGNE, C. F., GAY, D. & KRUISWIJK, F. 2017. Modulating the therapeutic response of tumours to dietary serine and glycine starvation. Great Britain: Nature Publishing Group.

MARTIN-BLANCO, E., GAMPEL, A., RING, J., VIRDEE, K., KIROV, N., TOLKOVSKY, A. M. & MARTINEZ-ARIAS, A. 1998. puckered encodes a phosphatase that mediates a feedback loop regulating JNK activity during dorsal closure in Drosophila. United States: CSH COLD SPRING HARBOR LABORATORY PRESS.

MARTINEZ, A. M., SCHUETTENGRUBER, B., SAKR, S., JANIC, A., GONZALEZ, C. & CAVALLI, G. 2009. Polyhomeotic has a tumor suppressor activity mediated by repression of Notch signaling. Great Britain: Nature Publishing Group.

MATTHEW, G. V. H., LEWIS, C. C. & CRAIG, B. T. 2009. Understanding the Warburg Effect: The Metabolic Requirements of Cell Proliferation. *Science,* 324**,** 1029.

MATTHEWS, K. A., KAUFMAN, T. C. & GELBART, W. M. 2005. Research resources for Drosophila: the expanding universe. *Nature Reviews. Genetics,* 6**,** 179-193.

MEDVEDEVA, Y. A., LENNARTSSON, A., EHSANI, R., KULAKOVSKIY, I. V., VORONTSOV, I. E., PANAHANDEH, P., KHIMULYA, G., KASUKAWA, T., DRABLØS, F. & CONSORTIUM, F. 2015. EpiFactors: a comprehensive database of human epigenetic factors and complexes. *Database (Oxford),* 2015**,** bav067.

MELONE, M. A. B., VALENTINO, A., MARGARUCCI, S., GALDERISI, U., GIORDANO, A. & PELUSO, G. 2018. The carnitine system and cancer metabolic plasticity.

MENENDEZ, J. A. & LUPU, R. 2007. Fatty acid synthase and the lipogenic phenotype in cancer pathogenesis. *Nature Reviews. Cancer,* 7**,** 763-777.

MILGRAUM, L. Z., WITTERS, L. A., PASTERNACK, G. R. & KUHAJDA, F. P. 1997. Enzymes of the Fatty Acid Synthesis Pathway Are Highly Expressed in in Situ Breast Carcinoma. United States: AMERICAN ASSOCIATION FOR CANCER RESEARCH, INC.

MORIN, X., DANEMAN, R., ZAVORTINK, M. & CHIA, W. 2001. A Protein Trap Strategy to Detect GFP-Tagged Proteins Expressed from Their Endogenous Loci in Drosophila. *Proceedings of the National Academy of Sciences - PNAS,* 98**,** 15050-15055.

MULLER, H. J. 1927. Artificial Transmutation of the Gene. *Science,* 66**,** 84.

MUSCARITOLI, M., MOLFINO, A., LAVIANO, A., RASIO, D. & ROSSI FANELLI, F. 2012. Parenteral nutrition in advanced cancer patients. *Critical Reviews in Oncology / Hematology,* 84**,** 26-36.

MUSSELMAN, L. P. & KUEHNLEIN, R. P. 2018. Drosophila as a model to study obesity and metabolic disease.

MUZ, B., DE LA PUENTE, P., AZAB, F. & AZAB, A. K. 2015. The role of hypoxia in cancer progression, angiogenesis, metastasis, and resistance to therapy. Dove Medical Press.

NARBONNE-REVEAU, K. & MAURANGE, C. 2019. Developmental regulation of regenerative potential in Drosophila by ecdysone through a bistable loop of ZBTB transcription factors. *PLoS biology,* 17**,** e3000149.

NATIONAL CANCER INSTITUTE 2022. available at. https://www.cancer.gov/publications/dictionaries/cancer-terms/def/dcis. Accessed on Nov 2022.

O'NEILL, L. A., KISHTON, R. J. & RATHMELL, J. 2016. A guide to immunometabolism for immunologists. Great Britain: Nature Publishing Group.

ORO, A. E., MCKEOWN, M. & EVANS, R. M. 1990. Relationship between the product of the Drosophila ultraspiracle locus and the vertebrate retinoid X receptor. *Nature (London),* 347**,** 298-301.

OTTO, W. 1956. On the Origin of Cancer Cells. *Science,* 123**,** 309.

OU, Q., MAGICO, A. & KING-JONES, K. 2011. Nuclear receptor DHR4 controls the timing of steroid hormone pulses during Drosophila development. *PLoS biology,* 9**,** e1001160.

PAN, M., REID, M. A., LOWMAN, X. H., KULKARNI, R. P., TRAN, T. Q., LIU, X., YANG, Y., HERNANDEZ-DAVIES, J. E., ROSALES, K. K. & LI, H. 2016. Regional glutamine deficiency in tumours promotes dedifferentiation through inhibition of histone demethylation. Great Britain: Nature Publishing Group.

PAVLOVA, NATALYA N. & THOMPSON, CRAIG B. 2016. The Emerging Hallmarks of Cancer Metabolism. *Cell Metabolism,* 23**,** 27-47.

PECK, B. & SCHULZE, A. 2019. Lipid Metabolism at the Nexus of Diet and Tumor Microenvironment. *Trends in cancer,* 5**,** 693-703.

PERRIMON, N., NI, J.-Q. & PERKINS, L. 2010. In vivo RNAi: today and tomorrow. *Cold Spring Harbor perspectives in biology,* 2**,** a003640.

PETAN, T., JARC, E. & JUSOVIC, M. 2018. Lipid Droplets in Cancer: Guardians of Fat in a Stressful World.

PHARMA, M. 2021. First Patient Dosed in Phase II OASIS Trial Evaluating the Potential Benefits of Oral SM-88 for Patients with Metastatic HR+/HER2- Breast Cancer After Treatment with a CDK4/6 Inhibitor.

PIPER, M. D., BLANC, E., LEITÃ£O-GONÃ§ALVES, R., YANG, M., HE, X., LINFORD, N. J., HODDINOTT, M. P., HOPFEN, C., SOULTOUKIS, G. A. & NIEMEYER, C.

2014. A holidic medium for Drosophila melanogaster. United States: Nature Publishing Group.
PLETCHER, R. C., HARDMAN, S. L., INTAGLIATA, S. F., LAWSON, R. L., PAGE, A. & TENNESSEN, J. M. 2019. A Genetic Screen Using the Drosophila melanogaster TRiP RNAi Collection To Identify Metabolic Enzymes Required for Eye Development. *G3 (Bethesda, Md.)*.
PRIOR, I. A., LEWIS, P. D. & MATTOS, C. 2012. A Comprehensive Survey of Ras Mutations in Cancer. *Cancer research (Chicago, Ill.),* 72**,** 2457-2467.
PUROHIT, V., RAPAKA, R. & SHURTLEFF, D. 2010. Role of Cannabinoids in the Development of Fatty Liver (Steatosis). *The AAPS journal,* 12**,** 233-237.
QIAN, X., ZHAO, J., CHEN, H. & HU, J. 2015. ATP citrate lyase expression is associated with advanced stage and prognosis in gastric adenocarcinoma. *International Journal of Clinical and Experimental Medicine,* 8**,** 7855-7860.
RAYMOND, A. P. & TIAN, X. 2003. A Genetic Screen in Drosophila for Metastatic Behavior. *Science,* 302**,** 1227.
RICH, J. T., NEELY, J. G., PANIELLO, R. C., VOELKER, C. C. J., NUSSENBAUM, B. & WANG, E. W. 2010. A practical guide to understanding Kaplan-Meier curves. *Otolaryngology-head and neck surgery,* 143**,** 331-336.
ROMERO-CALDERON, R., SHOME, R. M., SIMON, A. F., DANIELS, R. W., DIANTONIO, A. & KRANTZ, D. E. 2007. A screen for neurotransmitter transporters expressed in the visual system of Drosophila melanogaster identifies three novel genes. United States: JOHN WILEY & SONS, LTD.
ROUSSEAU, F., AUBREY, K. R. & SUPPLISSON, S. 2008. The glycine transporter GlyT2 controls the dynamics of synaptic vesicle refilling in inhibitory spinal cord neurons. *The Journal of Neuroscience,* 28**,** 9755-9768.
SAHU, N., DELA CRUZ, D., GAO, M., SANDOVAL, W., HAVERTY, PETER M., LIU, J., STEPHAN, J.-P., HALEY, B., CLASSON, M., HATZIVASSILIOU, G. & SETTLEMAN, J. 2016. Proline Starvation Induces Unresolved ER Stress and Hinders mTORC1-Dependent Tumorigenesis. *Cell metabolism,* 24**,** 753-761.
SANATI, S. 2019. Morphologic and Molecular Features of Breast Ductal Carcinoma in Situ. *The American journal of pathology,* 189**,** 946-955.
SCHULTE, M. L., FU, A., ZHAO, P., LI, J., GENG, L., SMITH, S. T., NICKELS, M. L., CHARLES MANNING, H., KONDO, J., COFFEY, R. J., BERLIN, J., KAY WASHINGTON, M., JOHNSON, M. O., RATHMELL, J. C., SHARICK, J. T., SKALA, M. C. & SMITH, J. A. 2018. Pharmacological blockade of ASCT2-dependent glutamine transport leads to antitumor efficacy in preclinical models. *Nature Medicine,* 24**,** 194-202.
SHAFER, O. T., HELFRICH-FORSTER, C., RENN, S. C. & TAGHERT, P. H. 2006. Reevaluation of Drosophila melanogasters neuronal circadian pacemakers reveals new neuronal classes. United States: John Wiley & Sons, Ltd.
SHELL, S., PARK, S.-M., RADJABI, A. R., SCHICKEL, R., KISTNER, E. O., JEWELL, D. A., FEIG, C., LENGYEL, E. & PETER, M. E. 2007. Let-7 Expression Defines Two Differentiation Stages of Cancer. *Proceedings of the National Academy of Sciences - PNAS,* 104**,** 11400-11405.
SHIRA NEUMAN-SILBERBERG, F., SCHEJTER, E., SHILO, B. Z. & MICHAEL HOFFMANN, F. 1984. The drosophila ras oncogenes: Structure and nucleotide sequence. *Cell,* 37**,** 1027-1033.
SIERRA, A. Y., GRATACOS, E., CARRASCO, P., CLOTET, J., URENA, J., SERRA, D., ASINS, G., HEGARDT, F. G. & CASALS, N. 2008. CPT1c Is Localized in

Endoplasmic Reticulum of Neurons and Has Carnitine Palmitoyltransferase Activity. United States: The American Society for Biochemistry and Molecular Biology.
SINGH, A., IRVINE, K. D., RUDRAPATNA, V. A., CAGAN, R. L. & DAS, T. K. 2012. Drosophila cancer models. *Developmental Dynamics***,** 107.
SON, J., LYSSIOTIS, C. A., YING, H., WANG, X., HUA, S., LIGORIO, M., PERERA, R. M., FERRONE, C. R., MULLARKY, E., SHYH-CHANG, N., KANG, Y. A., FLEMING, J. B., BARDEESY, N., ASARA, J. M., HAIGIS, M. C., DEPINHO, R. A., CANTLEY, L. C. & KIMMELMAN, A. C. 2013. Glutamine supports pancreatic cancer growth through a KRAS-regulated metabolic pathway. *Nature,* 496**,** 101-105.
SOUSA, C. O., BIANCUR, D. E., WANG, X., HALBROOK, C. J., SHERMAN, M. H., ZHANG, L., KREMER, D., HWANG, R. F., WITKIEWICZ, A. K. & YING, H. 2016. Pancreatic stellate cells support tumour metabolism through autophagic alanine secretion. Great Britain: Nature Publishing Group.
SREEKUMAR, A., POISSON, L. M., RAJENDIRAN, T. M., KHAN, A. P., CAO, Q., YU, J., LAXMAN, B., MEHRA, R., LONIGRO, R. J., LI, Y., NYATI, M. K., AHSAN, A., KALYANA-SUNDARAM, S., HAN, B., CAO, X., BYUN, J., OMENN, G. S., GHOSH, D., PENNATHUR, S., ALEXANDER, D. C., BERGER, A., SHUSTER, J. R., WEI, J. T., VARAMBALLY, S., BEECHER, C. & CHINNAIYAN, A. M. 2013. Corrigendum: Metabolomic profiles delineate potential role for sarcosine in prostate cancer progression. *Nature*.
SULLIVAN, M. R., MATTAINI, K. R., DENNSTEDT, E. A., NGUYEN, A. A., SIVANAND, S., REILLY, M. F., MEETH, K., MUIR, A., DARNELL, A. M., BOSENBERG, M. W., LEWIS, C. A. & VANDER HEIDEN, M. G. 2019. Increased Serine Synthesis Provides an Advantage for Tumors Arising in Tissues Where Serine Levels Are Limiting.
SYED, M. H., MARK, B. & DOE, C. Q. 2017. Steroid hormone induction of temporal gene expression in Drosophila brain neuroblasts generates neuronal and glial diversity. *eLife,* 6.
TALBOT, W. S., SWYRYD, E. A. & HOGNESS, D. S. 1993. Drosophila tissues with different metamorphic responses to ecdysone express different ecdysone receptor isoforms. *Cell,* 73**,** 1323-1337.
TANG, X., LIN, C.-C., SPASOJEVIC, I., IVERSEN, E. S., CHI, J.-T. & MARKS, J. R. 2014. A joint analysis of metabolomics and genetics of breast cancer. *Breast Cancer Research: BCR,* 16**,** 415-415.
TANNER, J. J., FENDT, S.-M. & BECKER, D. F. 2018. The Proline Cycle As a Potential Cancer Therapy Target. United States: ACS AMERICAN CHEMICAL SOCIETY.
TAPON, N. 2003. Modeling transformation and metastasis in Drosophila. *Cancer Cell,* 4**,** 333-335.
TAVSANLI, B. C., OSTRIN, E. J., BURGESS, H. K., MIDDLEBROOKS, B. W., PHAM, T. A. & MARDON, G. 2004. Structure–function analysis of the Drosophila retinal determination protein Dachshund. *Developmental Biology,* 272**,** 231-247.
TAYLOR, E., ALQADRI, N., DODGSON, L., MASON, D., LYULCHEVA, E., MESSINA, G. & BENNETT, D. 2017. MRL proteins cooperate with activated Ras in glia to drive distinct oncogenic outcomes. *Oncogene,* 36**,** 4311-4322.
THIMGAN, M. S., BERG, J. S. & STUART, A. E. 2006. Comparative sequence analysis and tissue localization of members of the SLC6 family of transporters in adult Drosophila melanogaster. Great Britain: THE COMPANY OF BIOLOGISTS LTD.
TRABALZINI, L. & RETTA, S. F. 2014. *Ras signaling methods and protocols / edited by Lorenza Trabalzini, Saverio Francesco Retta,* New York, Humana Press.

TZOLOVSKY, G., DENG, W. M., SCHLITT, T. & BOWNES, M. 1999. The function of the Broad-Complex during Drosophila melanogaster oogenesis. United States: WAVERLY PRESS INC.

UNG, P. M. U., SONOSHITA, M., SCOPTON, A. P., DAR, A. C., CAGAN, R. L. & SCHLESSINGER, A. 2019. Integrated computational and Drosophila cancer model platform captures previously unappreciated chemicals perturbing a kinase network. *PLoS Computational Biology,* 15**,** 1-19.

VENKEN, K. J. T. & BELLEN, H. J. 2005. Emerging technologies for gene manipulation in Drosophila melanogaster. *Nature Reviews. Genetics,* 6**,** 167-178.

VIDAL, M. 2010. The dark side of fly TNF: An ancient developmental proof reading mechanism turned into tumor promoter. United States: Landes Bioscience.

VIDAL, M. & CAGAN, R. L. 2006. Drosophila models for cancer research. *Current Opinion in Genetics & Development***,** 10.

WANG, L., LAM, G. & THUMMEL, C. S. 2010. Med24 and Mdh2 are required for Drosophila larval salivary gland cell death. United States: John Wiley & Sons, Ltd.

WANG, M. D., WU, H., FU, G. B., ZHANG, H. L., ZHOU, X., TANG, L., DONG, L. W., QIN, C. J., HUANG, S. & ZHAO, L. H. 2016. Acetyl-coenzyme A carboxylase alpha promotion of glucose-mediated fatty acid synthesis enhances survival of hepatocellular carcinoma in mice and patients. United States: John Wiley & Sons, Ltd.

WARR, C. G. 2019. Drosophila melanogaster: a model organism to study cancer.

WARR, C. G., SHAW, K. H., AZIM, A., PIPER, M. D. W. & PARSONS, L. M. 2018. Using Mouse and Drosophila Models to Investigate the Mechanistic Links between Diet, Obesity, Type II Diabetes, and Cancer.

WEI, L., ANNE, L., CHAD, H., ANDREW, N. L., CHI, V. D., TERESA, W. M. F. & JAMES, M. P. 2012. Reprogramming of proline and glutamine metabolism contributes to the proliferative and metabolic responses regulated by oncogenic transcription factor c-MYC. *Proceedings of the National Academy of Sciences of the United States of America,* 109**,** 8983.

WHITE, D. L., KANWAL, F. & EL–SERAG, H. B. 2012. Association Between Nonalcoholic Fatty Liver Disease and Risk for Hepatocellular Cancer, Based on Systematic Review. *Clinical gastroenterology and hepatology,* 10**,** 1342-1359.e2.

WU, M., PASTOR-PAREJA, J. C. & XU, T. 2017. Interaction between Ras(V12) and scribbled clones induces tumour growth and invasion (vol 463, pg 545, 2010).

XIAO, W., REN, M., ZHANG, C., LI, S. & AN, W. 2015. Amelioration of nonalcoholic fatty liver disease by hepatic stimulator substance via preservation of carnitine palmitoyl transferase-1 activity. *American Journal of Physiology: Cell Physiology,* 309**,** C215-C227.

XIN, M., LIU, J., SONG, S., ZHAO, X., MIAO, P., HUANG, G., QIAO, Z., TANG, T., WANG, L., DAI, K., LI, J., LIU, W. & YANG, X. 2016. MiR-22 inhibits tumor growth and metastasis by targeting ATP citrate lyase: Evidence in osteosarcoma, prostate cancer, cervical cancer and lung cancer. *Oncotarget,* 7**,** 44252-44265.

YAMANAKA, N., REWITZ, K. F. & O CONNOR, M. B. 2013. Ecdysone Control of Developmental Transitions: Lessons from Drosophila Research. United States: ANNUAL REVIEWS INC.

YANG, C., KO, B., HENSLEY, C. T., JIANG, L., WASTI, A. T., KIM, J., SUDDERTH, J., CALVARUSO, M. A., LUMATA, L. & MITSCHE, M. 2014. Glutamine Oxidation Maintains the TCA Cycle and Cell Survival during Impaired Mitochondrial Pyruvate Transport. United States: Elsevier Science B.V., Amsterdam.

YANG, C., SUDDERTH, J., DANG, T., BACHOO, R. G., MCDONALD, J. G. & DEBERARDINIS, R. J. 2009. Glioblastoma Cells Require Glutamate Dehydrogenase to Survive Impairments of Glucose Metabolism or Akt Signaling. United States: AMERICAN ASSOCIATION FOR CANCER RESEARCH.

YANG, L., ACHREJA, A., YEUNG, T.-L., MANGALA, LINGEGOWDA S., JIANG, D., HAN, C., BADDOUR, J., MARINI, JUAN C., NI, J., NAKAHARA, R., WAHLIG, S., CHIBA, L., KIM, SUN H., MORSE, J., PRADEEP, S., NAGARAJA, ARCHANA S., HAEMMERLE, M., KYUNGHEE, N., DERICHSWEILER, M., PLACKEMEIER, T., MERCADO-URIBE, I., LOPEZ-BERESTEIN, G., MOSS, T., RAM, PRAHLAD T., LIU, J., LU, X., MOK, SAMUEL C., SOOD, ANIL K. & NAGRATH, D. 2016. Targeting Stromal Glutamine Synthetase in Tumors Disrupts Tumor Microenvironment-Regulated Cancer Cell Growth. *Cell Metabolism*, 24**,** 685-700.

YANRUI, J., MAKIKO, S., TOMMY BEAT, S. & RENATO, P. 2018. An intrinsic tumour eviction mechanism in Drosophila mediated by steroid hormone signalling. *Nature Communications*, 9**,** 1-9.

YAO, C.-H., LIU, G.-Y., WANG, R., MOON, S. H., GROSS, R. W. & PATTI, G. J. 2018. Identifying off-target effects of etomoxir reveals that carnitine palmitoyltransferase I is essential for cancer cell proliferation independent of β-oxidation. *PLoS Biology,* 16**,** 1-26.

YAO, D., YAO, M., YAMAGUCHI, M., CHIDA, J. & KIDO, H. 2011. Characterization of compound missense mutation and deletion of carnitine palmitoyltransferase II in a patient with adenovirus-associated encephalopathy. *The journal of medical investigation,* 58**,** 210-218.

ZHANG, W., TRACHOOTHAM, D., LIU, J., CHEN, G., PELICANO, H., GARCIA-PRIETO, C., LU, W., BURGER, J. A., CROCE, C. M., PLUNKETT, W., KEATING, M. J. & HUANG, P. 2012. Stromal control of cystine metabolism promotes cancer cell survival in chronic lymphocytic leukaemia. *Nature cell biology,* 14**,** 276-286.

ZHAO, J., KILMAN, V. L., KEEGAN, K. P., PENG, Y., EMERY, P., ROSBASH, M. & ALLADA, R. 2003. Drosophila Clock Can Generate Ectopic Circadian Clocks. *Cell,* 113**,** 755-766.

ZHASMINE, M., MANUELA, S., MARIATERESA, A., ALICE MARIA, V., DANIELA, G. & PAOLA, B. 2019. Drosophila melanogaster: A Model Organism to Study Cancer. *Frontiers in Genetics*.

ZIRIN, J., HU, Y., LIU, L., YANG-ZHOU, D., COLBETH, R., YAN, D., EWEN-CAMPEN, B., TAO, R., VOGT, E., VANNEST, S., CAVERS, C., VILLALTA, C., COMJEAN, A., SUN, J., WANG, X., JIA, Y., ZHU, R., PENG, P., YU, J., SHEN, D., QIU, Y., AYISI, L., RAGOOWANSI, H., FENTON, E., EFREM, S., PARKS, A., SAITO, K., KONDO, S., PERKINS, L., MOHR, S. E., NI, J. & PERRIMON, N. 2020. Large-Scale Transgenic Drosophila Resource Collections for Loss- and Gain-of-Function Studies. *Genetics,* 214**,** 755-767.